Electronic Supplementary Material (ESI) for Chemical Science.

This version of the ESI published 20/03/2024 replaces the previous version published 04/03/2024 to update the refinement statistics presented in Table S7.

Modular Synthesis of Functional Libraries by Accelerated SuFEx Click Chemistry

Authors:

Joshua A. Homer[1], Rebecca A. Koelln[1], Andrew S. Barrow[2], Timothy L. Gialelis[2], Zlata Boiarska[3,4], Nikita S. Steinohrt[5,6], Erinna F. Lee[5,6,7], Wen-Hsuan Yang[1], Robert M. Johnson[1], Taemoon Chung[1], Amber N. Habowski[1], Dharmendra Vishwakarma[1], Debmalya Bhunia[1], Charlotte Avanzi[8], Adam D. Moorhouse[1], Mary Jackson[8], David A. Tuveson[1], Scott K. Lyons[1], Michael J. Lukey[1], W. Douglas Fairlie[5,6,7], Shozeb M. Haider[9], Michel O. Steinmetz[3,10], Andrea E. Prota[3], John E. Moses[*1,2]

Affiliations:

[1]Cancer Center, Cold Spring Harbor Laboratory, 1 Bungtown Rd, Cold Spring Harbor, NY 11724, USA
[2]La Trobe Institute for Molecular Science, La Trobe University, Melbourne, VIC 3086, Australia
[3]Laboratory of Biomolecular Research, Division of Biology and Chemistry, Paul Scherrer Institut, Villigen PSI, 5232, Switzerland
[4]Department of Chemistry, Università degli Studi di Milano, Via Golgi 19, 20133 Milan, Italy
[5]Olivia Newton-John Cancer Research Institute, Heidelberg, Victoria, 3084, Australia
[6]School of Cancer Medicine, La Trobe University, Melbourne, Victoria, 3086, Australia
[7]Department of Biochemistry and Chemistry, La Trobe Institute for Molecular Science, La Trobe University, Melbourne, Victoria, 3086, Australia
[8]Mycobacteria Research Laboratories, Department of Microbiology, Immunology and Pathology, Colorado State University, Fort Collins, CO 80523, USA
[9]School of Pharmacy, University College London, 29-39 Brunswick Square, London, WC1N 1AX, UK
[10]Biozentrum, University of Basel, 4056 Basel, Switzerland

Table of Contents

General Information

General Information: Commercial solvents and reagents were used as supplied. TLC was performed on Polygram® SIL/G_{25} plates and visualized using UV light. LCMS data was collected on a Thermo Scientific Vanquish Flex UHPLC with a Thermo Scientific ISQ™ EM Single Quadrupole Mass Spectrometer operating in APCI mode, using a Waters Xterra MS C18 Column (3.5 µm 4.6 x 100 mm).^{1}H, ^{13}C and ^{19}F NMR spectra were recorded on a Bruker Ascend™ 400 (400 MHz) as dilute solutions in the stipulated solvent. All chemical shifts (δ) are reported in parts per million (ppm) with ^{1}H and ^{13}C NMR referenced to solvent signals [^{1}H NMR: $CDCl_3$ (7.26), DMSO-d_6 (2.50), MeCN-d_3 (1.94); ^{13}C NMR: $CDCl_3$ (77.16), DMSO-d_6 (39.52), MeCN-d_3 (1.32)]. Coupling constants (*J*) are reported in Hertz (Hz) and recorded after averaging. The multiplicity of the ^{1}H NMR signals are designated by one of the following abbreviations: s=singlet, d=doublet, t=triplet, q=quartet, p=pentet, m=multiplet, br=broad signal. HRMS were obtained using a Thermo Scientific Q Exactive HF Hybrid Quadrupole-Orbitrap Mass Spectrometer utilizing a heated electrospray ionization (HESI-II) probe. Flash column chromatography was performed using a Biotage® Selekt™ on Biotage® Sfar Silica D Duo cartridges using ethyl acetate and hexane as elution solvents. Melting point data were collected using a Cole Parmer high resolution digital melting point apparatus.

Table S1. 96-Well Microplate ASCC Equipment.

Equipment	**Vendor**	**Part Number**
Single-channel micropipettes	IKA	0.5-10 µL – P/N: 0020011211 2-20 µL – P/N: 0020011213 20-200 µL – P/N: 0020011215 100-1000 µL – P/N: 0020011216 0.5-5 mL – P/N: 0020011217
12-channel micropipettes	Eppendorf	10-100 µL – P/N: 3125000044 120-1200 µL – P/N: 3125000222
Pipette Reservoir	VWR	490007-612
350 µL 96-well plates for reaction	VWR	82050-636
800 µL 96-well plates for LCMS	VWR	76210-524
Liquid reservoir	VWR	490007-612
Polyolefin sealing film	VWR	89134-428
Slitted silicone microplate cover	VWR	76397-828
Vacuum oven	VWR	89508-426
LC column	Waters	Xterra MS C18 Column (3.5 µm 4.6 x 100 mm)

Aryl Alcohols Used in the ASCC 96-Well Plate Reaction

Table S2. List of aryl alcohols and the total solution volume prepared for pipetting into 96-well plates. Font colors indicate the ratio of MeCN:DMSO used to dissolve the alcohol. Green = 1:2 MeCN:DMSO, Red = 1:1 MeCN:DMSO, Grey = 2:1 MeCN:DMSO, Brown = 5:2 MeCN:DMSO, Blue = 3:1 MeCN:DMSO, Yellow = 4:1 MeCN:DMSO, Orange = 5:1 MeCN:DMSO, Purple = 10:1 MeCN:DMSO, Black = MeCN only, Pink = DMSO only.

No.	Compound Name (CAS Number)	Structure	No.	Compound Name (CAS Number)	Structure	No.	Compound Name (CAS Number)	Structure
A01	Fulvestrant (129453-61-8)	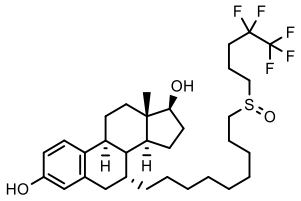	A07	Estrone (53-16-7)	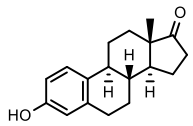	B01	4'-Demethylpodophyllotoxin (40505-27-9)	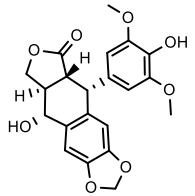
A02	beta-Estradiol (50-28-2)	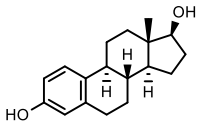	A08	Doxycycline HCl (10592-13-9)	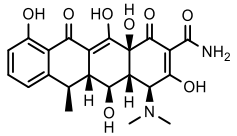	B02	3-Hydroxypyridine (109-00-2)	
A03	Estriol (50-27-1)	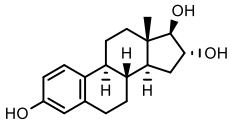	A09	meta-Topolin (75737-38-1)	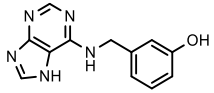	B03	Diethylstilbestrol (6898-97-1)	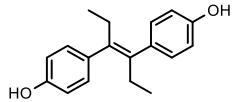
A04	Nonivamide (2444-46-4)	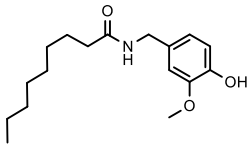	A10	Capsaicin (404-86-4)	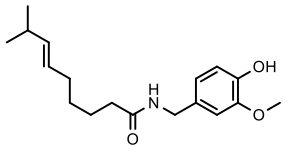	B04	Daidzin (552-66-9)	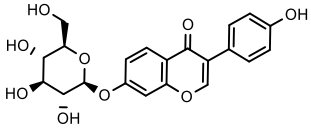
A05	Formononetin (485-72-3)	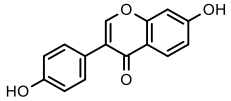	A11	Resorcinol (108-46-3)	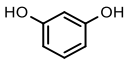	B05	2-{[2-(Methylamino) quinoline-8-yl]oxy} quinolin-8-ol (317375-40-9)	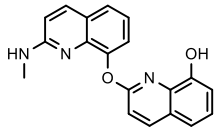
A06	Fenhexamid (126833-17-8)	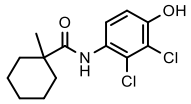	A12	3-{[3-Chloro-5-(trifluoromethyl)-2-pyridinyl]-oxy}benzenol (95711-07-2)	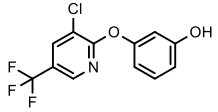	B06	7-Bromo-5-chloro-8-hydroxyquinoline (7640-33-7)	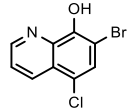

No.	Compound Name (CAS Number)	Structure	No.	Compound Name (CAS Number)	Structure	No.	Compound Name (CAS Number)	Structure
B07	4-Hydroxy-4′-isopropoxydiphenylsulfone (95235-30-6)	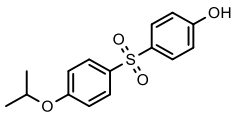	C02	3-Chloro-4-hydroxybenzonitrile (2315-81-3)	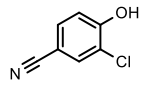	C09	2-Acetyl-4-cyanophenol (35794-84-4)	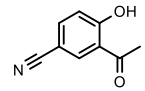
B08	beta-Isocupreidine (253430-48-7)	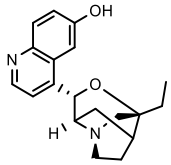	C03	2-(6,7,8,9-Tetrahydro-5H-1,2,4-triazolo[4,3-a] azepin-3-yl) phenol (108877-44-7)	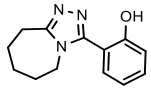	C10	3-(4-Hydroxyphenyl)-6,6-dimethyl-3-azabicyclo [3.1.0]hexane-2,4-dione (1415719-52-6)	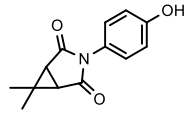
B09	2-Aminophenol (95-55-6)		C04	2-Acetyl-7-hydroxybenzofuran (40020-87-9)	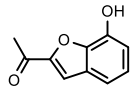	C11	(2Z)-6-Hydroxy-2-(3,4,5-trifluorobenzylidene)-1-benzofuran-3(2H)-one (1627411-97-5)	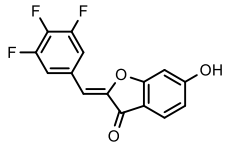
B10	5'-Chloro-3-hydroxy-2'-methyl-2-naphthanilide (135-63-7)	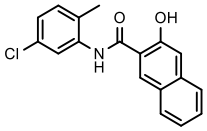	C05	Acridin-4-ol (18123-20-1)	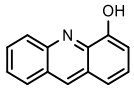	C12	4-Bromo-6-hydroxyisoindolin-1-one (808127-76-6)	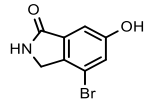
B11	3-Aminophenol (591-27-5)	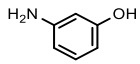	C06	1-Acetamido-7-hydroxynaphthalene (6470-18-4)	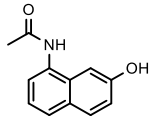	D01	2-(1H-Benzimidazol-2-ylsulfanyl)-N-(3-hydroxyphenyl)acetamide (352330-59-7)	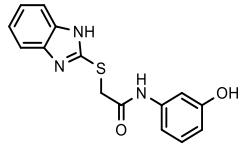
B12	2'-Hydroxychalcone (1214-47-7)	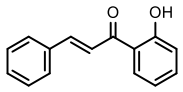	C07	3-(Prop-2-yn-1-yloxy)phenol (3692-88-4)	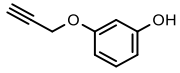	D02	2-(((3,5-Dimethoxyphenyl) amino)methyl)phenol (1019591-20-8)	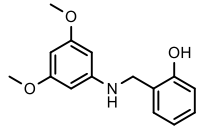
C01	4-Aminophenol (123-30-8)	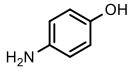	C08	6-Hydroxynaphthalene-2-boronic acid (173194-95-1)	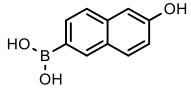	D03	2-(((4-Methoxyphenyl) amino)methyl)phenol (1019591-20-8)	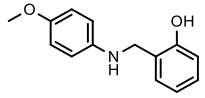

No.	Compound Name (CAS Number)	Structure	No.	Compound Name (CAS Number)	Structure	No.	Compound Name (CAS Number)	Structure
D04	2-(((4-Bromophenyl) amino)methyl)phenol (90383-20-3)	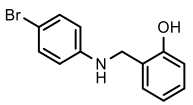	D11	2-((Phenylamino)methyl) -5-(prop-2-yn-1-yloxy)phenol	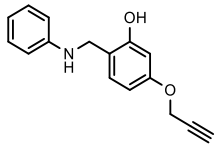	E06	n-Acetyltyramine (1202-66-0)	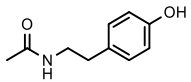
D05*	2-(((4-(Prop-2-yn-1-yloxy) phenyl)amino)methyl) phenol	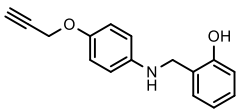	D12	2-Hydroxy-4-(prop-2-yn-1-yloxy)benzaldehyde (67268-54-6)	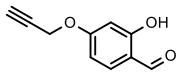	E07	5-Hydroxyisophthalonitrile (79370-78-8)	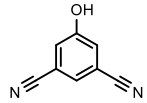
D06	N-(4-Hydroxyphenyl) acetamide (103-90-2)	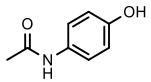	E01	1-Naphthol (90-15-3)		E08	4-(4-Hydroxy-3-methoxy phenyl)but-3-en-2-one (1080-12-2)	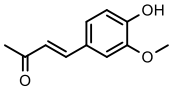
D07	2-((Phenylamino)methyl) phenol (93526-45-2)	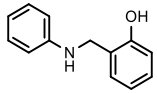	E02	4-Chloro-4'-hydroxybenzophenone (42019-78-3)	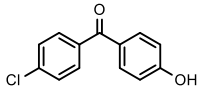	E09	1,2-Benzisoxazol-6-ol (65685-55-4)	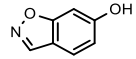
D08	2-{[(4-Methylphenyl) amino]methyl}phenol (14674-88-5)	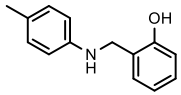	E03	tert-Butyl (4-hydroxyphenyl)carbamate (54840-15-2)	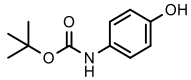	E10	5-Bromo-2-hydroxybenzaldehyde (1761-61-1)	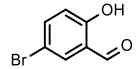
D09*	2-(((4-(Prop-2-yn-1-yloxy)phenyl)amino) methyl)phenol	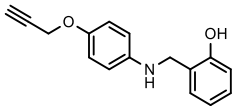	E04	3-Acetamidophenol (621-42-1)	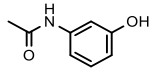	E11	4-(1-Adamantyl)phenol (29799-07-3)	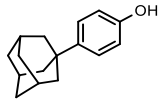
D10	2-(((4-Methoxy-2-methylphenyl)amino) methyl)phenol (1282863-10-8)	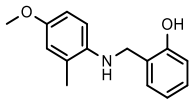	E05	(2Z)-2-(1,3-Benzodioxol-5-ylmethylene)-6-hydroxy -1-benzofuran-3(2H)-one (32396-84-2)	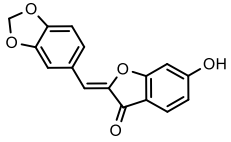	E12	4-Hydroxybenzaldehyde (123-08-0)	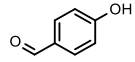

No.	Compound Name (CAS Number)	Structure	No.	Compound Name (CAS Number)	Structure	No.	Compound Name (CAS Number)	Structure
F01	Allyl 4-hydroxybenzoate (18982-18-8)	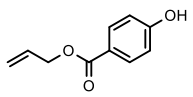	F08	2-(2,6-Dioxopiperidin-3-yl) -4-hydroxyisoindoline-1,3-dione (5054-59-1)	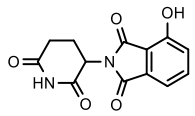	G03	1H-Benzimidazol-6-ol (41292-65-3)	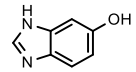
F02	4-{[(4-Chlorophenyl)(1,1-dioxido-1,2-benzisothiazol-3-yl)amino]methyl}-2-methoxyphenol (591242-71-6)	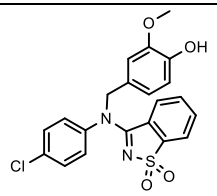	F09	2,2-Bis(4-Hydroxyphenyl) propane (80-05-7)	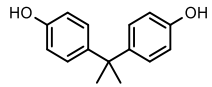	G04	4-Chloro-2-(1h-Pyrazol -3-yl)phenol (18704-67-1)	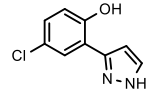
F03	*N*-Allyl-2-(3-hydroxybenzoyl) Hydrazinecarbothioamide (26036-14-6)	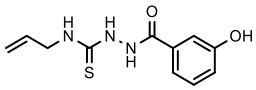	F10	5-Hydroxyindole (1953-54-4)	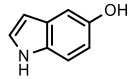	G05	9,9-Bis(4-hydroxyphenyl) fluorene (3236-71-3)	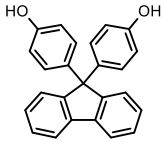
F04	2,2-Bis(3-amino-4-hydroxyphenyl) Hexafluoropropane (83558-87-6)	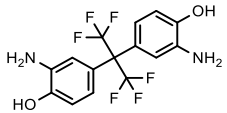	F11	D-Luciferin (2591-17-5)	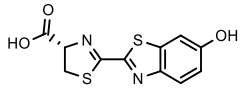	G06	4-Nitrophenol (100-02-7)	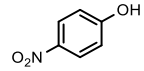
F05	3-Amino-4-hydroxy Benzenesulfonamide (98-32-8)	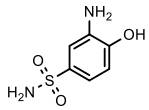	F12	4-Hydroxy-4'-nitrobiphenyl (3916-44-7)	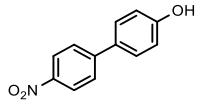	G07	Resveratrol (501-36-0)	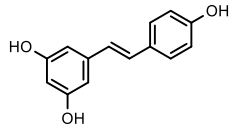
F06	Sesamol (533-31-3)	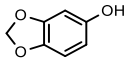	G01	4-Bromo-4'-hydroxybiphenyl (29558-77-8)	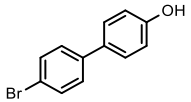	G08	Ethyl 4-[[(2-hydroxyphenyl)methyl] amino]benzoate (199190-52-8)	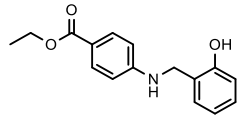
F07	3-(2-Hydroxy-5-methylphenyl)pyrazole (57148-86-4)	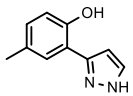	G02	4-Benzothiazolol (7405-23-4)		G09	3-Dimethylaminophenol (99-07-0)	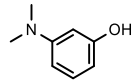

No.	Compound Name (CAS Number)	Structure	No.	Compound Name (CAS Number)	Structure	No.	Compound Name (CAS Number)	Structure
G10	1-Benzofuran-2-yl(5-hydroxy-1-benzofuran-3-yl)methanone (225217-53-8)	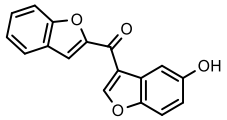	H05	4-((4-Bromo-2-fluorophenyl)amino)-6-methoxyquinazolin-7-ol (196603-96-0)	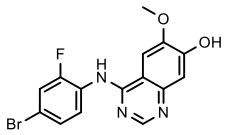	H12	3-Nitrophenol (554-84-7)	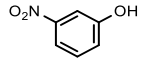
G11	3-Phenylphenol (580-51-8)	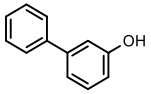	H06	4,4'-Dihydroxybenzophenone (611-99-4)	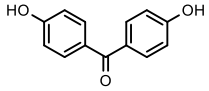	I01	2-Isopropyl-5-methylphenol (89-83-8)	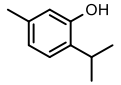
G12	2-[[(1,1-Dimethylethyl) amino]methyl]phenol (60399-04-4)	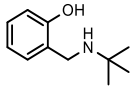	H07	O-Desmorpholinopropyl Gefitinib (184475-71-6)	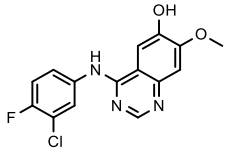	I02	4-(Diethylamino)-2-hydroxybenzaldehyde (17754-90-4)	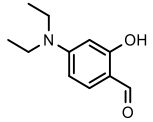
H01	7-Hydroxy-2H-chromen-2-one (93-35-6)	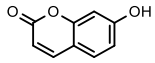	H08	3-Ethynylphenol (10401-11-3)	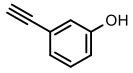	I03	4-Chloronaphthalen-1-ol (604-44-4)	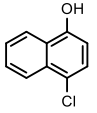
H02	2,6-Dimethoxyphenol (25511-61-9)	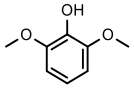	H09	3-(Dibutylamino)phenol (43141-69-1)	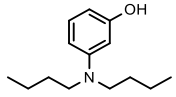	I04	Quinolin-8-ol (148-24-3)	
H03	Methyl 3-hydroxybenzoate (19438-10-9)	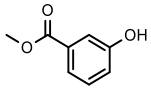	H10	2-Amino-5-fluorophenol (53981-24-1)	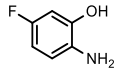	I05	5,6,7,8-Tetrahydronaphthalen-2-ol (1125-78-6)	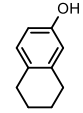
H04	2-Hydroxy-4-methoxybenzophenone (131-57-7)	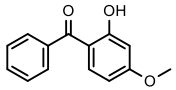	H11	2,7-Naphthalenediol (582-17-2)	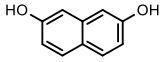	I06	4-(Methylsulfonyl)phenol (14763-60-1)	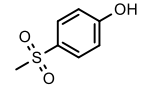

No.	Compound Name (CAS Number)	Structure	No.	Compound Name (CAS Number)	Structure	No.	Compound Name (CAS Number)	Structure
I07	2-Nitronaphthalen-1-ol (607-24-9)	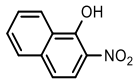	J02	4-(2-Phenylpropan-2-yl)phenol (599-64-4)	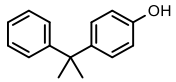	J09	2,6-Di-tert-butyl-4-methylphenol (128-37-0)	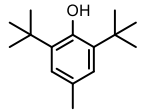
I08	3-Hydroxybenzaldehyde (100-83-4)	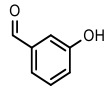	J03	7-Hydroxy-4-methyl-2H-chromen-2-one (90-33-5)	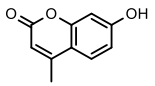	J10	Naphthalen-2-ol (135-19-3)	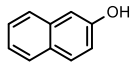
I09	2,3,4,5,6-Pentachlorophenol (87-86-5)	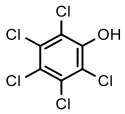	J04	4-Bromo-3,5-dimethylphenol (7463-51-6)	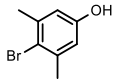	J11	4-Chloro-3-methylphenol (59-50-7)	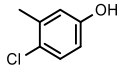
I10	Totarol (511-15-9)	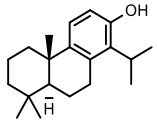	J05	2,6-Dimethylphenol (576-26-1)		J12	4-Hydroxy-3-methoxybenzaldehyde (121-33-5)	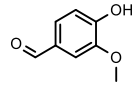
I11	2,4-Dichloronaphthalen-1-ol (2050-76-2)	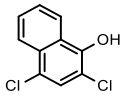	J06	4-(tert-Butyl)phenol (98-54-4)	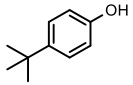	K01	[1,1'-Biphenyl]-4-ol (92-69-3)	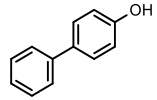
I12	4-(Phenyldiazenyl)phenol (1689-82-3)	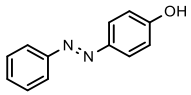	J07	4-Ethylphenol (123-07-9)	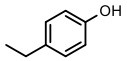	K02	6-Hydroxybenzo[d][1,3]oxathiol-2-one (4991-65-5)	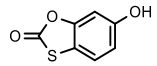
J01	4-Methoxyphenol (150-76-5)	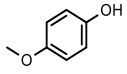	J08	3-Hydroxy-4,5-dimethoxybenzaldehyde (29865-90-5)	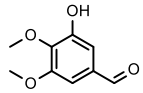	K03	9H-Carbazol-4-ol (52602-39-8)	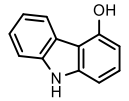

No.	Compound Name (CAS Number)	Structure	No.	Compound Name (CAS Number)	Structure	No.	Compound Name (CAS Number)	Structure
K04	4-(Methylthio)phenol (1073-72-9)	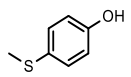	K11	2-(1H-Pyrazol-3-yl)phenol (34810-67-8)	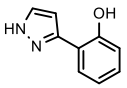	L06	3,5-Difluorophenol (2713-34-0)	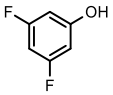
K05	5-Hydroxy-L-tryptophan (4350-09-8)	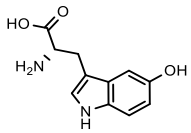	K12	Benzo[d]thiazol-6-ol (13599-84-3)	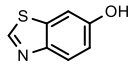	L07	3-Amino-4-fluorophenol (62257-16-3)	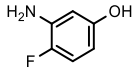
K06	5-Bromo-2-fluorophenol (112204-58-7)	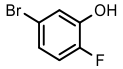	L01	2-Methyl-1H-indol-5-ol (13314-85-7)	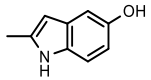	L08	2-Aminobenzo[d]thiazol-6-ol (26278-79-5)	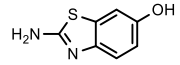
K07	7-Hydroxyquinolin-2(1H)-one (70500-72-0)	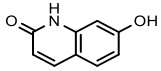	L02	4-(Pyridin-2-yl)phenol (51035-40-6)	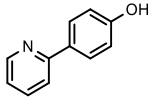	L09	3-(tert-Butyl)phenol (585-34-2)	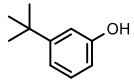
K08	4-Fluoro-2-methyl-1H-indol-5-ol (288385-88-6)	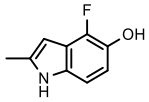	L03	6-Hydroxy-4-methyl-2H-chromen-2-one (2373-31-1)	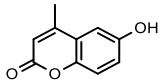	L10	4-Isopropylphenol (99-89-8)	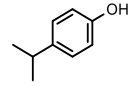
K09	(4-Hydroxyphenyl)boronic acid (71597-85-8)	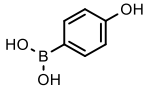	L04	3-(Hydroxymethyl)phenol (620-24-6)	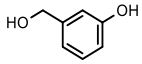	L11	2,3-Difluorophenol (6418-38-8)	
K10	6-Hydroxyquinolin-2(1H)-one (19315-93-6)	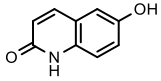	L05	6-Hydroxy-2H-chromen-2-one (6093-68-1)	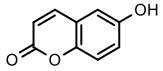	L12	4-(tert-Pentyl)phenol (80-46-6)	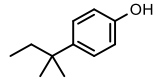

No.	Compound Name (CAS Number)	Structure	No.	Compound Name (CAS Number)	Structure	No.	Compound Name (CAS Number)	Structure
M01	2-Amino-4-chlorophenol (95-85-2)	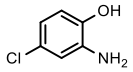	M08	2,4,6-Trimethylphenol (527-60-6)	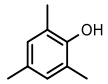	N03	1-(4-Hydroxyphenyl) propan-1-one (70-70-2)	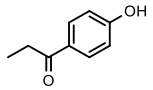
M02	2-(4-Hydroxyphenyl) acetonitrile (14191-95-8)	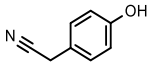	M09	3,4-Dimethylphenol (95-65-8)	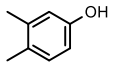	N04	2-Phenylphenol (90-43-7)	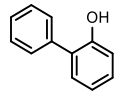
M03	4-((Trifluoromethyl) thio)phenol (461-84-7)	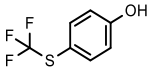	M10	2,6-Dichlorophenol (87-65-0)		N05	2-Methyl-3-nitrophenol (5460-31-1)	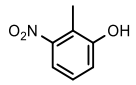
M04	3-Fluoro-4-methoxyphenol (452-11-9)	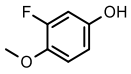	M11	2,4-Dichlorophenol (120-83-2)	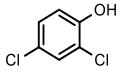	N06	2-Nitrophenol (88-75-5)	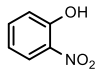
M05	2-Fluoro-5-hydroxybenzonitrile (104798-53-0)	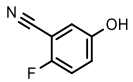	M12	3,4-Dichlorophenol (95-77-2)	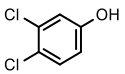	N07	1-(4-Hydroxyphenyl) ethan-1-one (99-93-4)	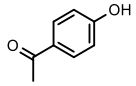
M06	3-Fluoro-5-hydroxybenzonitrile (473923-95-4)	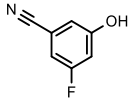	N01	2,4,5-Trichlorophenol (95-95-4)	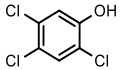	N08	2-Hydroxy-1-naphthaldehyde (708-06-5)	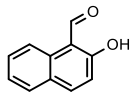
M07	4-Chloro-2-methylphenol (1570-64-5)	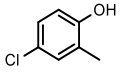	N02	1-Bromonaphthalen-2-ol (573-97-7)	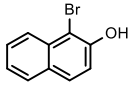	N09	3'-Hydroxyacetophenone (121-71-1)	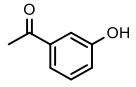

No.	Compound Name (CAS Number)	Structure	No.	Compound Name (CAS Number)	Structure	No.	Compound Name (CAS Number)	Structure
N10	4-(Hexyloxy)phenol (18979-55-0)	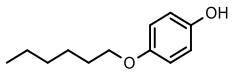	O05	2,3-Dimethylphenol (526-75-0)	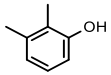	O12	3-(Trifluoromethyl)phenol (98-17-9)	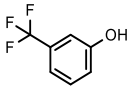
N11	3-Aminonaphthalen-2-ol (5417-63-0)	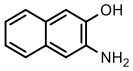	O06	2,5-Dimethylphenol (95-87-4)	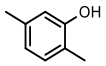	P01	4-Allyl-2-methoxyphenol (97-53-0)	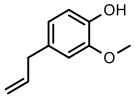
N12	1-(4-Hydroxy-2-methoxyphenyl) ethan-1-one (493-33-4)	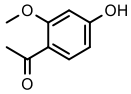	O07	1-(4-Hydroxy-3-methoxyphenyl)ethan-1-one (498-02-2)	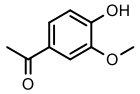	P02	Ethyl 2-hydroxybenzoate (118-61-6)	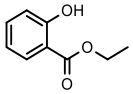
O01	2,4,6-Triiodophenol (609-23-4)	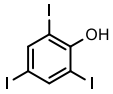	O08	2-Methylquinolin-8-ol (826-81-3)	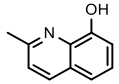	P03	3-(Trifluoromethoxy)phenol (827-99-6)	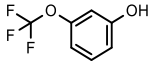
O02	5-Fluoro-2-nitrophenol (446-36-6)	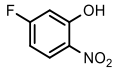	O09	2-Ethyl-6-methylphenol (1687-64-5)	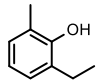	P04	2-(Methylthio)phenol (1073-29-6)	
O03	3-Hydroxybenzonitrile (873-62-1)	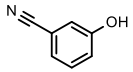	O10	2,2-Dimethyl-2,3-dihydrobenzofuran-7-ol (1563-38-8)	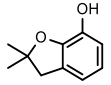	P05	3-Fluoro-4-methylphenol (452-78-8)	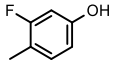
O04	2-Hydroxy-4,6-dimethoxybenzaldehyde (708-76-9)	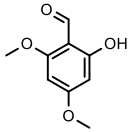	O11	2-Bromo-4-methylphenol (6627-55-0)	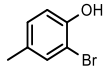	P06	Ethyl 2-hydroxy-5-methoxybenzoate (22775-40-2)	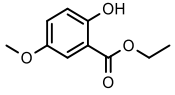

No.	Compound Name (CAS Number)	Structure	No.	Compound Name (CAS Number)	Structure	No.	Compound Name (CAS Number)	Structure
P07	4-Propylphenol (645-56-7)	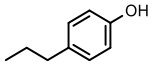	Q01	p-Cresol (106-44-5)	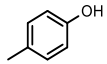	Q07	4-Chlorophenol (106-48-9)	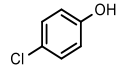
P08	3-Hydroxyphenyl acetate (102-29-4)	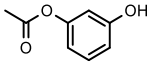	Q02	Phenol (108-95-2)		Q08	4-Bromophenol (106-41-2)	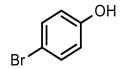
P09	2,4-Dimethylphenol (105-67-9)	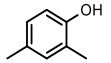	Q03	2-Hydroxybenzaldehyde (90-02-8)		Q09	2-Isopropylphenol (88-69-7)	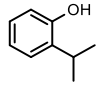
P10	3,4-Dihydroxybenzaldehyde (139-85-5)	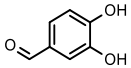	Q04	3-(1H-Pyrazol-5-yl)phenol (904665-39-0)	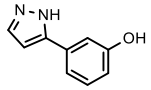	Q10	m-Cresol (108-39-4)	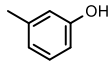
P11	4-Chloro-3,5-dimethylphenol (88-04-0)	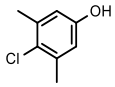	Q05	2,3,4,5,6-Pentamethylphenol (2819-86-5)	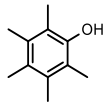	Q11	2,4-Dihydroxybenzaldehyde (95-01-2)	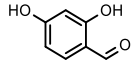
P12	Pyrocatechol (120-80-9)		Q06	o-Cresol (95-48-7)		Q12	Hydroquinone (123-31-9)	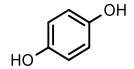

96-Well Microplate Preparation and ASCC Reaction Method

Preparation of Stock Solutions of Aryl Alcohols:
Approximately 20 mg of each aryl alcohol was transferred to an Eppendorf tube (203 unique aryl alcohols were used). The accurate weight of each was recorded and the solution volume needed to make a 0.15 M solution of each was calculated. The aryl alcohols were dissolved in either MeCN, DMSO, or a mixture thereof, depending on the compound's solubility. Refer to Table S2 above for details. Solutions were stored at 4 °C and re-prepared as necessary.

Preparation of 96-Well Microplates Containing Aryl Alcohols:
Using the stock solutions, aryl alcohols (3 μmol, ~20 μL) were added to a 350 μL polypropylene 96-well microplate, with each well containing a unique aryl alcohol. The plate was then placed in a vacuum oven (2 mbar, 50 ˚C, 3 h) to remove the solvent. The plate was subsequently sealed under nitrogen using a polyolefin sealing film and stored at 4 ˚C until required.

Model 96-Well Plate ASCC Reaction:

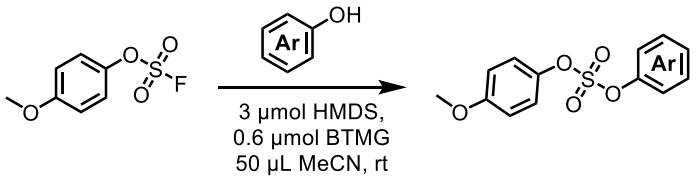

The 10 select aryl alcohol stock solutions (3 μmol, ~ 20 μL) were added to a 350 μL polypropylene 96-well microplate, with each well containing a unique aryl alcohol. The solvent was removed in a vacuum oven (2 mbar, 50 ˚C, 1 h). A stock solution containing 4-methoxyphenyl fluorosulfate (45 μmol), HMDS (45 μmol), and BTMG (9 μmol) in MeCN (750 μL) was prepared. After the 96-well plate had cooled to room temperature, 50 μL of this stock solution was added to each of the wells containing one of the 10 aryl alcohols and an empty control well – this delivered 3 μmol of 4-methoxyphenyl fluorosulfate, 3 μmol of HMDS and 0.6 μmol of BTMG to each well. The plate was sealed with a polyolefin film and agitated on an orbital plate shaker at 300 rpm for 24 h. After this time, the polyolefin sealing film was removed, and the plate was dried in a vacuum oven (2 mbar, 50 ˚C, 3 h). The reaction wells and control well were analyzed using the LCMS method detailed below.

Aryl alcohols used (see Table S2 for structures): **A02**, **A10**, **B08**, **C01**, **C07**, **C12**, **D05**, **D6**, **D8**, **D10**, **E1**, **E04**, **F10**, **G01**, **G10**, **G12**, **H03**, **H04**, **H09**, **H12**.

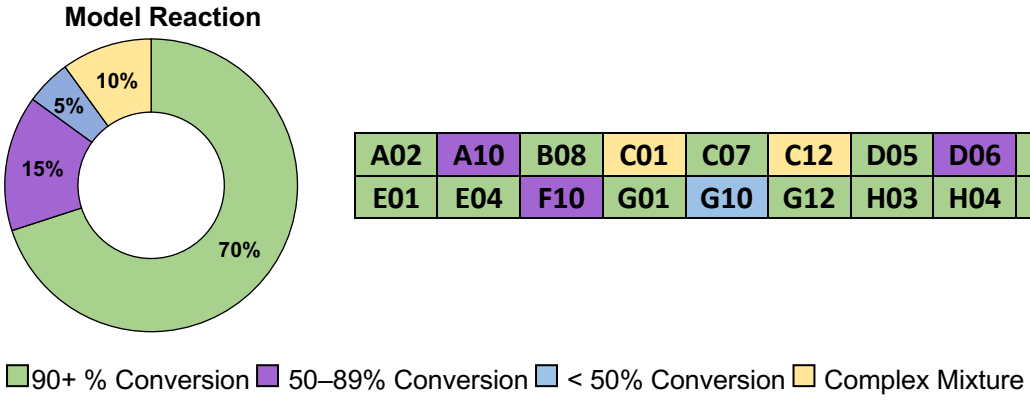

Figure S1. Results of the model 96-well plate ASCC reaction.

96-Well Plate SO_2F_2 ASCC Reaction:

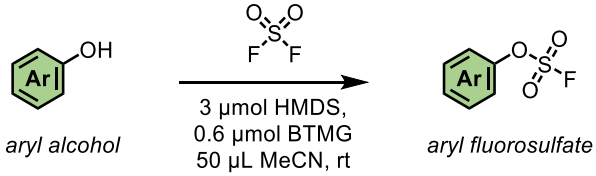

For each 96-well plate, HMDS (315 μmol) and BTMG (63 μmol) were dissolved in MeCN (5.25 mL), and the solution was stirred at room temperature for 15 minutes. This solution was sufficient for 96 reaction wells. The solution was transferred to a pipette reservoir, and, using a multichannel micropipette, 50 μL was dispensed into each well of a pre-prepared 96-well plate containing aryl alcohols (as described above) – this delivered 3 μmol of HMDS and 0.6 μmol of BTMG to each well. The plate was placed in a zip lock bag, and this was evacuated under vacuum, filled with SO_2F_2 gas, and left to agitate on

an orbital plate shaker at 300 rpm for 48 h. After shaking, the microplate was removed from the bag, and the solvent in each well was removed in a vacuum oven (2 mbar, 50 ˚C, 3 h). The progress of each reaction was determined using the below LCMS method.

96-Well Plate ASCC Reaction:

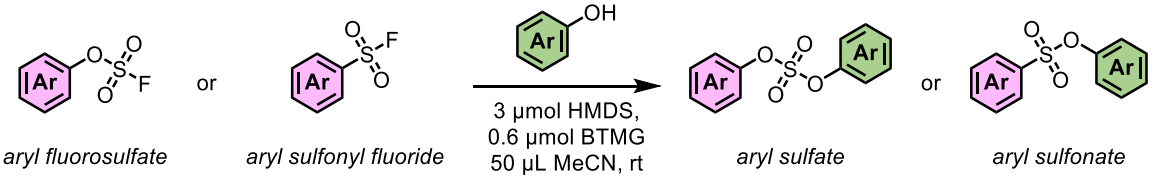

For each 96-well plate, the required fluorosulfate or sulfonyl fluoride (315 μmol) was dissolved in MeCN (5.25 mL). HMDS (315 μmol) and BTMG (63 μmol) were added, and the solution was stirred at room temperature for 15 minutes. This solution was sufficient for 96 reaction wells. The solution was transferred to a pipette reservoir, and, using a multichannel pipette, 50 μL was dispensed into each well of a pre-prepared 96-well plate containing aryl alcohols (as described above) – this delivered 3 μmol of the required fluorosulfate or sulfonyl fluoride, 3 μmol of HMDS, and 0.6 μmol of BTMG to each well. The plate was sealed with a polyolefin sealing film and agitated on an orbital plate shaker at 300 rpm for 24 h. After shaking, the polyolefin sealing film was removed, and the solvent in each well was removed in a vacuum oven (2 mbar, 50 ˚C, 3 h). The progress of each reaction was determined using the below LCMS method.

Analysis of ASCC Reactions

Preparation of Aryl Alcohol Standards for LCMS Analysis:
MeCN (200 μL) was used to resuspend the aryl alcohols in each well of a pre-prepared 96-well microplate. The plate was sealed with a polyolefin sealing film and placed on an orbital plate shaker for ~20 min at 600 rpm. Using a multichannel micropipette, a 50 μL aliquot from each well was transferred to an 800 μL 96-well microplate with each well prefilled with 450 μL of 1:1 MeCN:H_2O. The 800 μL plate was sealed with a slitted silicone microplate cover and the plate was agitated on an orbital plate shaker at 600 rpm for ~20 min to mix the samples prior to LCMS analysis thoroughly.

Preparation of Reaction Plates for LCMS Analysis:
MeCN (200 μL) was used to resuspend the reaction mixture of each well of 96-well microplate. The plate was sealed with a polyolefin sealing film and agitated on an orbital plate shaker for ~20 min at 600 rpm. Using a multichannel micropipette, a 50 μL aliquot of each reaction mixture was transferred to a 96-well microplate with each well prefilled with 450 μL of 1:1 MeCN:H_2O. The 800 μL plate was sealed with a slitted silicone microplate cover and the plate was agitated on an orbital plate shaker at 600 rpm for ~20 min to mix the samples prior to LCMS analysis thoroughly. The solvent (MeCN) was removed from the original reaction mixture plate in a vacuum oven (2 mbar, 50 ˚C, 3 h), and the plate was subsequently sealed using a polyolefin sealing film and stored at 4 ˚C until needed for biological testing.

LCMS Method:
Column: XTerra MS C18 Column (3.5 μm 4.6 x 100 mm)
Mobile phase A: 0.1% formic acid in H_2O
Mobile phase B: 0.1% formic acid in MeCN
UV absorption: 280 nm
Injection volume: 10 μL
Ionization source: APCI
Program:

Time (min)	% B	Flow (mL/min)
0	30	0.5
9	90	0.5
12	90	0.5
12.1	90	2
13.1	30	2
13.2	30	0.5
15	30	0.5

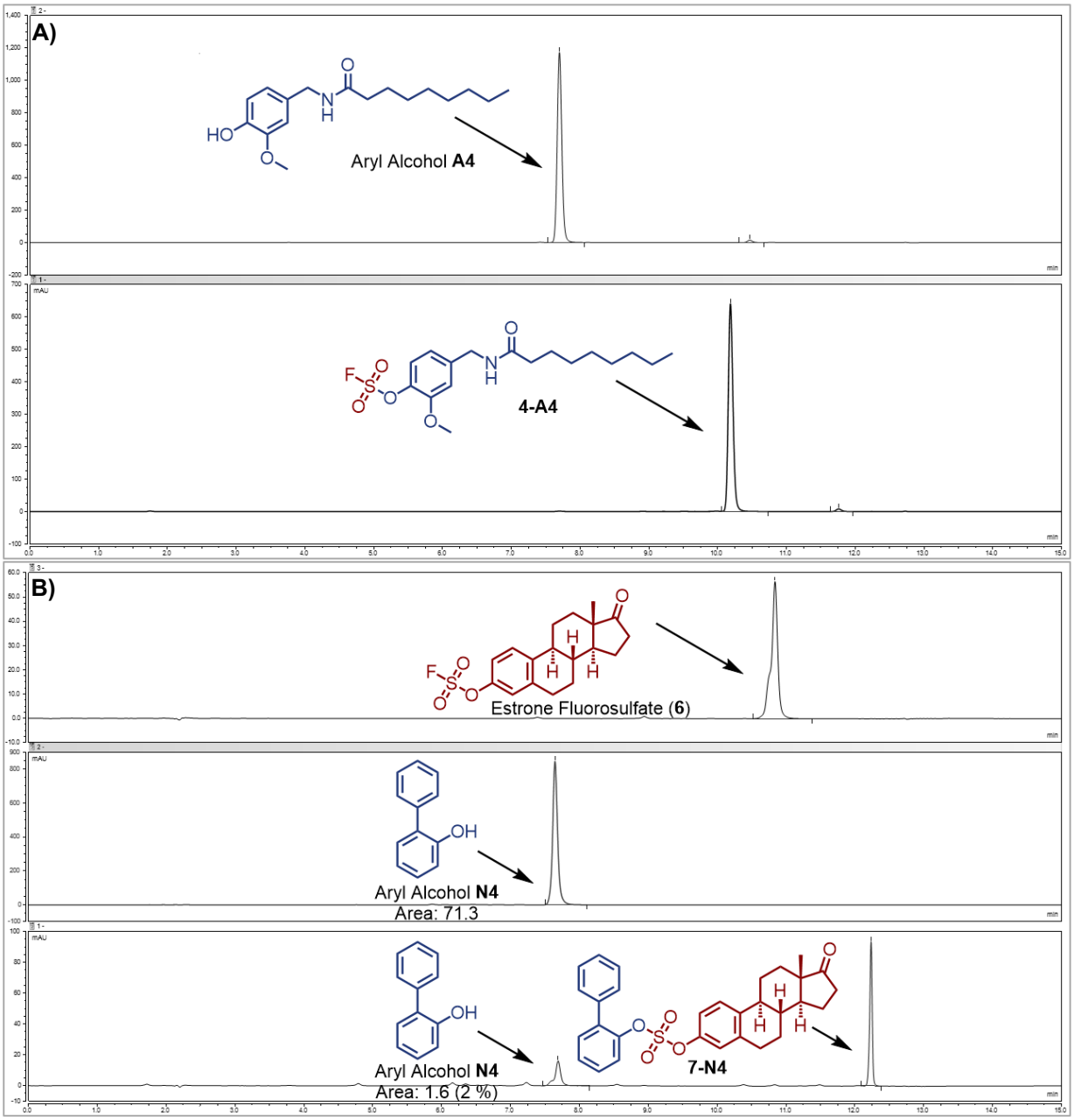

Figure S2: Example LC traces used to determine reaction completion using the above method. A) Top: LC trace of aryl alcohol **A4** standard; Bottom: Reaction mixture from 96-well plate ASCC reaction between sulfuryl fluoride and aryl alcohol A4 after shaking for 48 h. B) Top: LC trace of estrone fluorosulfate (**6**) standard; Middle: LC trace of aryl alcohol **N04** standard; Bottom: Reaction mixture from 96-well plate ASCC reaction between **6** and aryl alcohol **N04** after shaking for 24 h.

NMR Analysis:

In instances where the chemoselectivity of the ASCC reaction needs to be confirmed, NMR analysis can be used. To achieve this, the contents of a reaction well were dissolved in $CDCl_3$ (500 µL) and transferred directly to an NMR tube.

Example: The NMR analysis of the model reaction between aryl alcohol **D08** and 4-methoxyphenyl fluorosulfate is presented below. In this instance, the disappearance of the OH signal (blue box, Fig S3) of **D08** confirms the SuFEx reaction occurred at the aryl alcohol and not at the aniline (green box, Fig S3) functional group.

^{1}H NMR Spectrum for Aryl Alcohol **D08** (400 MHz, $CDCl_3$)

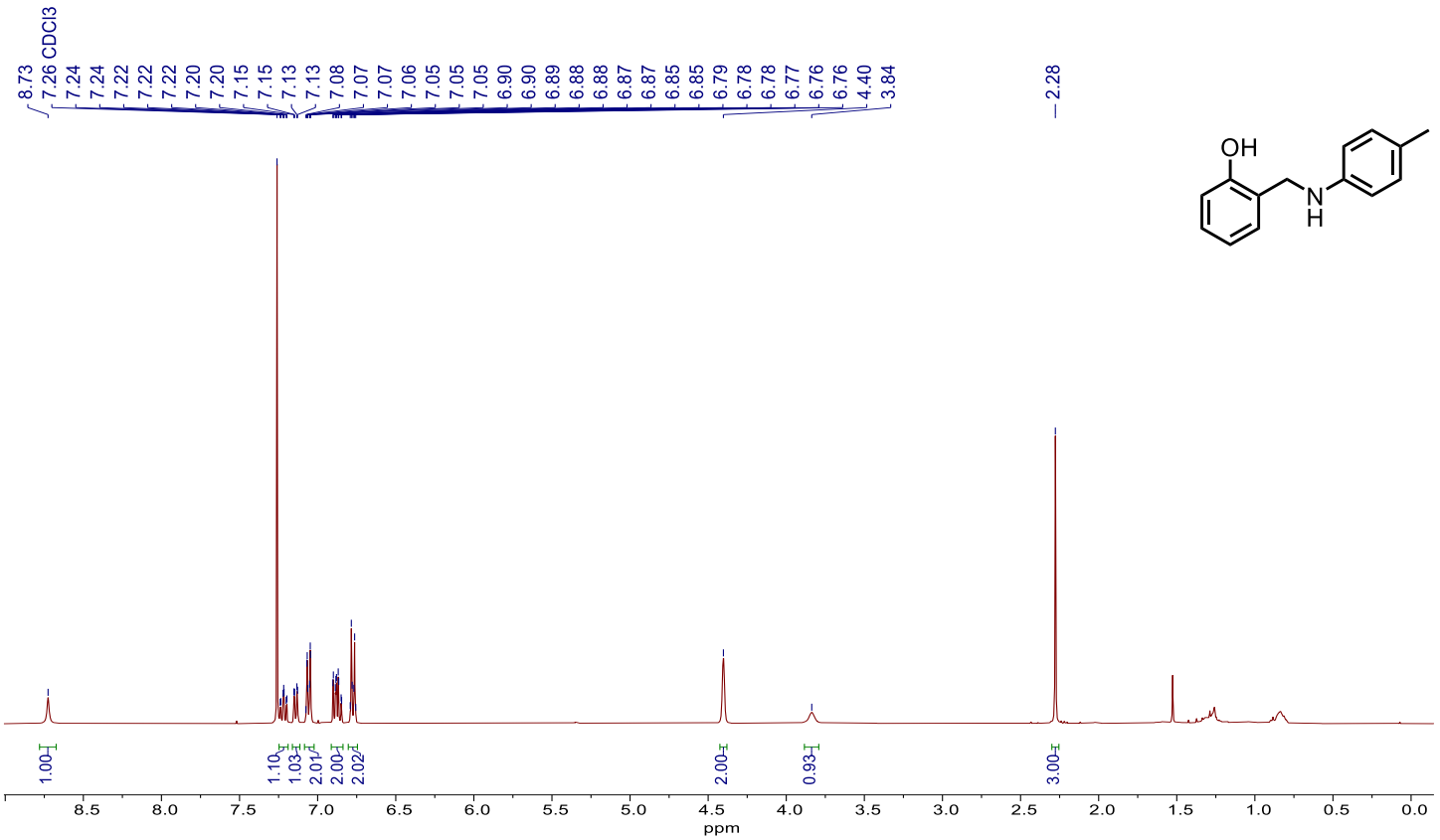

^{1}H NMR Spectrum for Compound **3-D08** (400 MHz, $CDCl_3$, unpurified)

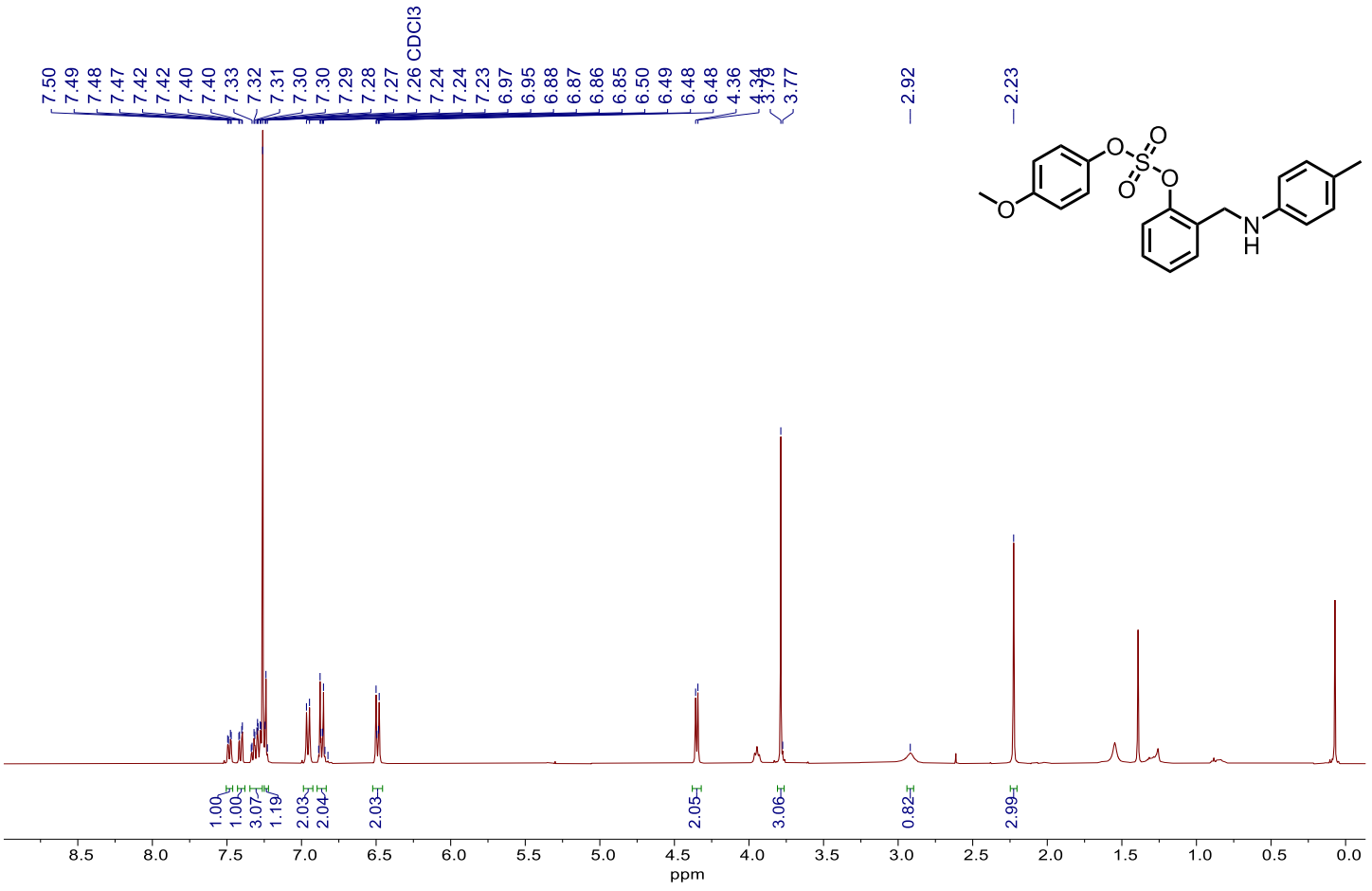

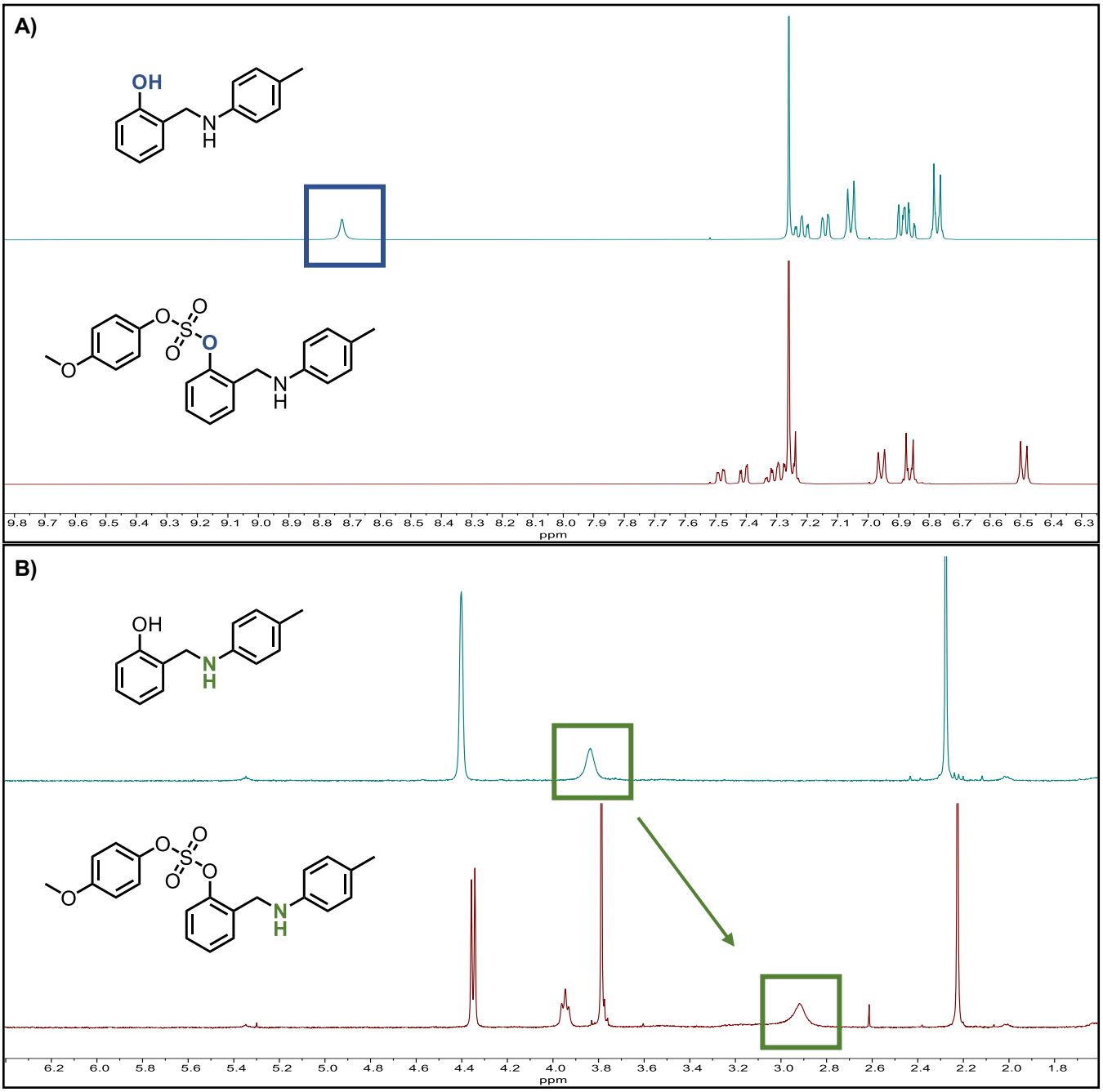

Figure S3. ^{1}H NMR comparison of aryl alcohol **D08** (top) and unpurified reaction mixture containing sulfate **3-D08** (bottom) in $CDCl_3$. A) 9.8–6.3 ppm region. B) 4.7–0.0 ppm region.

Thin-Layer Chromatography (TLC) Analysis:

For the 96-well plate ASCC reaction of 3,4,5-trimethoxybenzenesulfonyl fluoride (**13**), it was possible in most cases to monitor reaction completion by TLC. In cases where the aryl alcohol and product could not be seen under either 254 or 366 nm wavelengths, the LCMS method outlined above was used to monitor the reactions.

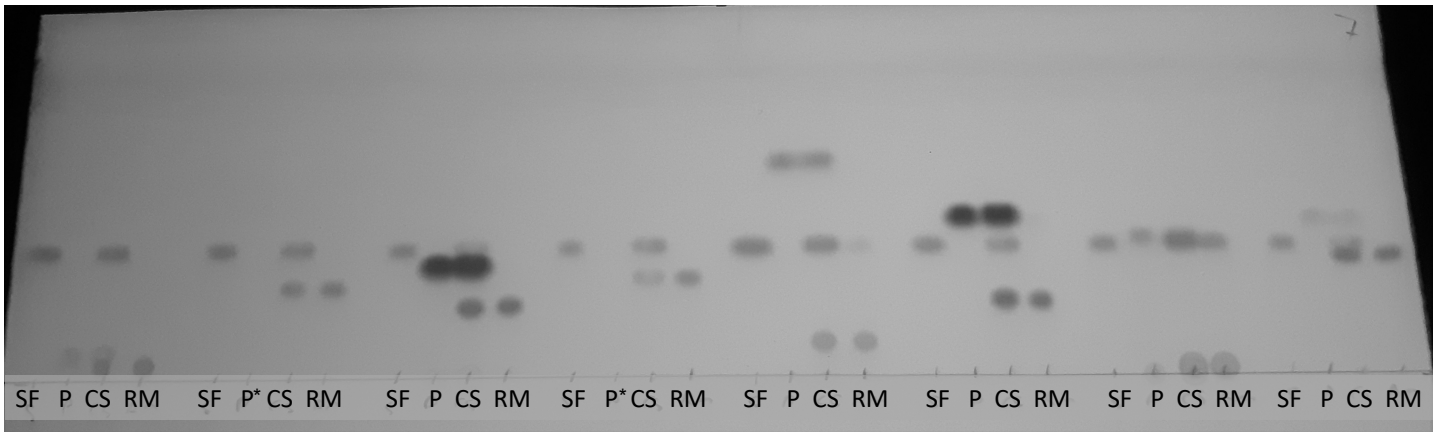

Figure S4: Representative TLC for reaction monitoring (observed under a Spectroline ENF-240C/FE UV lamp at 254 nm). Color removed to improve clarity. SF = sulfonyl fluoride **13**, P = aryl alcohol, CS = co-spot, RM = reaction mixture.
*Note: Two aryl alcohols are not visible under UV light (indicated with *), but a new product spot was identified.*

Synthesis of Starting Materials, Lead Compounds, and Control Compounds

Synthesis of *p*-methoxyphenyl fluorosulfate (**2**):

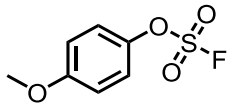

p-Methoxyphenol (300 mg, 2.42 mmol) was dissolved in MeCN (14 mL) in a round bottom flask. HMDS (506 µL, 2.42 mmol) was added, followed by BTMG (51 µL, 0.24 mmol). SO_2F_2 gas was bubbled through the solution for 5 minutes and then the reaction mixture was left stirring at room temperature under an atmosphere of SO_2F_2 until deemed complete by TLC analysis (30 min). After this time, the reaction mixture was concentrated under reduced pressure and purified by flash column chromatography. The title compound was isolated as a colorless oil (430 mg, 86%). **^{1}H NMR** (400 MHz, $CDCl_3$) δ 7.29–7.22 (m, 2H), 6.98–6.91 (m, 2H), 3.83 (s, 3H); **^{13}C NMR** (101 MHz, $CDCl_3$) δ 159.5, 143.8, 122.1, 115.3, 55.9; **^{19}F NMR** (376 MHz, $CDCl_3$) δ 36.4. Characterization data was in agreement with literature values[1].

Synthesis of estrone fluorosulfate (**6**):

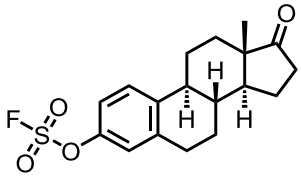

Estrone (1.00 g, 3.7 mmol) was dissolved in 4:1 MeCN:DMSO (25 mL) in a round-bottom flask. HMDS (0.77 mL, 3.7 mmol) was added, followed by BTMG (0.037 mL, 0.18 mmol). SO_2F_2 gas was bubbled through the solution for 2 minutes and then the reaction mixture was left stirring at room temperature under an atmosphere of SO_2F_2 until deemed complete by TLC analysis (17 h). After this time, H_2O was added to the reaction mixture causing a white solid to precipitate. The precipitate was filtered under vacuum and lyophilized to remove residual DMSO and H_2O. The title compound was isolated as a colorless solid (1.24 g, 95 %). **^{1}H NMR** (400 MHz, $CDCl_3$) δ 7.37 (d, *J* = 8.6 Hz, 1H), 7.11 (dd, *J* = 8.7, 2.7 Hz, 1H), 7.06 (d, *J* = 2.7 Hz, 1H), 2.95 (dd, *J* = 8.9, 4.4 Hz, 2H), 2.52 (dd, *J* = 18.8, 8.7 Hz, 1H), 2.45–2.37 (m, 1H), 2.31 (td, *J* = 10.7, 4.3 Hz, 1H), 2.21–1.95 (m, 4H), 1.68–1.46 (m, 6H), 0.92 (s, 3H); **^{19}F NMR** (376 MHz, $CDCl_3$) δ 37.5. Characterization data was in agreement with literature values[2].

Synthesis of 5-(diethylamino)-2-formylphenyl ((8*R*,9*S*,13*S*,14*S*)-13-methyl-17-oxo-7,8,9,11,12,13,14,15,16,17-decahydro-6*H*-cyclopenta[a]phenanthren-3-yl) sulfate (**7-I02**):

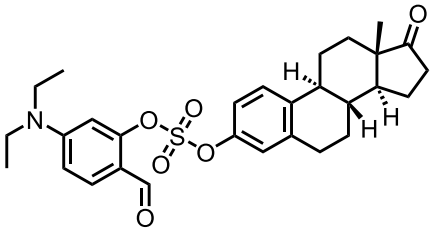

Estrone fluorosulfate (**6**) (100 mg, 0.284 mmol) and **I02** (55.1 mg, 0.285 mmol) were dissolved in MeCN (2 mL) in a round bottom flask. HMDS (77.0 µL, 0.368 mmol) and BTMG (14.8 µL, 0.073 mmol, 25 mol%) were added, and the reaction mixture was stirred at room temperature under an atmosphere of nitrogen until deemed complete by TLC analysis (24 h). The reaction mixture was concentrated under reduced pressure and purified by flash column chromatography. The title compound was isolated as a yellow oil (97.9 mg, 66%). **^{1}H NMR** (400 MHz, $CDCl_3$) δ 9.89 (s, 1H), 7.79 (d, J = 9.6 Hz, 1H), 7.32 (dd, J = 8.8, 1.1 Hz, 1H), 7.13 – 7.01 (m, 2H), 6.61 (tt, J = 4.8, 2.5 Hz, 2H), 3.41 (q, J = 7.1 Hz, 4H), 2.90 (dd, J = 9.0, 4.3 Hz, 2H), 2.56 – 2.45 (m, 1H), 2.44 – 2.35 (m, 1H), 2.28 (ddd, J = 11.9, 7.9, 3.0 Hz, 1H), 2.22 – 1.88 (m, 4H), 1.75 – 1.32 (m, 6H), 1.20 (t, J = 7.1 Hz, 6H), 0.91 (s, 3H); **^{13}C NMR** (101 MHz, $CDCl_3$) δ 185.4, 154.4, 153.1, 148.4, 139.9, 139.2, 130.7, 127.2, 121.2, 118.3, 116.5, 110.5, 103.1, 50.5, 48.0, 45.4, 44.2, 37.9, 36.7, 35.9, 31.6, 29.5, 26.2, 25.8, 21.7, 13.9, 12.4; **HRMS** (ESI): m/z calc'd for $C_{29}H_{35}NO_6S$ $[M+H]^+$: 526.2258, found: 526.2258; **IR** ν_{max} (ATR)/cm^{-1} 2972, 2931, 2865, 2766, 1735, 1674, 1602, 1530, 1490, 1473, 1454, 1399, 1380, 1355, 1293, 1263, 1213, 1194, 1171, 1143, 1132, 1075, 1007, 964, 932, 920, 881, 838, 825, 772, 729, 704, 689, 662, 648, 633, 580, 563, 530, 464.

Synthesis of 5-formyl-2,3-dimethoxyphenyl ((8*R*,9*S*,13*S*,14*S*)-13-methyl-17-oxo-7,8,9,11,12,13,14,15,16,17-decahydro-6*H*-cyclopenta[a]phenanthren-3-yl) sulfate (**7-J08**):

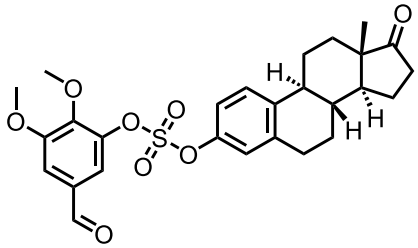

Estrone fluorosulfate (**6**) (101 mg, 0.287 mmol) and **J08** (52.3 mg, 0.287 mmol) were dissolved in MeCN (2 mL) in a round bottom flask. HMDS (77.0 µL, 0.368 mmol) and BTMG (14.8 µL, 0.073 mmol, 25 mol%) were added, and the reaction mixture was stirred at room temperature under an atmosphere of nitrogen until deemed complete by TLC analysis (24 h). The reaction mixture was concentrated under reduced pressure, dissolved in CH_2Cl_2, and passed through a short plug of silica to purify. The title compound was isolated as a colorless solid (130.1 mg, 88%). **m.p.** 57–59 °C; **^{1}H NMR** (400 MHz, $CDCl_3$) δ 9.83 (s, 1H), 7.42 (d, *J* = 1.8 Hz, 1H), 7.38 (d, *J* = 1.8 Hz, 1H), 7.35 (d, *J* = 8.6 Hz, 1H), 7.18 (dd, *J* = 8.6, 2.7 Hz, 1H), 7.14 (d, *J* = 2.6 Hz, 1H), 3.99 (s, 3H), 3.96 (s, 3H), 2.94 (dd, J = 9.0, 4.3 Hz, 2H), 2.52 (dd, J = 18.8, 8.6 Hz, 1H), 2.45 – 2.37 (m, 1H), 2.31 (td, J = 10.8, 4.2 Hz, 1H), 2.21 – 1.92 (m, 4H), 1.71 – 1.41 (m, 6H), 0.92 (s, 3H); **^{13}C NMR** (101 MHz, $CDCl_3$) δ 189.6, 154.5, 148.6, 147.2, 143.7, 139.8, 139.1, 131.5, 127.1, 121.3, 118.4, 117.9, 110.5, 61.7, 56.6, 50.6, 48.0, 44.3, 38.0, 35.9, 31.7, 29.6, 26.3, 25.9, 21.7, 14.3, 14.0; **HRMS** (ESI): m/z calc'd for $C_{27}H_{30}O_8S$ $[M+H]^+$: 515.1734, found: 515.1736; **IR** ν_{max} (ATR)/cm^{-1} 2932, 2859, 1735, 1695, 1600, 1582, 1504, 1492, 1455, 1413, 1323, 1301, 1246, 1209, 1194, 1181, 1130, 1074, 1055, 998, 931, 920, 899, 884, 858, 838, 800, 755, 729, 704, 648, 620, 588, 559, 546, 487.

Synthesis of (8*R*,9*S*,13*S*,14*S*)-13-methyl-17-oxo-7,8,9,11,12,13,14,15,16,17-decahydro-6*H*-cyclopenta[a]phenanthren-3-yl (2-oxo-1,2-dihydroquinolin-7-yl) sulfate (**7-K07**):

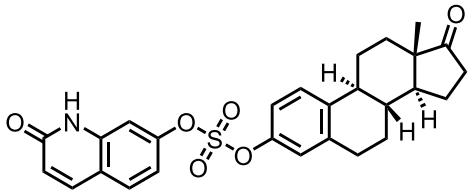

Estrone fluorosulfate (**6**) (103 mg, 0.292 mmol) and **K07** (48.4 mg, 0.300 mmol) were dissolved in MeCN (2 mL) in a round bottom flask. HMDS (77.0 µL, 0.368 mmol) and BTMG (14.8 µL, 0.073 mmol, 25 mol%) were added and the reaction mixture was stirred at room temperature under an atmosphere of nitrogen until deemed complete by TLC analysis (24 h). The reaction mixture was concentrated under reduced pressure, dissolved in ethyl acetate, and passed through a short plug of silica to purify. The title compound was isolated as a colorless solid (67.2 mg, 47%) **m.p.** decomposed at 160 °C; **^{1}H NMR** (400 MHz, $CDCl_3$) δ 7.81 (d, *J* = 9.5 Hz, 1H), 7.63 (d, *J* = 8.6 Hz, 1H), 7.43 (d, *J* = 2.3 Hz, 1H), 7.33 (d, *J* = 8.6 Hz, 1H), 7.24 (dd, *J* = 8.7, 2.3 Hz, 1H), 7.12 (dd, *J* = 8.6, 2.7 Hz, 1H), 7.08 (d, *J* = 2.7 Hz, 1H), 6.73 (d, *J* = 9.5 Hz, 1H), 2.98 – 2.86 (m, 2H), 2.51 (dd, *J* = 18.9, 8.7 Hz, 1H), 2.40 (dt, *J* = 12.7, 3.7 Hz, 1H), 2.29 (td, *J* = 10.9, 4.1 Hz, 1H), 2.22 – 1.91 (m, 4H), 1.70 – 1.38 (m, 6H), 0.91 (s, 3H); **^{13}C NMR** (101 MHz, $CDCl_3$) δ 164.4, 151.8, 148.5, 140.6, 139.8, 139.5, 139.2, 129.8, 127.2, 122.0, 121.1, 119.1, 118.2, 116.1, 108.7, 50.6, 48.0, 44.3, 38.0, 35.9, 31.7, 29.6, 26.3, 25.9, 21.7, 14.0; **HRMS** (ESI): m/z calc'd for $C_{27}H_{27}NO_6S$ $[M+H]^+$: 494.1632, found: 494.1632; **IR** ν_{max} (ATR)/cm^{-1} 2933, 1734, 1692, 1668, 1582, 1506, 1490, 1454, 1413, 1303, 1249, 1210, 1194, 1128, 1074, 1056, 989, 921, 873, 856, 839, 829, 792, 766, 728, 703, 637, 625, 587, 559, 538, 459.

Synthesis of 4-fluoro-2-methyl-1H-indol-5-yl ((8*R*,9*S*,13*S*,14*S*)-13-methyl-17-oxo-7,8,9,11,12,13,14,15,16,17-decahydro-6*H*-cyclopenta[a]phenanthren-3-yl) sulfate (**7-K08**):

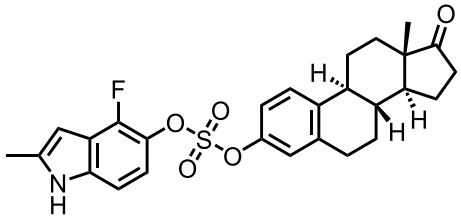

Estrone fluorosulfate (**6**) (101 mg, 0.292 mmol) and **K08** (48.4 mg, 0.287 mmol) were dissolved in MeCN (2 mL) in a round bottom flask. HMDS (77.0 µL, 0.368 mmol) and BTMG (14.8 µL, 0.073 mmol, 25 mol%) were added and the reaction mixture was stirred at room temperature under an atmosphere of nitrogen until deemed complete by TLC analysis (24 h). The reaction mixture was concentrated under reduced pressure, dissolved in ethyl acetate, and passed through a short plug of

silica to purify. The title compound was isolated as a colorless solid (67.2 mg, 47%) **m.p.** 149–151 °C; **^{1}H NMR** (400 MHz, $CDCl_3$) δ 8.18 (s, 1H), 7.32 (d, J = 8.6 Hz, 1H), 7.22 – 7.06 (m, 3H), 6.99 (d, J = 8.8 Hz, 1H), 6.33 (s, 1H), 2.92 (dd, J = 9.0, 4.3 Hz, 2H), 2.52 (dd, J = 18.9, 8.7 Hz, 1H), 2.44 (s, 4H), 2.29 (td, J = 10.7, 4.3 Hz, 1H), 2.22 – 1.91 (m, 4H), 1.71 – 1.37 (m, 6H), 0.92 (s, 3H); **^{13}C NMR** (101 MHz, $CDCl_3$) δ 148.8, 146.7 (d, J = 252.9 Hz), 139.4, 138.9, 137.3, 137.0 (d, J = 11.2 Hz), 130.3 (d, J = 11.3 Hz), 127.0, 121.2, 119.0 (d, J = 19.0 Hz), 118.3, 115.7, 106.3 (d, J = 3.8 Hz), 97.5, 60.5, 50.6, 48.1, 44.3, 38.0, 36.0, 31.7, 29.5, 26.3, 25.9, 21.7, 14.0, 13.8; **HRMS** (ESI): m/z calc'd for $C_{27}H_{28}FNO_5S$ $[M+H]^+$: 498.1745, found: 498.1747; **IR** ν_{max} (ATR)/cm^{-1} 3297, 2931, 2866, 1721, 1593, 1556, 1514, 1489, 1450, 1412, 1396, 1349, 1244, 1224, 1207, 1193, 1180, 1164, 1141, 1132, 1086, 1061, 1012, 998, 976, 933, 925, 900, 862, 833, 800, 781, 759, 736, 706, 672, 659, 616, 603, 588, 562, 538, 516, 499, 474.

Synthesis of 2-((4-((4-aminophenyl)sulfonyl)phenyl)amino)ethane-1-sulfonyl fluoride (**9**):

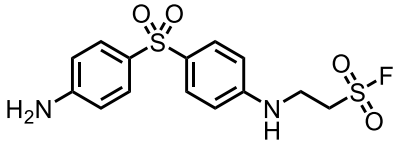

Dapsone (991 mg, 3.99 mmol) was dissolved in MeCN (8.0 mL). ESF (640 µL, 8.00 mmol) was added dropwise. The reaction mixture was warmed to 50 ˚C and stirred for 48 h. After this time, the reaction mixture was concentrated under reduced pressure and purified by flash column chromatography. The title compound was isolated as an off-white solid (500 mg, 35%). **m.p.** 150–152 °C; **^{1}H NMR** (400 MHz, DMSO-d_6) δ 7.63–7.56 (m, 2H), 7.56–7.48 (m, 2H), 6.91 (br s, 1H), 6.81–6.70 (m, 2H), 6.69–6.60 (m, 2H), 6.06 (br s, 2H), 4.16 (q, J = 6.1 Hz, 2H), 3.71 (q, J = 5.8 Hz, 2H); **^{13}C NMR** (101 MHz, DMSO-d_6) δ 152.8, 150.7, 129.6, 128.6, 128.4, 127.7, 112.8, 111.6, 49.3 (d, *J* = 11.3), 36.8; **^{19}F NMR** (376 MHz, DMSO-d_6) δ 57.9; **LCMS** (HESI): m/z calc'd for $C_{14}H_{15}FN_2O_4S_2$ $[M+H]^+$: 359.05, found: 359.12; **IR** ν_{max} (ATR)/cm^{-1} 3398, 1622, 1591, 1521, 1396, 1302, 1285, 1277, 1259, 1191, 1141, 1106, 1072, 824, 805 721, 687.

Synthesis of 3,4,5-trimethoxybenzenesulfonyl fluoride (**13**):

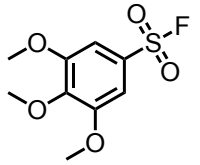

Potassium bifluoride (404 mg, 5.17 mmol) was dissolved in water (4.0 mL) in a round bottom flask. MeCN (8.0 mL) was added, followed by 3,4,5-trimethoxybenzenesulfonyl chloride[3] (600 mg, 2.25 mmol). The resultant biphasic mixture was stirred vigorously at room temperature until deemed complete by TLC analysis (6 h). After this time, the reaction mixture was diluted with ethyl acetate (50 mL) and washed with water (50 mL). The organic phase was dried over anhydrous $MgSO_4$, filtered, concentrated under reduced pressure, and purified by flash column chromatography. The title compound was isolated as a colorless solid (531 mg, 94%). **^{1}H NMR** (400 MHz, $CDCl_3$) δ 7.22 (s, 2H), 3.96 (s, 3H), 3.95 (s, 6H); **^{19}F NMR** (376 MHz, $CDCl_3$) δ 66.6. Characterization data was in agreement with literature values[4].

Synthesis of 2-methyl-*1H*-indol-5-yl 3,4,5-trimethoxybenzenesulfonate (**1-L01**):

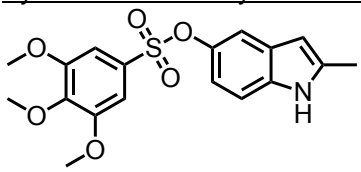

Sulfonyl fluoride **13** (173 mg, 0.693 mmol) and 5-hydroxy-2-methylindole (101 mg, 0.692 mmol) were dissolved in MeCN (3.5 mL) in a round bottom flask. HMDS (145 µL, 0.692 mmol) and BTMG (7.0 µL, 0.035 mmol, 5 mol%) were added and the reaction mixture was stirred at room temperature under an atmosphere of nitrogen until deemed complete by TLC analysis (1 h). The reaction mixture was concentrated under reduced pressure and purified by flash column chromatography (ethyl acetate and hexane). The title compound was isolated as a colorless solid (202.7 mg, 78%). **m.p.** 122–124 °C; **^{1}H NMR** (400 MHz, $CDCl_3$) δ 7.92 (s, 1H), 7.17–7.10 (m, 2H), 7.01 (s, 2H), 6.71 (dd, *J* = 8.7, 2.4 Hz, 1H), 6.16 (dt, *J* = 2.1, 1.0 Hz, 1H), 3.91 (s, 3H), 3.78 (s, 6H), 2.43 (s, 3H); **^{13}C NMR** (101 MHz, $CDCl_3$) δ 153.1, 143.6, 137.1, 134.5, 130.1, 129.2, 115.4, 113.0, 110.4, 106.1, 101.1, 77.2, 61.1, 56.5, 13.8; **HRMS** (ESI): m/z calc'd for $C_{18}H_{19}NO_6S$ $[M+H]^+$: 378.1006, found: 378.1005; **IR** ν_{max} (ATR)/cm^{-1} 3423, 2922, 1731, 1674, 1588, 1498, 1457, 1411, 1369, 1308, 1239, 1179, 1155, 1128, 1100, 1074, 986, 946, 918, 898, 870, 849, 815, 782, 728, 667, 616, 577, 545, 531, 496, 457.

Synthesis of 4-fluoro-2-methyl-1*H*-indol-5-yl 3,4,5-trimethoxybenzenesulfonate (**1-K08**):

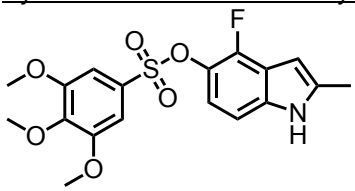

Sulfonyl fluoride **13** (305 mg, 1.22 mmol) and 4-fluoro-5-hydroxy-2-methylindole (201 mg, 1.22 mmol) were dissolved in MeCN (12.2 mL) in a round bottom flask. HMDS (256 µL, 1.22 mmol) and BTMG (12.3 µL, 0.061 mmol, 5 mol%) were added and the reaction mixture was stirred at room temperature under an atmosphere of nitrogen until deemed complete by TLC analysis (1 h). The reaction mixture was concentrated under reduced pressure and purified by flash column chromatography (ethyl acetate and hexane). The title compound was isolated as an off-white solid (250 mg, 52%). **m.p.** decomposed at 167 °C; **^{1}H NMR** (400 MHz, $CDCl_3$) δ 8.00 (s, 1H), 7.09 (s, 2H), 6.96 (d, *J* = 8.8 Hz, 1H), 6.89 (dd, *J* = 8.7, 6.7 Hz, 1H), 6.25 (dd, *J* = 2.3, 1.2 Hz, 1H), 3.92 (s, 3H), 3.81 (s, 6H), 2.43 (d, *J* = 0.9 Hz, 3H); **^{13}C NMR** (101 MHz, $CDCl_3$) δ 153.2, 142.9, 136.7, 129.9, 116.9, 106.1, 105.8, 105.8, 97.3, 77.2, 61.5, 56.5, 13.7, 2 x C not observed; **^{19}F NMR** (377 MHz, $CDCl_3$) δ -137.2; **HRMS** (ESI): m/z calc'd for $C_{18}H_{18}FNO_6S$ $[M+H]^+$: 396.0912, found: 396.0912; **IR** ν_{max} (ATR)/cm^{-1} 3424, 2919, 2216, 1728, 1686, 1588, 1497, 1457, 1410, 1369, 1349, 1308, 1239, 1197, 1178, 1155, 1127, 1100, 1076, 985, 947, 898, 870, 848, 821, 801, 781, 750, 727, 667, 609, 576, 546, 526, 495, 458.

Synthesis of 3,4,5-trimethoxyphenyl fluorosulfate (**S1**):

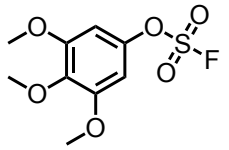

3,4,5-Trimethoxyphenol (500 mg, 2.71 mmol) was dissolved in MeCN (13.6 mL) in a round bottom flask. HMDS (568 µL, 2.71 mmol) was added followed by BTMG (27 µL, 0.136 mmol, 5 mol%). SO_2F_2 gas was bubbled through the solution for 5 minutes and then the reaction mixture was left stirring at room temperature under an atmosphere of SO_2F_2 until deemed complete by TLC analysis (24 h). The reaction mixture was concentrated under reduced pressure and purified by flash column chromatography (ethyl acetate and hexane). The title compound was isolated as a colorless solid (400.6 mg, 56%). **^{1}H NMR** (400 MHz, $CDCl_3$) δ 6.56 (s, 2 H), 3.88 (s, 6 H), 3.85 (s, 3 H); **^{13}C NMR** (101 MHz, $CDCl_3$) 154.0, 146.0, 138.1, 98.7, 61.2, 56.6; **^{19}F NMR** (376 MHz, $CDCl_3$) δ 37.2. Characterization data was in agreement with literature values[5].

Synthesis of 2-methyl-*1H*-indol-5-yl (3,4,5-trimethoxyphenyl) sulfate (**14-L01**):

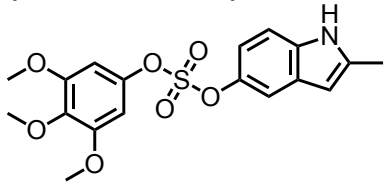

Fluorosulfate **S1** (53.2 mg, 0.20 mmol) and 5-hydroxy-2-methylindole (29.4 mg, 0.20 mmol) were dissolved in MeCN (1 mL). HMDS (41.92 µL, 0.20 mmol) and BTMG (2.02 µL, 0.01 mmol, 20 mol%) were added, and the reaction mixture was stirred at room temperature until deemed complete by TLC analysis (1 h). The reaction mixture was concentrated under reduced pressure and purified by flash column chromatography (ethyl acetate and hexane). The title compound was isolated as an off-white solid (41.7 mg, 53%). **m.p.** 99–101 °C; **^{1}H NMR** (400 MHz, $CDCl_3$) δ 8.11 (s, 1H), 7.47 (d, *J* = 2.4 Hz, 1H), 7.26–7.24 (m, 1H), 7.06 (dd, *J* = 8.8, 2.4 Hz3 1H), 6.48 (s, 2H), 6.24 (br s, 1H), 3.82 (s, 3H), 3.76 (s, 6H), 2.44 (s, 3H); **^{13}C NMR** (101 MHz, $CDCl_3$) δ 153.7, 146.6, 144.5, 137.8, 137.0, 134.8, 129.4, 114.3, 112.1, 111.0, 101.2, 99.0, 61.1, 56.3, 13.9; **HRMS** (ESI): m/z calc'd for $C_{18}H_{19}NO_7S$ $[M+H]^+$: 394.0955, found: 394.0957; **IR** ν_{max} (ATR)/cm^{-1} 3346, 2919, 1722, 1611, 1588, 1558, 1500, 1468, 1451, 1408, 1385, 1369, 1313, 1226, 1200, 1154, 1125, 1103, 997, 982, 945, 885, 871, 846, 823, 814, 788, 729, 665, 654, 596, 556, 547, 519, 491, 456.

Synthesis of 4-fluoro-2-methyl-*1H*-indol-5-yl (3,4,5-trimethoxyphenyl) sulfate (**14-K08**):

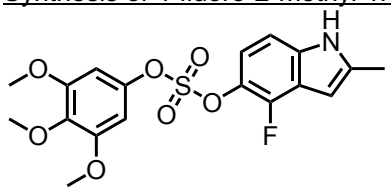

Fluorosulfate **S1** (53.2 mg, 0.20 mmol) and 4-fluoro-5-hydroxy-2-methylindole (33.0 mg, 0.20 mmol) were dissolved in MeCN (1 mL). HMDS (41.92 µL, 0.20 mmol) and BTMG (2.02 µL, 0.01 mmol, 20 mol%) were added, and the reaction mixture was stirred at room temperature until deemed complete by TLC analysis (1 h). The reaction mixture was concentrated under reduced pressure and purified by flash column chromatography (ethyl acetate and hexane). The title compound was isolated as a colorless solid (21.1 mg, 26%). **m.p.** 96–98 °C; **^{1}H NMR** (400 MHz, $CDCl_3$) δ 8.21 (s, 1H), 7.10 (dd, *J* = 8.8, 6.9 Hz, 1H), 7.01 (dt, *J* = 8.8, 0.8 Hz, 1H), 6.61 (s, 2H), 6.34 (dt, *J* = 2.2, 1.0 Hz, 1H), 3.82 (d, *J* = 6.5 Hz, 9H), 2.44 (d, *J* = 1.1 Hz, 3H); **^{13}C NMR** (101 MHz, $CDCl_3$) δ 153.7, 146.7, 146.6 (d, *J* = 252.6 Hz), 137.5, 137.0 (d, *J* = 11.5 Hz), 130.1 (d, *J* = 11.5 Hz), 129.2 (d, *J* = 131.8 Hz), 118.9 (d, *J* = 19.4), 115.6, 106.4 (d, *J* = 4.7 Hz), 99.0, 97.5, 61.1, 56.4, 13.8; **HRMS** (ESI): m/z calc'd for $C_{18}H_{19}NO_7S$ $[M+H]^+$: 412.0861, found: 412.0862; **IR** ν_{max} (ATR)/cm^{-1} 3288, 3138, 3118, 3010, 2924, 1719, 1615, 1595, 1552, 1519, 1501, 1467, 1433, 1410, 1353, 1332, 1311, 1261, 1246, 1227, 1198, 1175, 1167, 1147, 1120, 1065, 996, 971, 909, 862, 847, 825, 819, 775, 758, 738, 724, 684, 653, 607, 597, 566, 548, 523, 498, 469.

Synthesis of 2-methoxy-5-(2,3,4-trimethoxyphenyl)cyclohepta-2,4,6-trien-1-one (**MTC**):
The synthesis of MTC was accomplished by modifying the procedure from Potenziano *et al.*[6]

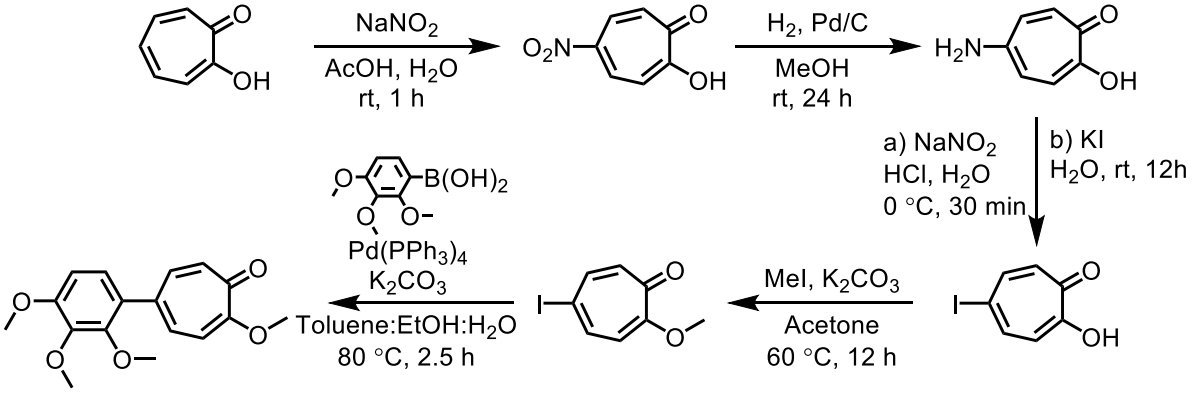

2-Hydroxy-5-nitrocyclohepta-2,4,6-trien-1-one (**S2**):

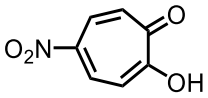

Tropolone (2.0 g, 5.31 mmol) was dissolved in warm water (15 mL) in a round bottom flask. A solution of sodium nitrite (2.2 g, 32 mmol) in water (40 mL) was then added dropwise. The reaction mixture was stirred at room temperature for 30 min, before glacial acetic acid (3.8 mL) was added. The reaction was stirred for an additional 30 min, during which time a tan precipitate formed. The precipitate was filtered under vacuum and washed with cold H_2O, affording the title compound as a brown solid (2.2 g, 82%). **m.p.** > 200 °C; **^{1}H NMR** (400 MHz, DMSO-d_6) δ 13.97 (s, 1H), 7.69 (d, *J* = 13.0 Hz, 1H), 7.21 (d, *J* = 12.8 Hz, 1H), 6.56 (dd, *J* = 13.0, 7.1 Hz, 2H); **^{13}C NMR** (101 MHz, DMSO-d_6) δ 185.6, 184.1, 152.2, 139.5, 130.2, 128.0, 124.1; **HRMS** (ESI): m/z calc'd for $C_7H_5NO_3Na$ $[M+Na]^+$ with loss of one oxygen: 174.0161, found 174.0161; **IR** ν_{max} (ATR)/cm^{-1} 3156, 3091, 3044, 1649, 1602, 1519, 1314, 1109, 1013, 845, 781, 635, 534.

5-Amino-2-hydroxycyclohepta-2,4,6-trien-1-one (**S3**):

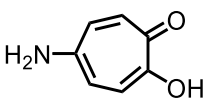

Nitro-tropolone **S2** (500 mg 3.0 mmol) was dissolved in MeOH (15 mL) in a round bottom flask. Pd/C (100 mg, 10 mol%, 20 wt%) was added. The reaction mixture was purged with H_2 gas and then stirred at room temperature until deemed complete by TLC analysis (24 h). The reaction mixture was then filtered through a short pad of Celite® and the filtrate was concentrated under reduced pressure. The title compound was isolated as a dark brown solid (403 mg, 98%). **m.p.** 163–165 °C; **^{1}H NMR**

(400 MHz, DMSO-d_6) δ 7.12 (d, *J* = 11.8 Hz, 2H), 6.80 (d, *J* = 11.8 Hz, 2H), 5.75 (s, 2H), 1 x OH not observed; **^{13}C NMR** (101 MHz, DMSO-d_6) δ 164.7, 151.7, 127.7, 120.8; **HRMS** (ESI): m/z calc'd for $C_7H_8NO_2$ $[M+H]^+$: 138.0549, found 138.0549; **IR** ν_{max} (ATR)/cm^{-1} 3420, 3336, 3201, 3059, 1662,1531, 1514, 1422, 1210, 854, 755, 704, 579.

2-Hydroxy-5-iodocyclohepta-2,4,6-trien-1-one (**S4**):

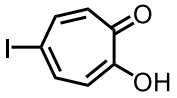

Hydrochloric acid (1.2 mL, fuming) and distilled H_2O (1.7 mL) were added to a round bottom flask containing 5-aminotropolone **S3** (300 mg, 2.19 mmol) and the resulting solution was cooled to 0 °C. A solution of sodium nitrite (166.2 mg, 2.41 mmol) in H_2O (1 mL) was added dropwise to this solution over 10 minutes and the reaction mixture was stirred for 30 min. After this time, a solution of potassium iodide (3.6 g, 21.9 mmol) in H_2O (3.5 mL) was added dropwise to the reaction mixture over 10 minutes. The reaction mixture was then allowed to warm to room temperature and stirred at room temperature until deemed complete by TLC analysis (12 h). The reaction mixture was then diluted with EtOAc (20 mL) and filtered. The organic layer of the filtrate was washed with brine (10 mL), dried over sodium sulfate, and concentrated under reduced pressure. The title compound was isolated as a dark brown solid (502 mg, 92%). **m.p.** 172–174 °C; **^{1}H NMR** (400 MHz, DMSO-d_6) δ 7.84 (d, *J* = 11.5 Hz, 2H), 6.82 (d, *J* = 11.5 Hz, 2H), 1 x OH not observed; **^{13}C NMR** (101 MHz, DMSO-d_6) δ 171.8, 145.6, 124.1, 95.5; **HRMS** (ESI): m/z calc'd for $C_7H_6IO_2$ $[M+H]^+$: 248.9407, found 248.9407; **IR** ν_{max} (ATR)/cm^{-1} 3218, 3061, 2921, 1698, 1585, 1519, 1445, 1417, 1355, 1272, 1188, 1063, 837, 646, 581, 562, 505.

5-Iodo-2-methoxycyclohepta-2,4,6-trien-1-one (**S5**):

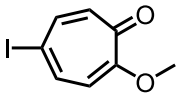

Iodo-tropolone **S4** (180 mg, 0.725 mmol) and K_2CO_3 (200 mg, 1.45 mmol) were dissolved in dry acetone (2 mL) in a round bottom flask. Iodomethane (85 mL, 1.45 mmol) was added to the solution and the resulting reaction mixture was stirred at 60 °C until deemed complete by TLC analysis (12 h). After this time, the reaction mixture was filtered through a short pad of Celite® and the filtrate was concentrated under reduced pressure. The title compound was isolated as a brown solid (150 mg, 78%). **m.p.** 123–125 °C. **^{1}H NMR** (400 MHz, DMSO-d_6) δ 7.77 (d, *J* = 10.4 Hz, 1H), 7.64 (d, *J* = 12.6 Hz, 1H), 6.66 (d, *J* = 12.6 Hz, 1H), 6.62 (d, *J* = 10.5 Hz, 1H), 3.82 (s, 3H); **^{13}C NMR** (101 MHz, DMSO-d_6) δ 178.7, 164.9, 144.8, 141.9, 135.6, 113.3, 95.5, 56.3. **HRMS** (ESI): m/z calc'd for $C_8H_8IO_2$ $[M+H]^+$: 262.9563, found 262.9563; **IR** ν_{max} (ATR)/cm^{-1} 2958, 2925, 2854, 1606, 1580, 1515, 1435, 1393, 1230, 826, 734, 666, 508.

2-Methoxy-5-(2,3,4-trimethoxyphenyl)cyclohepta-2,4,6-trien-1-one (**MTC**):

5-Iodo-2-methoxytropone **S5** (100 mg, 0.38 mmol), 2,3,4-trimethoxyphenylboronic acid (89 mg, 0.42 mmol), and K_2CO_3 (138.2 mg, 0.76 mmol) were dissolved in a mixture of toluene (2 mL), ethanol (1.2 mL), and H_2O (0.8 mL) in a round bottom flask under N_2 atmosphere. $Pd(PPh_3)_4$ (30 mg, 0.025 mmol) (freshly recrystallized from MeOH) was added to the solution and the resulting reaction mixture was stirred at 80 °C for 2.5 h. After this time, the reaction was diluted with water and extracted with EtOAc (3 x 10 mL). The combined organic layer was dried over sodium sulfate and concentrated under reduced pressure and the product was purified by flash column chromatography (ethyl acetate and hexane). The title compound was isolated as a brown solid (134 mg 85%). **m.p.** 116–118 °C; **^{1}H NMR** (400 MHz, $CDCl_3$) δ 7.44 (dd, J = 12.6, 1.9 Hz, 1H), 7.29–7.21 (m, 1H), 7.16 (dd, J = 10.4, 1.9 Hz, 1H), 6.96 (d, J = 8.7 Hz, 1H), 6.80 (d, J = 10.4 Hz, 1H), 6.72 (d, J = 8.6 Hz, 1H), 3.97 (s, 3H), 3.91 (s, 3H), 3.90 (s, 3H), 3.71 (s, 3H); **^{13}C NMR** (101 MHz, CDCl3) δ 180.2, 164.3, 154.0, 151.1, 142.6, 140.0, 138.9, 136.0, 132.7, 129.5, 124.5, 112.8, 107.6, 61.2, 61.2, 56.4, 56.2; **HRMS** (ESI): calc'd for $C_{17}H_{19}O_5$ $[M+H]^+$: 303.1227, found 303.1226; **IR** ν_{max} (ATR)/cm^{-1} 2999, 2953, 2933, 2835, 1624, 1580, 1489, 1448, 1244, 1075, 801, 699, 484. Characterization data was in agreement with literature values[6].

Stability tests of **1-K08**:

Procedure: Stability tests were conducted in a 1:9 mixture of DMSO (to aid solubility) and the appropriate aqueous phosphate buffer (i.e., pH = 4.8, 7.4, or 8.8) at a concentration of 5 mg/mL. Reactions were stirred vigorously at room temperature to ensure thorough mixing. Aliquots (50 µL) were taken immediately and after 3 h, 1 day, 2 days, 3 days, and 14 days, added to 650 µL of MeCN, filtered to remove solid material (i.e., phosphates), and analyzed by LCMS.

Results: No change to compound peak areas or the formation of new compound peaks were noted during the course of this experiment.

Stability tests of **7-J08**:

Procedure: Stability tests were conducted as described above. Aliquots (50 µL) were taken immediately and after 1 day, 2 days, 3 days, and 7 days, added to 650 µL of MeCN, filtered to remove solid material (i.e., phosphates), and analyzed by LCMS.

Results: No change to compound peak areas or the formation of new compound peaks were noted when **7-J08** was stirred in neutral or basic phosphate buffers. Under acidic conditions, **7-J08** decomposed; after 24 h, a 17% conversion to the hydrolyzed products was noted and after 7 days complete consumption of **7-J08** was observed.

Cell Viability Assays for Diaryl Sulfate Estrone Derivatives

Compounds: Two 96-well plates containing unpurified reaction mixtures or aryl alcohol controls were dissolved in DMSO at a concentration of 20 mM. These solutions were transferred from the 96-well plate to an Echo Qualified 384 well PP 2.0 Microplate (LABCYTE Cat # PP-0200) using an Eppendorf epMotion 96 dispenser (Eppendorf Cat # 5069000004). Compounds that had antiproliferative activity in the initial screen (below) were prepared on a larger scale and purified by flash column chromatography to afford analytically pure material.

Cell Culture: Authenticated MCF-7 cells, which had been tested for mycoplasma contamination, were obtained from the Tissue Culture Core Facility at Cold Spring Harbor Laboratory. These cells were maintained in DMEM with 10% FBS at 37 °C and 5% CO_2. The MCF-7 cells were harvested using TrypLE™ Express Enzyme (Gibco Cat # 12605010) once they had reached 90% confluence. The quantity of viable cells was measured using a DeNovix CellDrop Cell Counter (DeNovix Cat # CellDrop FL-UNLTD) with ViaStain™ AOPI Staining Solution (Nexcelom Cat # CS2-0106-5mL).

Viability Assay: The MCF-7 cells were seeded on a 1536 well plate (Greiner Bio-one Cat # 782092) in 7.5 µL of DMEM (10% FBS) using a Multidrop™ Combi Reagent Dispenser (Thermo Scientific Cat # 5840340) at a density of 250 cells per well. Compound derivatives or control aryl alcohols were acoustically dispensed into each 1536 well culture plate of MCF-7 cells using Echo 650 Liquid Handler (Backman Coulter Cat # 001-16079) 24 hours after seeding. After incubating for 72 hours, 2 µL of premixed CellTiter-Glo® Luminescent Cell Viability Assay reagent (Promega Cat # G7572) was added to each well. The total viability was measured via luminescence reading by an EnVision XCite 2105 Multimode Plate Reader (Perkin Elmer Cat # 2105-0010). Raw data of luminescence readings were analyzed using Microsoft Excel.

Results, Initial Screen: The cells were incubated with unpurified reaction mixtures or aryl alcohol controls at four different concentrations in triplicate (198.01 µM, 63.65 µM, 21.22 µM and 7.07 µM). This allowed for the calculation of IC_{50} ranges, but not absolute values due to the range and number of concentrations used. Of the compounds tested, 4 were found to be more potent than estrone fluorosulfate (**6**), and a further 8 compounds were found to have the same IC_{50} range as **6** (see Table S3)

Table S3: IC_{50} ranges determined from initial cell viability assays (values reported in µM). Unpurified reaction mixtures used.

Compound	IC_{50} Range	Aryl Alcohol	IC_{50} Range
7-I02	7–21	**I02**	>200
7-J08	7–21	**J08**	>200
7-K07	7–21	**K07**	>200
7-K08	7–21	**K08**	>200
7-I01	21–64	**I01**	>200
7-I03	21–64	**I03**	64–200
7-J07	21–64	**J07**	>200
7-K03	21–64	**K03**	64–200
7-K06	21–64	**K06**	>200
7-K10	21–64	**K10**	>200
7-L07	21–64	**L07**	64–200
7-N12	21–64	**N12**	64–200
Estrone FS (**6**)	21–64	n/a	n/a
7-I04	64–200	**I04**	>200
7-K11	64–200	**K11**	>200
7-L01	64–200	**L01**	>200
Estrone (**5**)	>200	n/a	n/a

Results, Accurate IC_{50} Determination: The cells were incubated with purified products at fourteen different concentrations in triplicate (198.02 µM, 99.01 µM, 46.20 µM, 26.40 µM, 13.20 µM, 6.60 µM, 3.30 µM, 1.52 µM, 792 nM, 396 nM, 198 nM, 99 nM, 46 nM, 26 nM). IC_{50} values were calculated using Prism. Of the compounds tested, all were found to be more potent than estrone fluorosulfate (**6**).

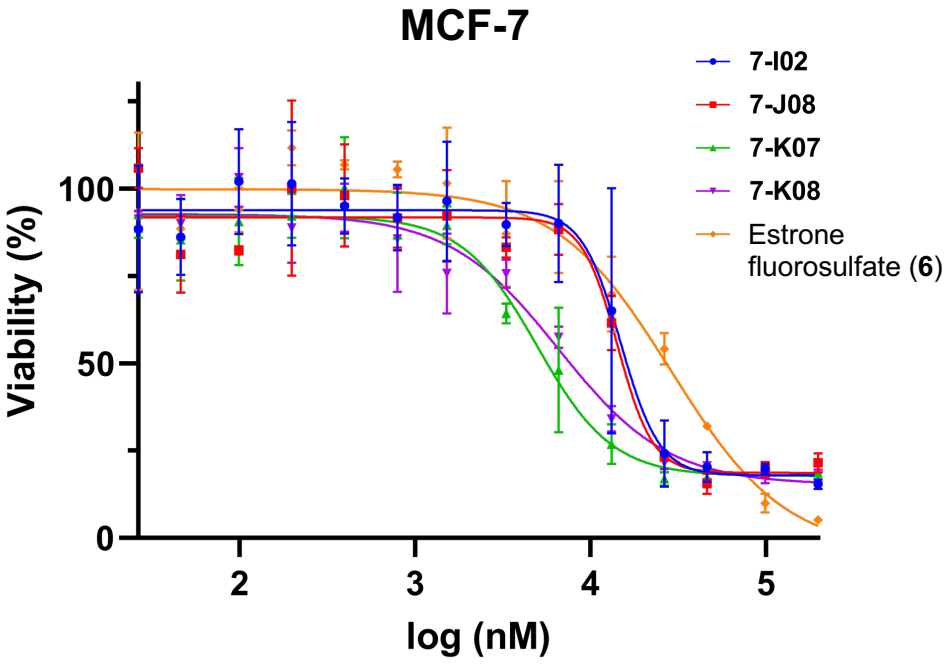

Compound	IC_{50} (µM)	95% CI	R^2
7-I02	14.9	12.647 to 17.899	0.9835
7-J08	14.3	10.824 to 18.904	0.9594
7-K07	5.0	3.894 to 6.356	0.9864
7-K08	6.6	4.527 to 9.628	0.9803
Estrone fluorosulfate (**6**)	28.7	17.527 to 83.415	0.9674

Figure S5: Dose-response curves of the purified hit sulfate diester estrone derivatives **7** and estrone fluorosulfate (**6**) against the MCF-7 breast cancer cell line. Data is the mean from N = 3 separate assays.

Human Estrogen Receptor Alpha Luciferase Reporter Assay

Protocol (Agonistic Effect): The "Human ERα Reporter Assay Kit" (INDIGO Biosciences, product #IB00401) was used to determine the agonistic effects of the novel estrone derivatives at the ERα. The assay was conducted based on the manufacturer's standard protocol. In short, stock solutions of each tested compound were prepared to 100 μM in DMSO. The receptor cells (with luciferase reporter gene functionally linked to an ERα-responsive promoter) were treated with the known agonist 17-β-estradiol (provided) and other compounds (**6**, **7-J08** and **7-K07**). The treated concentrations were from 100 nM to 6 pM [100 nM, 20 nM, 4 nM, 0.8 nM, 160 pM, 32 pM and 6 pM] [DMSO<0.2%] where n=1. After successful treatment, cells were incubated for 24 h at 37 °C, inside a humidified 5% CO_2 incubator. After 24 h of incubation, all media was discarded. The luciferase detection reagent was then added, and plates were allowed to rest for 5 min at room temperature. Finally, the luminescence signals from each well were quantified. The instrument (Molecular Device, SpectraMax i3x) was set to perform a single 5 sec "plate shake" prior to reading the first well. Read time was set to 140 mSec (0.14 sec) per well. The observed data was plotted using OriginPro 8.5 software using log10[Conc] as X-axis and luminescence response as Y-axis.

Results: The diaryl sulfate estrone derivatives **7-J08** and **7-K07** and estrone fluorosulfate (**6**) were found to have no significant agonistic effects at the ERα.

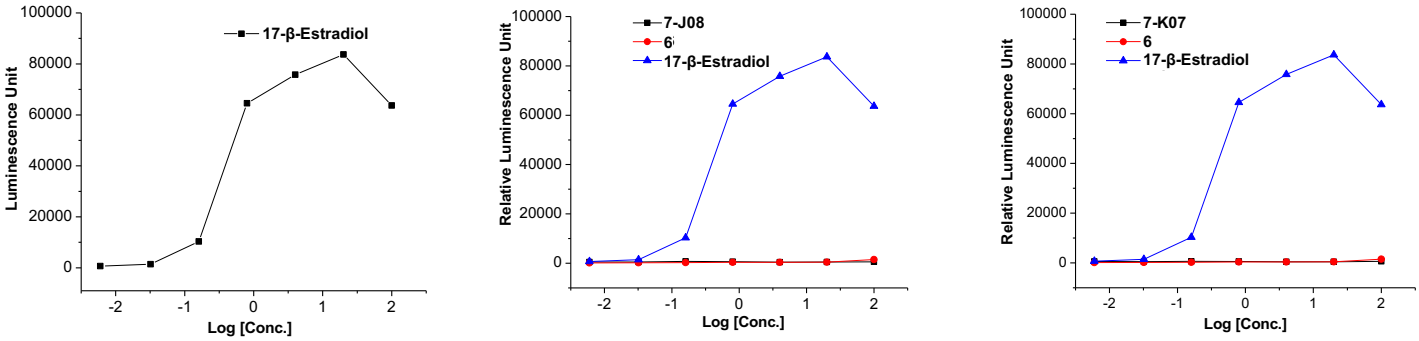

Figure S6: Agonistic effect of tested compounds against the ERα. An increase in relative luminescence indicates receptor agonism.

Protocol (Antagonistic Effect): The "Human ERα Reporter Assay Kit" (INDIGO Biosciences, product #IB00401) was used to determine the antagonistic effects of the novel estrone derivatives at the ERα. The assay was conducted based on the manufacturer's standard protocol. In short, stock solutions of each tested compound were prepared to 100 μM in DMSO. The antagonistic effect of each compound was measured by varying the concentration (above mentioned) of each test compound in the presence of 17-β-estradiol [1 nM] where n=3. After 24 h of incubation, all media was discarded. The luciferase detection reagent was then added, and plates were allowed to rest for 5 min at room temperature. Finally, the luminescence signals from each well were quantified. The instrument (Molecular Device, SpectraMax i3x) was set to perform a single 5 sec "plate shake" prior to reading the first well. Read time was set to 140 mSec (0.14 sec) per well. The observed data was plotted using OriginPro 8.5 software using concentration (nM) as X-axis and luminescence response as Y-axis. Plotted luminescence response (antagonist) is the averaged value of triplicated dataset and variability is plotted as standard error.

Results: The diaryl sulfate estrone derivative **7-J08** and estrone fluorosulfate (**6**) were found to show notable dose-dependent antagonistic effects at the ERα when delivered in the presence of 17-β-estradiol.

Molecular Modeling of Diaryl Sulfate Estrone Compounds

Computational methods: The structures of the estrogen receptor alpha (PDB ID = 1ERE) and the 17β-hydroxysteroid dehydrogenase 1 (PDB ID = 1FDT) were downloaded from the Protein Data Bank. The crystallized ligands were removed, and their empty binding sites were used as sites to dock our ligands. The side chains of the binding sites were locally minimized to accommodate our larger ligands. The docking was carried out using the ICM-Pro MolSoft suite (www.molsoft.com). The ligands were sketched in the LigEditor module and then converted into 3D. The docking was run using the default parameters with a docking effort of 10. The Radial topological convolutional neural net (RTCNN) scoring, which is independent of any molecular mechanics or physical energy terms is used as a measure of binding. The lower the RTCNN score the better the predicted ligand-receptor interaction.

Results (estrogen receptor alpha): The diaryl sulfate derivatives **7-I02**, **7-J08**, and **7-K07** were found to dock to the receptor binding site with lower RTCNN scores (-37.68 – -35.46) to estrone (-33.99). Estrone fluorosulfate (**6**) was found to bind with an intermediate RTCNN score of -35.51.

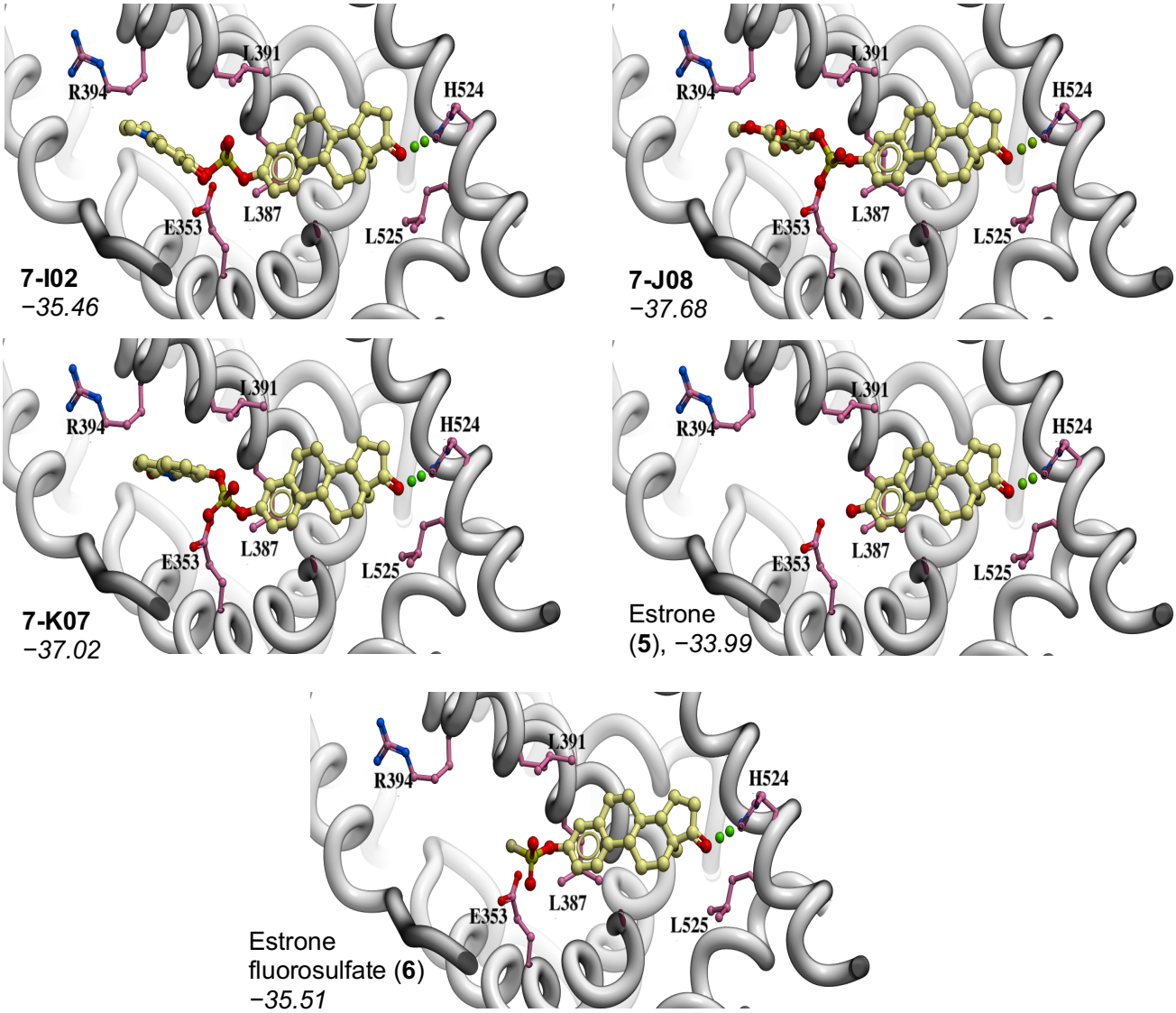

Figure S7: Computational modeling of estrone, estrone fluorosulfate, and the hit diaryl sulfate estrone derivatives with the structure of the estrogen receptor alpha (PDB = 1ERE). RTCNN scores are shown in italics.

Results (17β-hydroxysteroid dehydrogenase 1): The diaryl sulfate estrone derivatives **7-I02**, **7-J08**, and **7-K07** were found to bind to the enzyme active site with lower RTCNN scores (-42.14 – -38.41) than the known inhibitor STX1040 (-33.38). A similar binding orientation between the diaryl sulfate derivatives and STX1040 was observed.

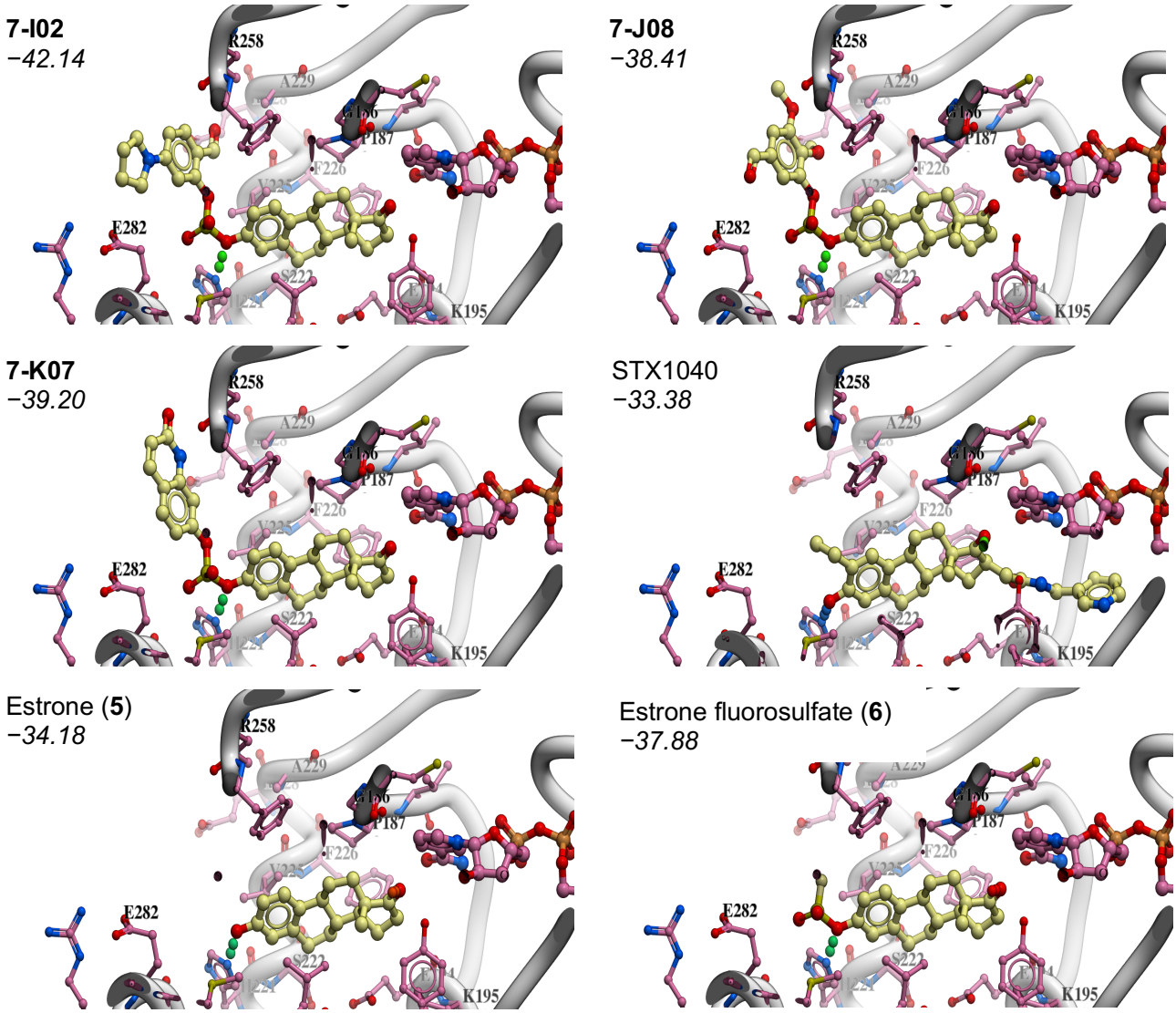

Figure S8: Computational modeling of estrone, estrone fluorosulfate, and the hit estrone diaryl sulfate derivatives with the structure of 17β-HSD1 (PDB = 1FDT). STX1040 included as a known inhibitor of 17β-HSD1. RTCNN scores are shown in italics.

Biological Evaluation of Dapsone Derivatives Against *Mycobacterium tuberculosis*

Compounds: Dapsone derivatives were provided in dry powder form in 96-well plates. Only compounds provided with a purity >50% as determined by LCMS analysis were evaluated (n=36).

Bacterial strains: Compounds were tested against the *M. tuberculosis* $mc^2$7000 Δ*pabC* strain previously described to be highly sensitive to anti-folates[7]. Drugs that were found to be active against $mc^2$7000 Δ*pabC* were also tested against a drug-resistant *M. tuberculosis* strain, 100x (mutation in *folP1,* specifically P55L).

Determination of Minimum Inhibitory Concentrations (MICs) against Mycobacterium tuberculosis*:* The activities of drugs against the *M. tuberculosis* $mc^2$7000 Δ*pabC* strain were tested using the pellet reading method in 96-well plates as previously described[7] with minor modifications. Briefly, a mid-logarithmic-phase culture of H37Rv (optical density at 600 nm [OD_{600}], approximately 0.5) was diluted Middlebrook 7H9 broth supplemented with 0.2% glycerol, 10% oleic acid-albumin-dextrose-catalase (OADC), 0.05% tyloxapol and 50 µg/mL pantothenate to an OD_{600} of 0.001 (approximately 3×10^5 CFU/mL). Bacteria (100 µL) were then dispensed in transparent round-bottom 96-well plates. Two-fold serial dilutions of each drug (resuspended in DMSO, stock concentration 400 µM) were prepared and added to the wells. Each plate further included dapsone as positive control and a negative control corresponding to culture medium without drug. The plates were incubated for 12 days at 37 °C at which point the plates were visually scanned for bacterial growth. When inhibition was observed, MICs were repeated using a 10 mM stock solution, and each of the compounds was diluted 16 times in a two-fold dilution. OD_{600} was used to determine the MIC_{90} (concentration of compound leading to 90% inhibition of bacterial growth). Relevant control fragments (i.e., the aryl alcohols used to prepare the compounds) were then tested.

Results: Among the 36 compounds tested, only two showed a MIC <4 µM during the initial screening phase: compounds **10-F01** and **10-F05**. Detailed MIC data for these compounds and the relevant controls against the *M. tuberculosis* strains are shown below.

Table S4: MIC values against *M. tuberculosis* (values reported in µM).

Compound	**Δ*pabC* (wildtype)**	**100x (*folP1* P55L)**
10-F01	1.56	25
F01	50	50–100
10-F05	6.25	100
F05	No effect at >100 µM	No effect at >100 µM
Dapsone (**8**)	0.5–1	50

Cell Viability Assays for MTA Compounds

Initial Compound Screen:

Compounds: 80 compounds, synthesized as outlined above, were prepared as 10 mM solutions in DMSO. Colchicine (**11**) was included as a positive control alongside sulfonyl fluoride **13**.

Cell culture: Cancer cell lines HCT-15 (colorectal cancer) and NCI-H460 (large cell lung cancer) were obtained from ATCC. Cells were cultured in RPMI medium (Thermo Fisher Scientific) supplemented with 10% (v/v) fetal bovine serum (PAA Laboratories, Australia), 100 U/mL penicillin, and 100 mg/mL streptomycin (Gibco), 2 mM L-Glutamine (Gibco) and maintained at 37 °C with 5% CO_2.

Viability assays: Briefly, cells were plated in white 96-well plates at 1000 cells/well then 4 h later treated with novel compounds. Cell viability was assessed after 72 h using the CellTiter-Glo (Promega) viability assay according to the manufacturer's instructions. Luminescence was measured on an Ensight Multimode plate reader, and results normalized to the highest % (v/v) of vehicle (DMSO). The IC_{50} values were determined using non-linear regression algorithms in Prism software (GraphPad) using the data from at least three separate assays.

An initial time-course experiment was performed on a subset of representative compounds to gauge their relative efficacy over time. Significant activity was observed in both cell lines at 48 h, and this increased further at 72 h. Accordingly, all subsequent assays were performed at 72 h.

Results: All compounds were initially screened in the cell viability assays at 1.5 μM. Those compounds that induced >50% reduction in cell viability were then re-tested in full 8-point titration to determine their IC_{50} values. In general, the compounds were more potent in the HCT-15 (multidrug-resistant) cell line compared to NCI-H460 cells. There were 8 compounds that were more potent than the reference compound, colchicine (**11**), in the HCT-15 cell line, with four of these being 4–10 fold more potent. The order of potency for the top 10 most active compounds on HCT-15 cells was identical between cell lines, though only the two most potent of these (**1-L01** and **1-K08**) were more active than **11** in the NCI-H460 cells. Only one compound (**1-K02**) was more active on NCI-H460 cells compared to HCT-15 cells.

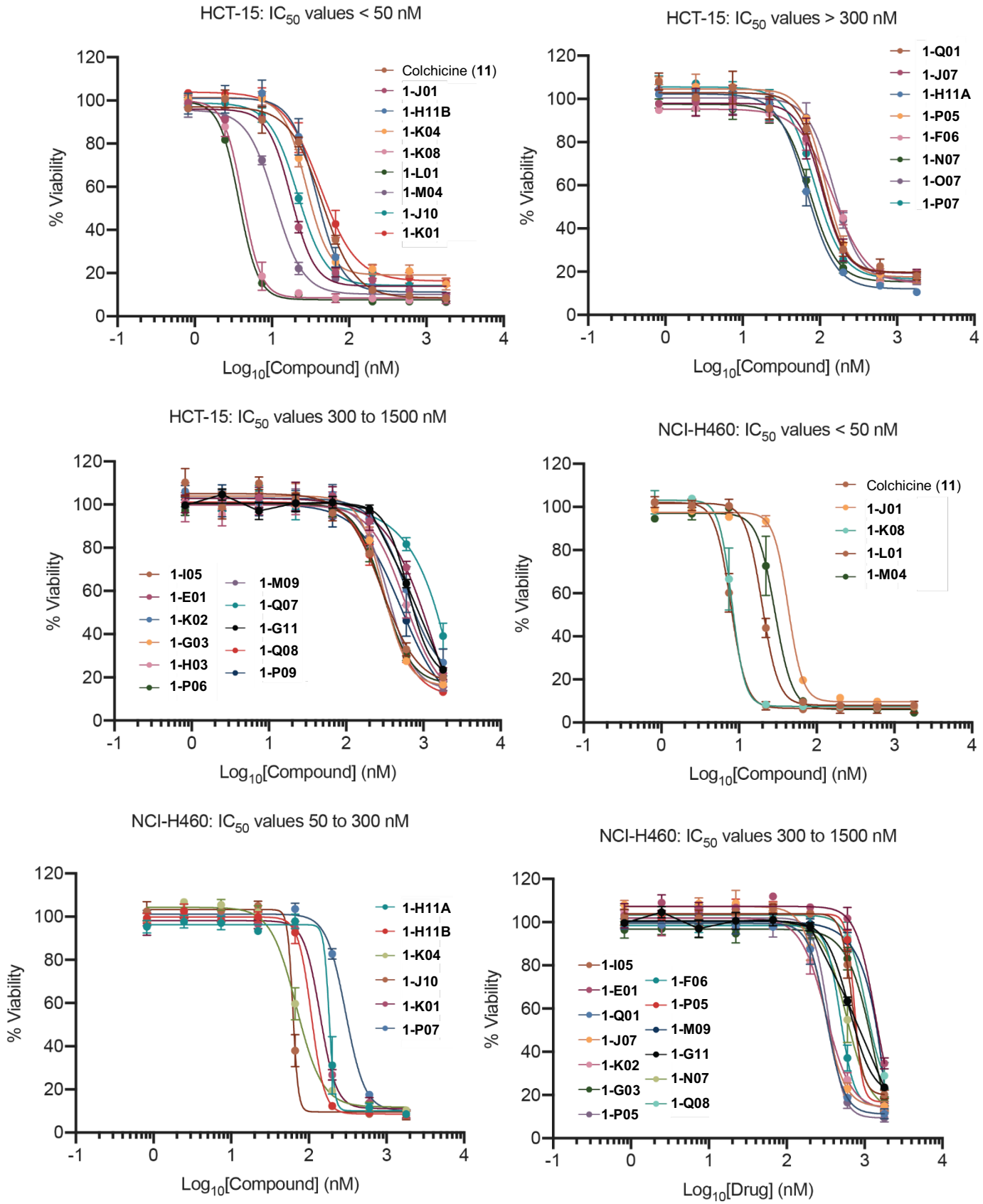

Figure S9: Dose-response curves of sulfonate-linked MTAs against HCT-15 and NCI-H460. Data is the mean ± standard deviation from n=3– 4 separate assays.

Table S5: IC_{50} values determined from initial cell viability assays (values reported in nM).

Compound	HCT-15	Std Dev	NCI-H460	Std Dev
Colchicine (**11**)	44.7	3.22	19.6	2.76
Sulfonyl fluoride **13**	>1500	N.D.	>1500	N.D.
1-L01	3.71	0.03	7.96	1.2
1-K08	4.16	0.73	8.34	1.62
1-M04	10.8	0.22	32.7	6.02
1-J01	17.9	0.72	44.2	5.19
1-J10	21.3	0.59	60.8	7.34
1-K04	28	3.21	69.8	13.62
1-H11B	37.4	10.22	123	41.6
1-K01	43.3	12.89	140	4.04
1-H11A	67.5	14.49	169	37.11
1-N07	74.1	9.28	613	173.4
1-P07	84.2	6.67	298	2.85
1-Q01	106	11.64	327	43.16
1-J07	108	29.46	302	28.58
1-P05	118	12.55	347	11.71
1-F06	148	16.81	487	111.08
1-O07	156	16.34	>1500	N.D.
1-I05	302	47.55	744	137.62
1-P06	303	55.49	999	180.01
1-G03	304	39.98	1130	297.62
1-Q08	318	53.41	910	230.41
1-M09	357	27.92	1297	581.61
1-P09	599	195.24	>1500	N.D.
1-H03	629	184.4	>1500	N.D.
1-K02	723	381.84	318	32.77
1-E01	946	168.75	1384	441.89
1-Q07	1289	272.78	>1500	N.D.

Further Biological Evaluation Against 2D Cancer Cell Lines:

Compounds: Lead compounds **1-L01** and **1-K08** were freshly prepared and provided as analytically pure, dry powder.

Cell culture: The pancreatic ductal adenocarcinoma cancer cell lines MIA PaCa-2 and SUIT-2, as well as the triple-negative breast cancer cell line MDA-MB-231 were cultured in RPMI-1640 medium (Gibco #11875) supplemented with 10% fetal bovine serum at 37 ˚C with 5% CO_2.

Cell proliferation assay: The cancer cells were plated in 96-well black plates at a density of 2000 cells per well and then incubated with the indicated drug concentrations. 2×2 technical replicates were conducted for each treatment group. The medium was changed every other day. The viability was evaluated using the CyQUANT proliferation assay (Thermo #C35013) in accordance with manufacturer's instructions when the control well had reached confluence (MIA PaCa-2 = 5 days, SUIT-2 = 3 days, MDA-MB-231 = 5 days). The GraphPad Prism software was used to calculate the IC_{50} values.

Legend:

- **compound 1-L01**
- **compound 1-K08**
- **compound 14-L01**
- **compound 14-K08**
- **colchicine** (**11**)
- **combretastatin A4** (**12**)

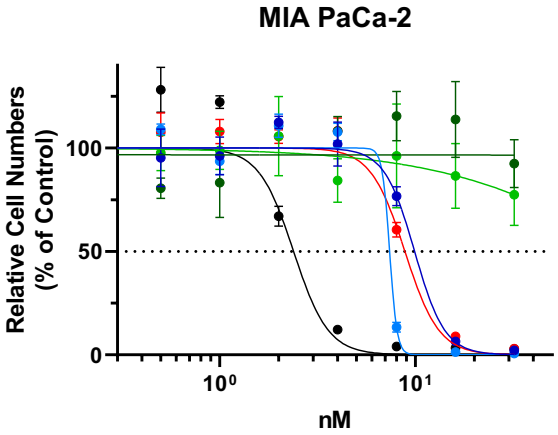

Compound	IC_{50} (nM)	SEM
1-L01	9.90	0.87
1-K08	7.38	N.D.
14-L01	N.D.	N.D.
14-K08	N.D.	N.D.
colchicine (**11**)	8.83	0.46
combretastatin A4 (**12**)	2.38	0.20

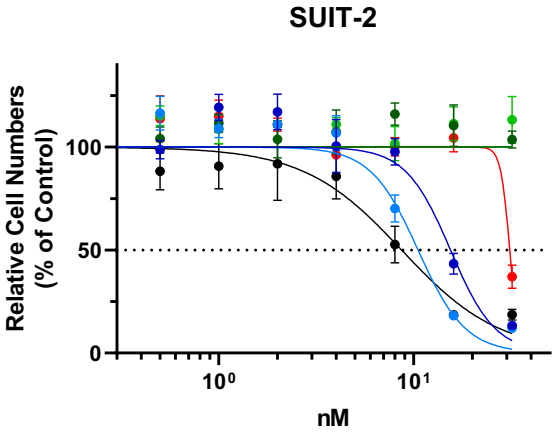

Compound	IC_{50} (nM)	SEM
1-L01	15.44	1.36
1-K08	10.52	0.90
14-L01	N.D.	N.D.
14-K08	N.D.	N.D.
colchicine (**11**)	31.11	N.D.
combretastatin A4 (**12**)	8.66	1.26

Figure S10: Dose-response curves of lead compounds **1-L01** and **1-K08** against pancreatic ductal adenocarcinoma cell lines.

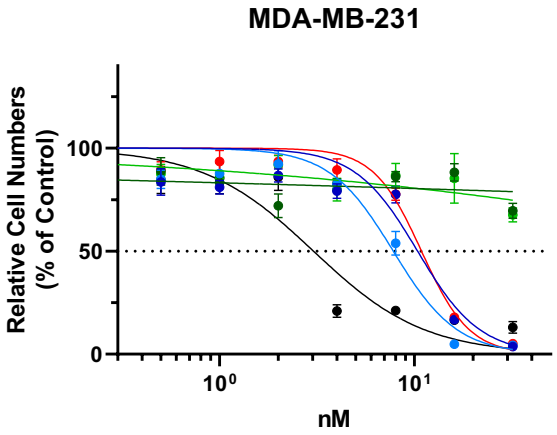

Compound	IC_{50} (nM)	SEM
1-L01	10.37	0.97
1-K08	7.79	0.62
14-L01	N.D.	N.D.
14-K08	N.D.	N.D.
colchicine (**11**)	10.87	0.53
combretastatin A4 (**12**)	3.03	0.35

Figure S11: Dose-response curves of lead compounds **1-L01** and **1-K08** against triple-negative breast cancer cell lines.

Organoid Viability Assays

General Information: Previously established and published human pancreatic cancer organoid lines hM1A, hM1E, hT1, and hF70, and human normal pancreatic organoid line hN39, were plated in Matrigel (Corning #356231) and grown in PDAC human complete tumor organoid media (advanced DMEM/F12, HEPES 10 mM, GlutaMAX 1X, Primocin 1X, A83-01 500 nM, hEGF-10 50 nM, mNoggin 100 nM, hFGF10 100 nM, hGastrin I 0.01 µM, N- acetylcysteine 1.25 mM, Nicotinamide 10 mM, B27 supplement 1X final, R-spondin1 10 nM, NGS Wnt 0.2 nM (ImmunoPrecise #N001) as previously described by Tiriac at al.[8] The normal pancreas line, hN39, was grown in human complete tumor organoid media supplemented 1 µM PGE2. Organoids were maintained at 37 °C with 5 % CO_2 and >90 % humidity, culture media was routinely changed, and passaging occurred as needed to expand/maintain PDO cultures. During passaging PDOs were removed from Matrigel using cell recovery solution and broken down to cell clusters/single cells with 5 to 10 min incubation in TrypLE at 37 °C with mild agitation followed by mechanical breaking. All organoid models were isolated, established, and cultured at Cold Spring Harbor Laboratory and routinely tested for *Mycoplasma*.

Organoid viability assays: Organoids were passaged as described above and dissociated using TrypLE and mechanical force and then passed through a 40 µm filter to form a single cell suspension. An organoid/media slurry with 5 % Matrigel was dispensed into 384-well plates (1,000 cells per well) using a Multidrop Combi liquid dispenser and mixed with the desired dosage of drug that was dispensed using an ECHO 650 drug dispenser. On day 6, CellTiter-Glo was added to each well using the Multidrop Combi and luminescence was read using a Perkin Elmer Envision 2105 plate reader. All compounds were dissolved in DMSO and assayed in triplicates in 12-point dose response using a concentration range from 5e-5 to 10 µM. Data from each compound was normalized to vehicle-DMSO only treated wells and analyzed in Graphpad Prism to determine dose-response curves using a non-linear regression and corresponding IC_{50} and area under the curve (AUC) values. Normalized AUCs were calculated by dividing each AUC value by the maximum/100% AUC value for each given compound over the specified dose range.

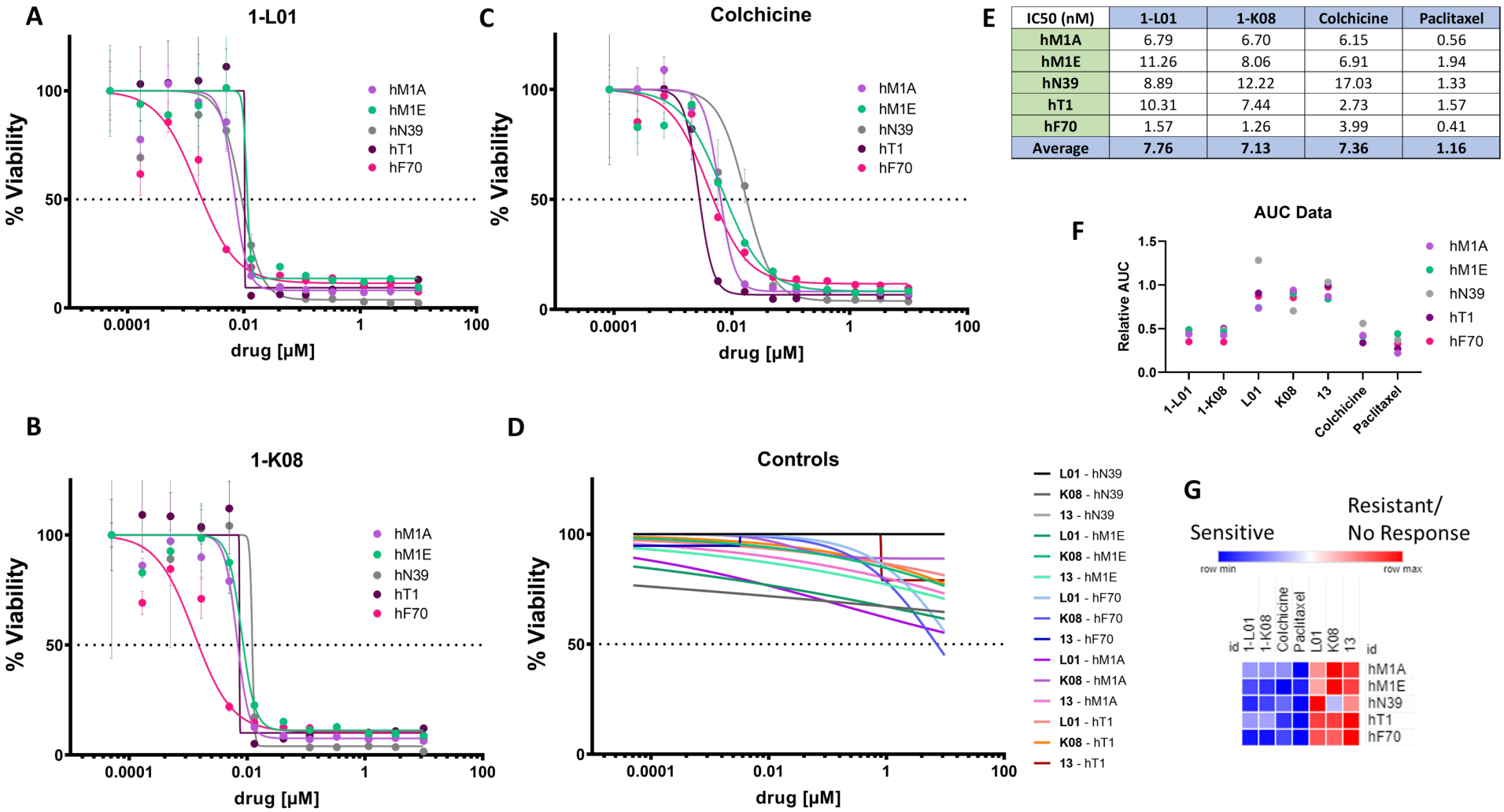

IC50 (nM)	1-L01	1-K08	Colchicine	Paclitaxel
hM1A	6.79	6.70	6.15	0.56
hM1E	11.26	8.06	6.91	1.94
hN39	8.89	12.22	17.03	1.33
hT1	10.31	7.44	2.73	1.57
hF70	1.57	1.26	3.99	0.41
Average	**7.76**	**7.13**	**7.36**	**1.16**

Figure S12: Organoid viability assay results. Dose response curves comparing concentration (x-axis) and cell viability (y-axis) for human pancreatic cancer tumor organoids (hM1A, hM1E, hT1, and hF70) and normal pancreas organoid line hN39 for **A) 1-L01**, **B) 1-K08**, **C)** colchicine (**11**), and **D)** controls (**13**, **L01**, and **K08**). **E)** Table of calculated IC_{50} based on dose response curves across all organoid lines. **F)** Relative area under the curve (AUC) across all compounds and organoids. **G)** Heatmap of AUC row normalized by organoid to show sensitive (blue) versus resistant/no response (red).

Mechanism of Action Studies

Tubulin Polymerization Assay:

General Information: Microplates used for the in vitro tubulin polymerization assays were 96-well, black, flat-bottom Corning Costar plates (Cat #3686). Tubulin polymerization assay kit was purchased from Cytoskeleton, Inc. (Cat #BK011P) and was used as received according to the manufacturer's instructions. Fluorescence spectra were recorded using a Molecular Devices SpectraMax i3x thermal control fluorometer with excitation and emission wavelengths set at 360 nm and 420 nm, respectively. The data was plotted using OriginPro 8.5 software.

Polymerization Protocol: Following the manufacturer's protocol, the *in vitro* tubulin polymerization assay of **1-L01** and **1-K08** was prepared in a black flat bottom 96-well plate, on a 3 μM scale at 37 °C, following the manufacturer's standard procedure. HTS tubulin was used as a negative control, and paclitaxel (microtubule stabilizing drug) and colchicine (**11**) (microtubule destabilizing drug) were used as positive controls. The assay was conducted at 37 °C for 1 hour. Fluorescence readings were taken from above the plate every 30 seconds, with shaking for 5 sec prior to each reading.

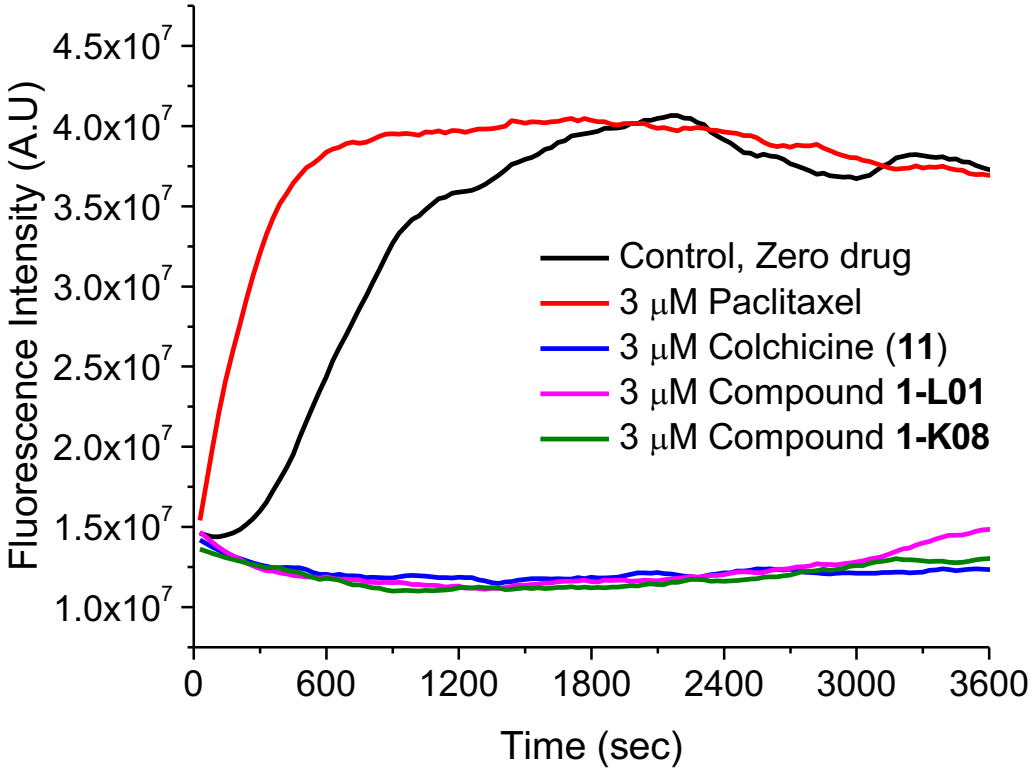

Figure S13: The tubulin polymerization assay (fluorescence based) of compounds **1-L01** and **1-K08**.

X-ray Crystallography Experiments:

Proteins and Compounds: The production of the stathmin-like domain of RB3 and chicken TTL in bacteria, as well as the reconstitution of the T_2R-TTL complex was done as described by Prota *et al.*[9,10]**.** The compounds used in the subsequent experiments are shown below (Fig S13).

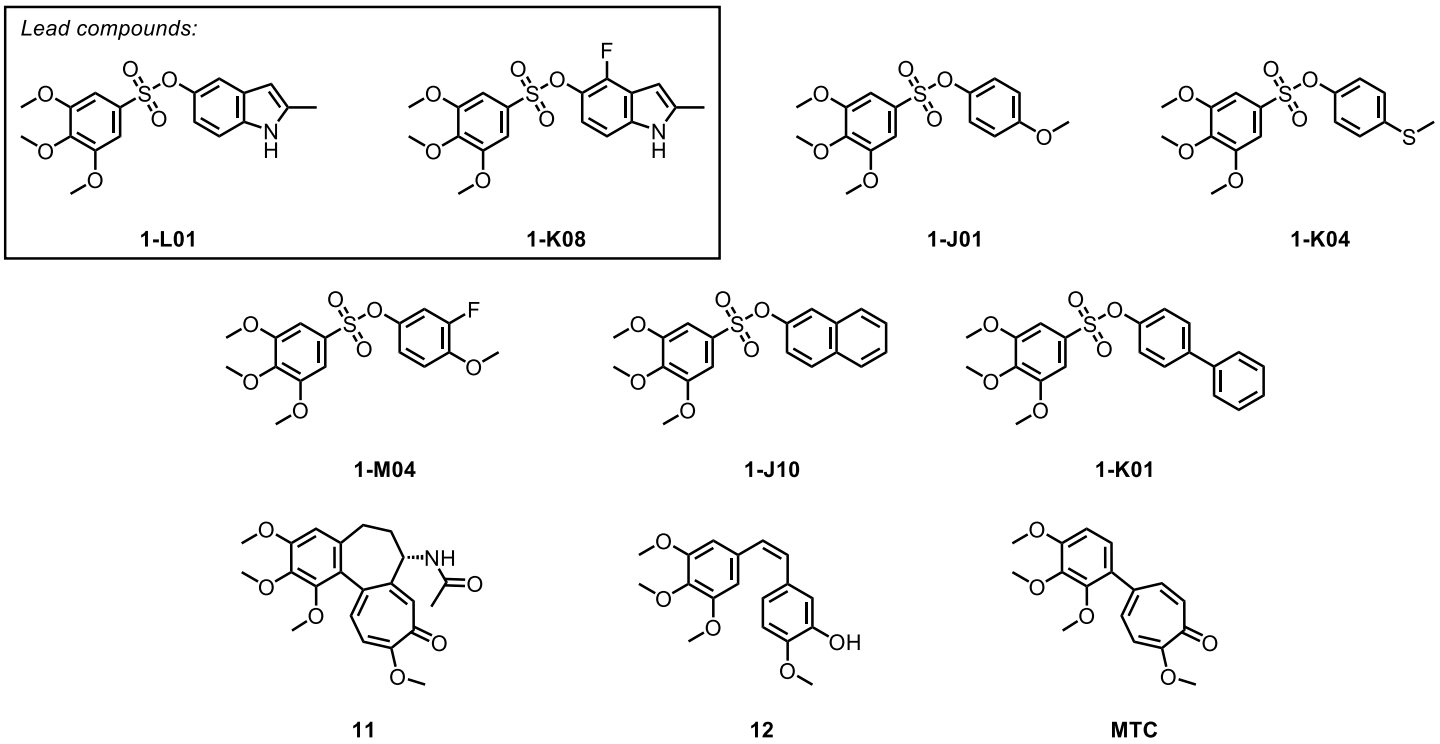

Figure S14: Chemical structures of **CA-4** and the sulfonate **CA-4** mimetics used in the crystallography experiments.

Crystallization, data collection, and structure determination: Crystals of T_2R-TTL were grown by the vapor-diffusion method following the established protocols by Prota *et al.*[9,10] The complex crystallized overnight at 20 °C in reservoir solutions composed of 4% PEG 4K, 9–10% glycerol, 30 mM $MgCl_2$, 30 mM $CaCl_2$, 5 mM tyrosine and 100 mM MES/Imidazole pH 6.5. The crystals were soaked for 5 hours at 20 °C in reservoir solutions containing 5 mM of each of the compounds (Fig S13). The crystals were transferred consecutively to cryo-protectant solutions containing the reservoir solution supplemented with 16% and 20% glycerol, before flash-freezing in liquid nitrogen and subsequent data collection. Native data were collected at 100K at beamline X06SA of the Swiss Light Source (Paul Scherrer Institut, Villigen PSI, Switzerland). Data were processed and merged with XDS[11]. The T_2R-TTL structures were determined using the difference Fourier method using the phases of a T_2R-TTL complex in the absence of ligands and solvent molecules as a starting point for refinement (PDB ID 5LXT). Initial refinement included 10 cycles of rigid body and restrained refinement in Refmac[12], followed by further refinement cycles in Phenix[13]. The resulting models were further improved through iterative model rebuilding in Coot[14] and refinement in Phenix. The quality of the structures was assessed with MolProbity[15].

Chains in the T_2R-TTL complex were defined as follows: chain A, α1-tubulin; chain B, β1-tubulin; chain C, α2-tubulin; chain D, β2-tubulin; chain E, RB3; chain F, TTL. Structure visualization, molecular editing and figure preparation were performed with the PyMOL molecular graphics system (The PyMOL Molecular Graphics System, Version 2.5.2 Schrödinger, LLC).

Table S7. Data collection and refinement statistics.

	T_2R-TTL-1-K08	**T_2R-TTL-1-L01**
PDB ID	8RIV	8RIW
Data collection		
Wavelength	1.00000	1.00000
Resolution range	48.11 - 2.78 (2.81 - 2.78)	47.99 - 2.57 (2.6 - 2.57)
Space group	P 21 21 21	P 21 21 21
Unit cell	104.9 156.4 183.1 90 90 90	104. 7 156.1 182.5 90 90 90
Total reflections	1050959 (33403)	1329010 (44180)
Unique reflections	144994 (4671)	181996 (6020)
Multiplicity	7.2 (7.2)	7.3 (7.3)
Completeness (%)	99.24 (94.99)	99.28 (98.40)
Mean I/sigma (I)	11.64 (0.79)	10.58 (0.51)
Wilson B-factor	83.79	80.71
R_{merge}	0.09764 (1.96)	0.1033 (3.169)
R_{meas}	0.1052 (2.114)	0.1112 (3.406)
R_{pim}	0.03877 (0.7846)	0.04086 (1.242)
$CC^{1/2}$	0.999 (0.378)	0.999 (0.175)
CC*	1 (0.741)	1 (0.545)
Refinement		
Reflections in refinement	75601 (2407)	94644 (3080)
Reflections for R_{free}	3780 (120)	4732 (153)
R_{work}	0.1799 (0.4304)	0.1887 (0.4125)
R_{free}	0.2307 (0.4414)	0.2282 (0.4299)
Number of non-hydrogen atoms	17689	17779
macromolecules	17339	17392
ligands	235	245
solvent	115	142
Protein residues	2187	2195
RMS(bonds)	0.002	0.125
RMS(angles)	0.56	1.52
Ramachandran statistics		
favored (%)	97.27	98.48
allowed (%)	2.73	1.52
outliers (%)	0.00	0.00
Rotamer outliers (%)	0.37	0.58
Clashscore	1.71	3.72
Average B-factor	109.14	104.42
macromolecules	109.53	104.79
ligands	99.48	96.54
solvent	74.02	76.06
Number of TLS groups	28	28

Statistics for the highest-resolution shell are shown in parentheses.

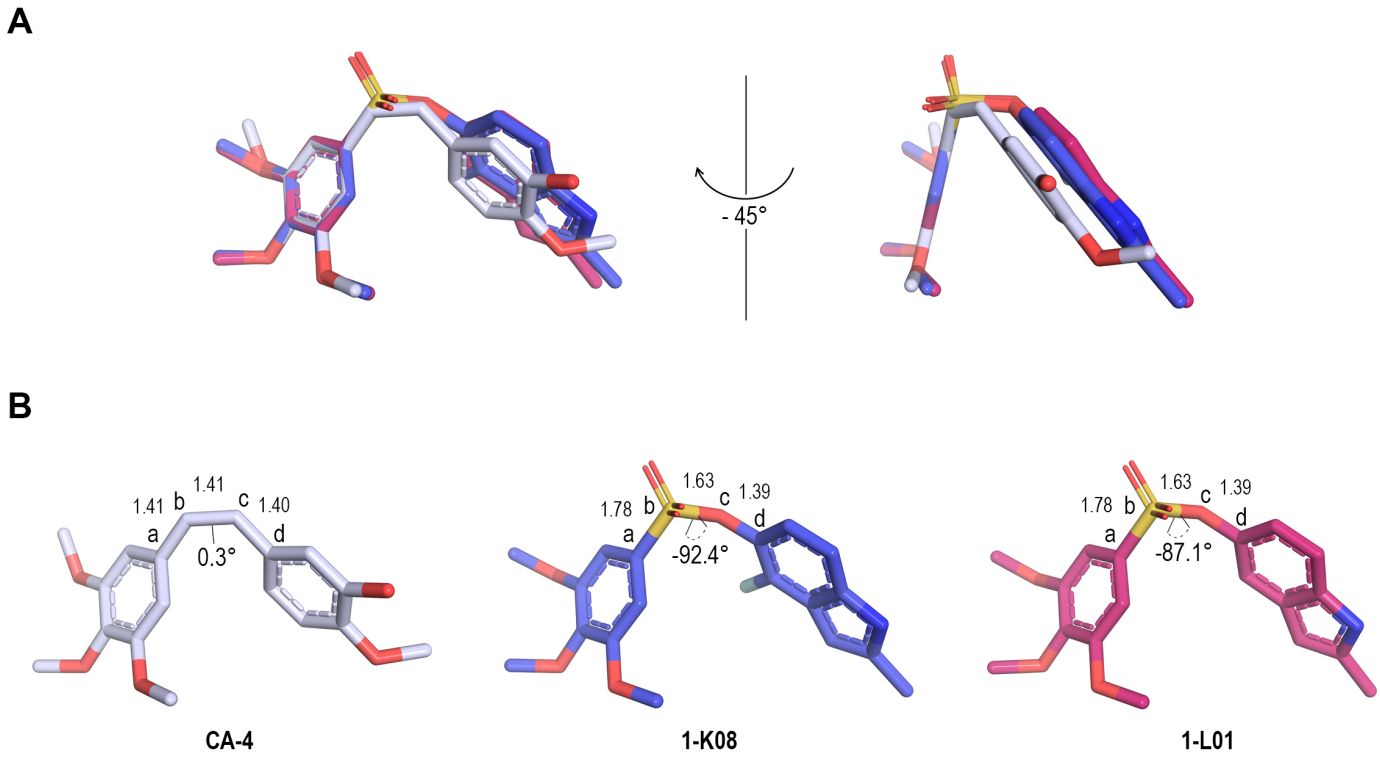

Figure S15. Comparison of the dihedral angles and bond lengths observed for **CA-4**, **1-K08**, and **1-L01** bound to the colchicine binding site of tubulin. The ligands are superimposed onto their 3,4,5-trimethoxybenzene rings. A) Overview of binding orientation, B) Dihedral angles measured along the atoms a,b,c,d.

Competition Assay with **MTC**:

Protocol: Lyophilized tubulin was suspended on ice in 10 mM NaPi with 0.1 mM GTP as a buffer. Tubulin was spun down using MLA 120 rotor at 50,000 rpm at 4°C to remove the aggregates (10-20 min). Then, the emission spectra of each compound were measured separately to determine the background emission. The excitation wavelength was chosen based on the UV absorbance spectra of **MTC** and the studied compounds (Fig S7) and nocodazole as a control). 350 nm was the maximum value of the **MTC** absorbance where the other compounds presented no to minimum (in case of compounds **1-J10**, **1-K01** and nocodazole) absorbance.

10 μM of tubulin and 10 μM of **MTC** were mixed in a buffer and left on ice for 10 min, then the fluorescence intensity of the complex was measured. The compounds were then added to 150 μL of the complex (appropriate for the cuvette) in triplicates at concentrations of 0.1 μM, 0.5 μM, 1 μM, 2.5 μM, 5 μM, 10 μM, 15 μM, 20 μM, 30 μM, and 40 μM. 15 min incubation was done for each sample, after which they were measured using a Cary Eclipse spectrophotometer (Agilent®). Emission maximum values at 421 nm were used to calculate the displacement ratios with the help of the Prism software. The formula used for the calculation: logEC50=log(10^logKi*(1+HotNM/HotKdNM)) Y=(Top-Bottom)/(1+10^(XLogEC50))+Bottom, where X is the logmolar concentration of the measured ligand and Y is the percentage of binding.

Table S7. Binding affinities determined for the compounds **1-J01, 1-K04, 1-L01, 1-K08 1-M04, 1-J10,** and **1-K01**.

Compound	**nocodazole**	**1-J01**	**1-K04**	**1-L01**	**1-K08**	**1-M04**	**1-J10**	**1-K01**
K_D (M^{-1})	$2.0x10^6$	$2.7x10^6$	$2.7x10^6$	$1.7x10^6$	$3.0\ x10^6$	$1.8x10^6$	$1.4x10^6$	$1.3x10^6$

Live Cell Imaging Assays:

Construction of cell cycle reporter: Lentivirus-based cell cycle reporter was described previously[16]. Briefly, the geminin degron was conjugated to the C-terminus of red luciferase (PRE9) to indicate cell cycle and constitutively-expressed green luciferase (CBG99) was used as an imaging internal control. Red fluorescence from mStrawberry expression was used for the positive selection of reporter gene-transduced cells. All the gene cassettes were built into a single lentiviral vector (pBOB lentiviral backbone). Reporter genes (CBG99, PRE9 and mStrawberry) along with geminin protein degron sequences were all synthesized from GenScript USA (New Jersey).

The generation of cell cycle reporter expressing cells: The three lentiviral packaging plasmids (pMDL, pRSV-REV, pCMV-VSVG) and the lentiviral cell cycle reporter plasmid (GemLuc) were transfected into HEK293T packaging cells using Lipofectamine 3000 (Invitrogen, Waltham, MA; according to the manufacturer's recommended protocol) to produce GemLuc lentivirus[17]. The lentiviral supernatant was collected 48 hours and 72 hours later, aliquoted, and then stored at –80°C.

MIA PaCa-2 cells were seeded on a 6-well plate at a density of $3x10^5$ cells/well and transduced with GemLuc lentiviral supernatant along with polybrene to a final concentration of 8 µg/mL. After expanding the transduced cells, FACS sorting was conducted for mStrawberry expression (BD-FACS Aria, BD Bioscience, Franklin Lakes, NJ) to select for MIA PaCa-2 cells stably transduced with GemLuc expression (MIA PaCa-2/GemLuc).

Cell cycle imaging and drug treatment in vitro*:* Images of the cell cycle were taken with an IVIS Spectrum scanner (Perkin Elmer) as previously described[16]. $5x10^3$ MIA PaCa-2/GemLuc cells were plated day –1 on a black-walled 96-well plate (Cellvis, Mountain View, CA). The next day, the cells were treated with escalating doses (0, 25, 50, 100 nM) in triplicate of compounds **1-L01**, **1-K08**, colchicine (**11**), **13**, **L01**, and **K08**. After 24 hours of drug treatment, multiple bioluminescent images were acquired 2 minutes after adding 150 µg/mL of D-luciferin (Goldbio, Saint Louis, MO), through a series of 20 nm bandpass optical filters, ranging from 520 to 660 nm. Using single-color CBG99 and PRE9 reference spectra, green and red emitted light was spectrally unmixed using the Imaging Wizard in Living Imaging software 4.0 (Perkin Elmer). All *in vitro* images were acquired with a field-of-view C and focused at a subject height of 0.5 cm. Photon flux from each well was quantified as photons/second/steradian/cm^2.

References

1 C. Ma, C.-Q. Zhao, X.-T. Xu, Z.-M. Li, X.-Y. Wang, K. Zhang and T.-S. Mei, *Org. Lett.*, 2019, **21**, 2464–2467.
2 P. Gilles, C. Veryser, S. Vangrunderbeeck, S. Ceusters, L. Van Meervelt and W. M. De Borggraeve, *J. Org. Chem.*, 2019, **84**, 1070–1078.
3 Y.-Z. Ji, H.-J. Li, J.-Y. Zhang and Y.-C. Wu, *Chem. Commun.*, 2019, **55**, 11864–11867.
4 T. Zhong, M.-K. Pang, Z.-D. Chen, B. Zhang, J. Weng and G. Lu, *Org. Lett.*, 2020, **22**, 3072–3078.
5 X. Wang, M. Zhou, Q. Liu, C. Ni, Z. Fei, W. Li and J. Hu, *Chem. Commun.*, 2021, **57**, 8170–8173.
6 J. Potenziano, R. Spitale and M. E. Janik, *Synth. Commun.*, 2005, **35**, 2005–2016.
7 J. M. Thiede, S. L. Kordus, B. J. Turman, J. A. Buonomo, C. C. Aldrich, Y. Minato and A. D. Baughn, *Scientific Reports*, 2016, **6**, 38083.
8 H. Tiriac, P. Belleau, D. D. Engle, D. Plenker, A. Deschênes, T. D. D. Somerville, F. E. M. Froeling, R. A. Burkhart, R. E. Denroche, G.-H. Jang, K. Miyabayashi, C. M. Young, H. Patel, M. Ma, J. F. LaComb, R. L. D. Palmaira, A. A. Javed, J. C. Huynh, M. Johnson, K. Arora, N. Robine, M. Shah, R. Sanghvi, A. B. Goetz, C. Y. Lowder, L. Martello, E. Driehuis, N. LeComte, G. Askan, C. A. Iacobuzio-Donahue, H. Clevers, L. D. Wood, R. H. Hruban, E. Thompson, A. J. Aguirre, B. M. Wolpin, A. Sasson, J. Kim, M. Wu, J. C. Bucobo, P. Allen, D. V. Sejpal, W. Nealon, J. D. Sullivan, J. M. Winter, P. A. Gimotty, J. L. Grem, D. J. DiMaio, J. M. Buscaglia, P. M. Grandgenett, J. R. Brody, M. A. Hollingsworth, G. M. O'Kane, F. Notta, E. Kim, J. M. Crawford, C. Devoe, A. Ocean, C. L. Wolfgang, K. H. Yu, E. Li, C. R. Vakoc, B. Hubert, S. E. Fischer, J. M. Wilson, R. Moffitt, J. Knox, A. Krasnitz, S. Gallinger and D. A. Tuveson, *Cancer Discov.*, 2018, **8**, 1112–1129.
9 A. E. Prota, K. Bargsten, D. Zurwerra, J. J. Field, J. F. Díaz, K.-H. Altmann and M. O. Steinmetz, *Science*, 2013, **339**, 587–590.
10 A. E. Prota, M. M. Magiera, M. Kuijpers, K. Bargsten, D. Frey, M. Wieser, R. Jaussi, C. C. Hoogenraad, R. A. Kammerer, C. Janke and M. O. Steinmetz, *J. Cell Biol.*, 2013, **200**, 259–270.
11 W. Kabsch, *Acta Crystallogr. D Biol. Crystallogr.*, 2010, **66**, 125–132.
12 G. N. Murshudov, P. Skubák, A. A. Lebedev, N. S. Pannu, R. A. Steiner, R. A. Nicholls, M. D. Winn, F. Long and A. A. Vagin, *Acta Crystallogr. D Biol. Crystallogr.*, 2011, **67**, 355–367.
13 P. D. Adams, P. V. Afonine, G. Bunkoczi, V. B. Chen, I. W. Davis, N. Echols, J. J. Headd, L. W. Hung, G. J. Kapral, R. W. Grosse-Kunstleve, A. J. McCoy, N. W. Moriarty, R. Oeffner, R. J. Read, D. C. Richardson, J. S. Richardson, T. C. Terwilliger and P. H. Zwart, *Acta Crystallogr. D Biol. Crystallogr.*, 2010, **66**, 213–221.
14 P. Emsley and K. Cowtan, *Acta Crystallogr. D Biol. Crystallogr.*, 2004, **60**, 2126–2132.
15 I. W. Davis, L. W. Murray, J. S. Richardson and D. C. Richardson, *Nucleic Acids Res.*, 2004, **32**, W615–W619.
16 T. Chung, L. Garcia, M. M. Swamynathan, F. E. M. Froeling, L. C. Trotman, D. A. Tuveson and S. K. Lyons, *Anal. Chem.*, 2023, **95**, 5661–5670.
17 G. Tiscornia, O. Singer and I. M. Verma, *Nat. Protoc.*, 2006, **1**, 241–245.

NMR Spectra

^{1}H NMR Spectrum for Compound **2** (400 MHz, $CDCl_3$)

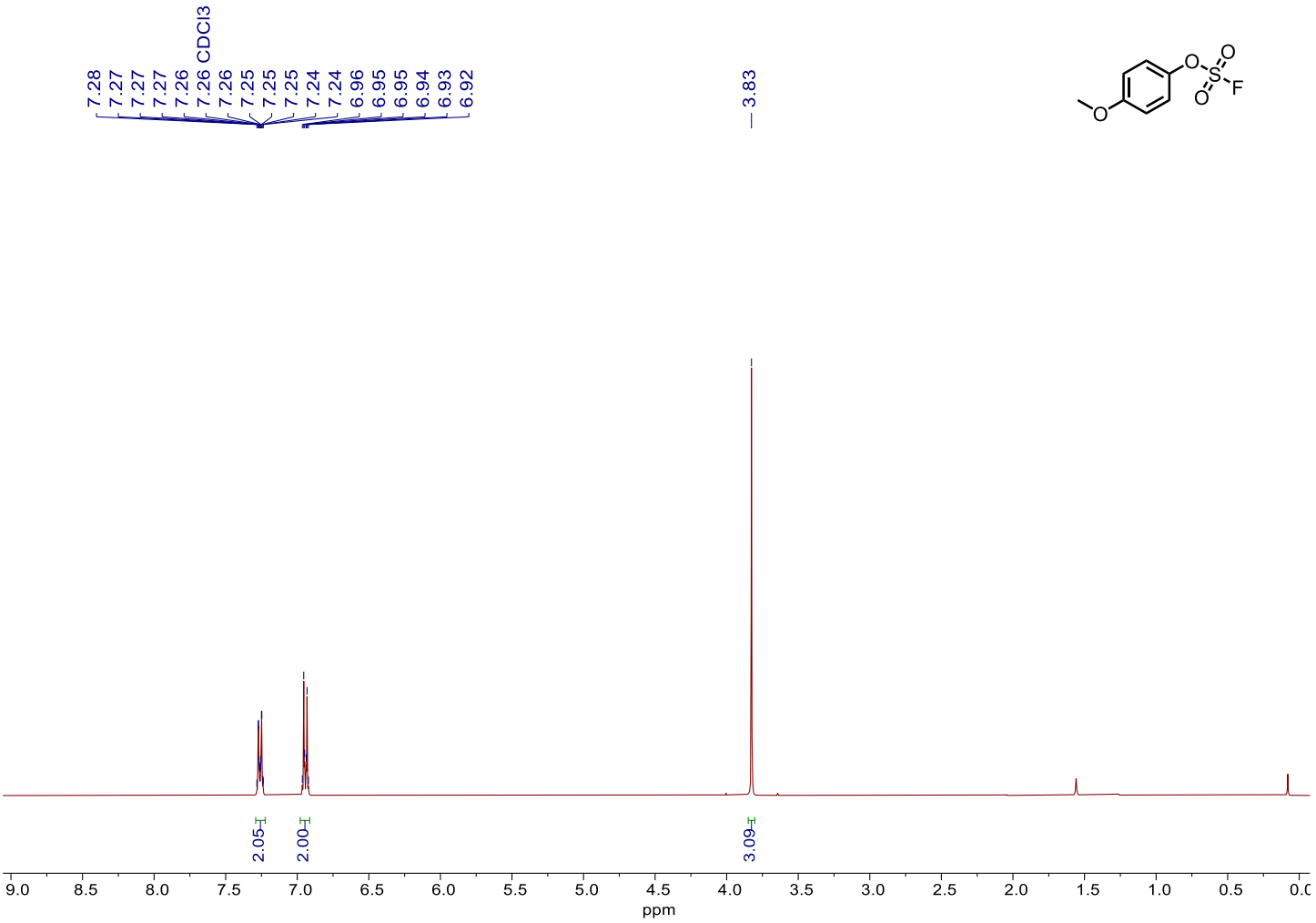

^{13}C NMR Spectrum for Compound **2** (101 MHz, $CDCl_3$)

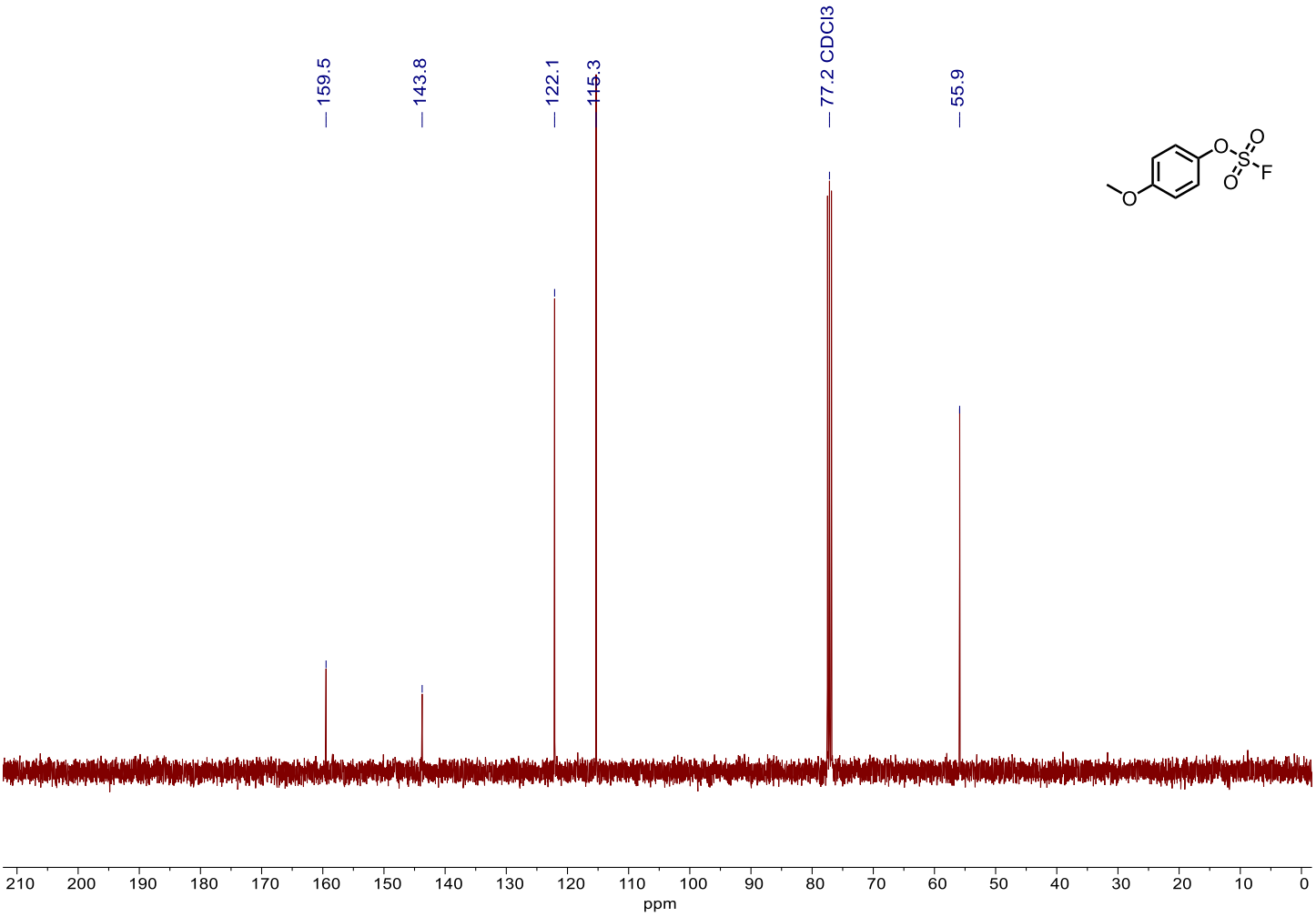

^{19}F NMR Spectrum for Compound **2** (376 MHz, $CDCl_3$)

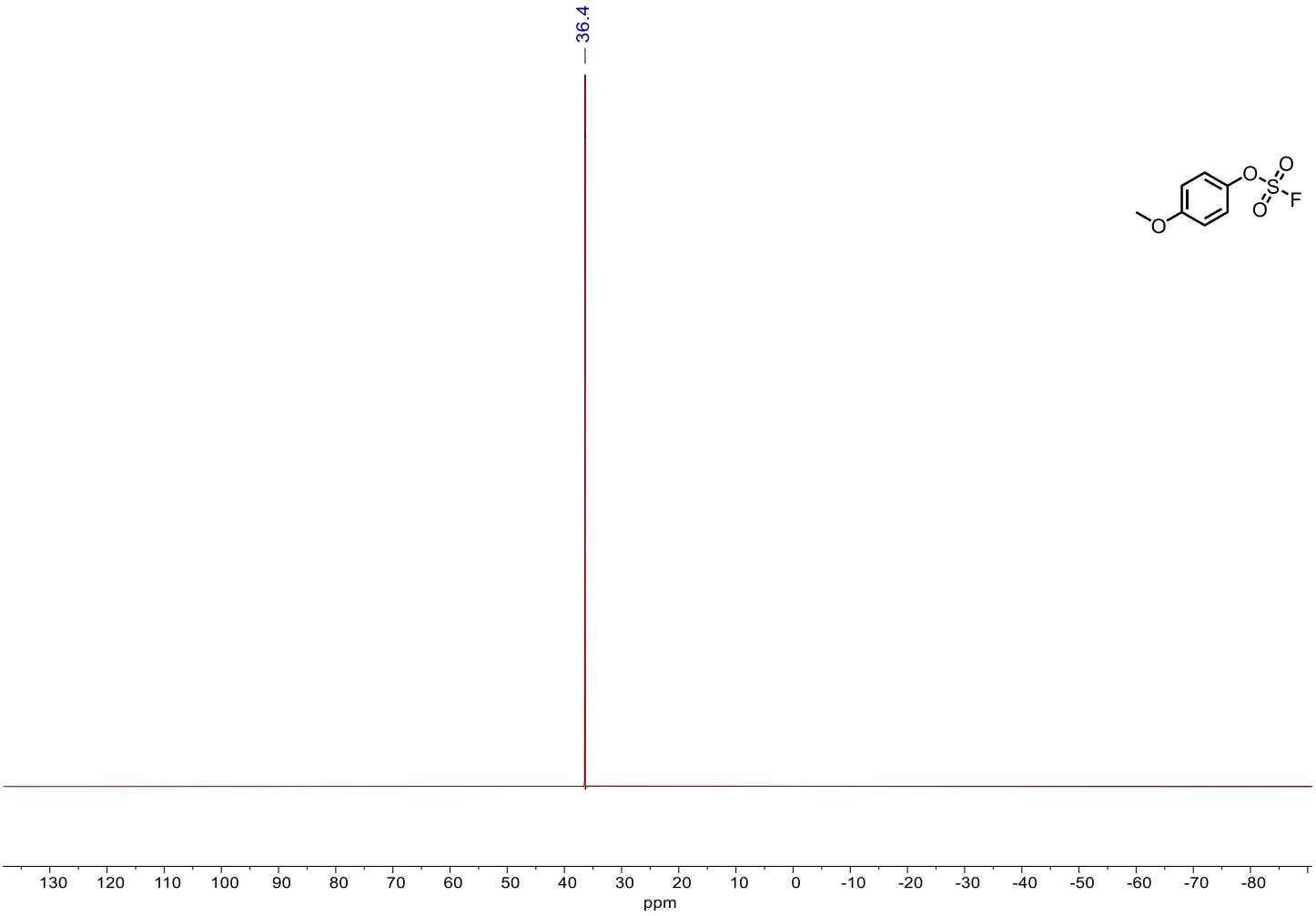

^{1}H NMR Spectrum for Compound **6** (400 MHz, $CDCl_3$)

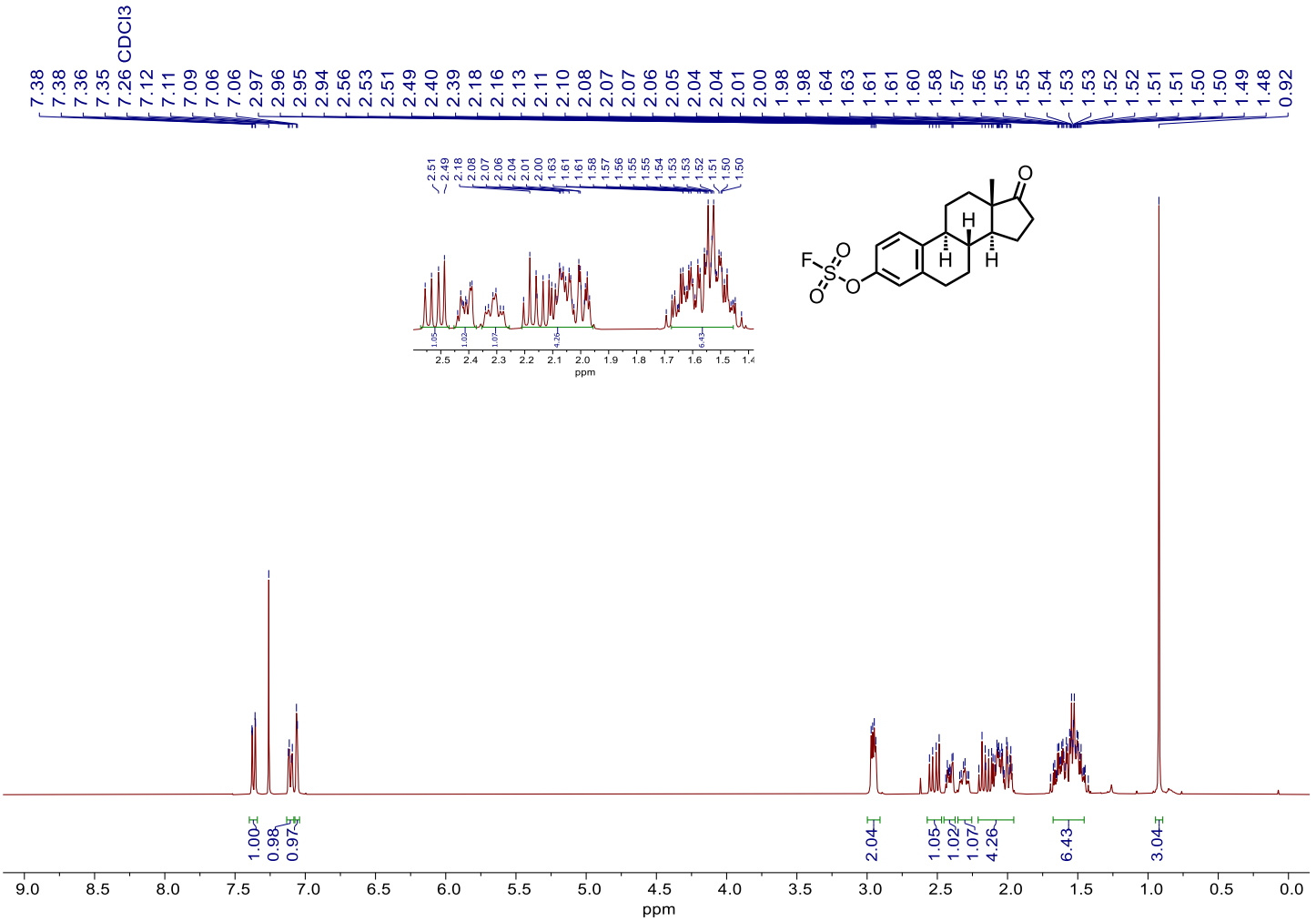

^{19}F NMR Spectrum for Compound **6** (376 MHz, $CDCl_3$)

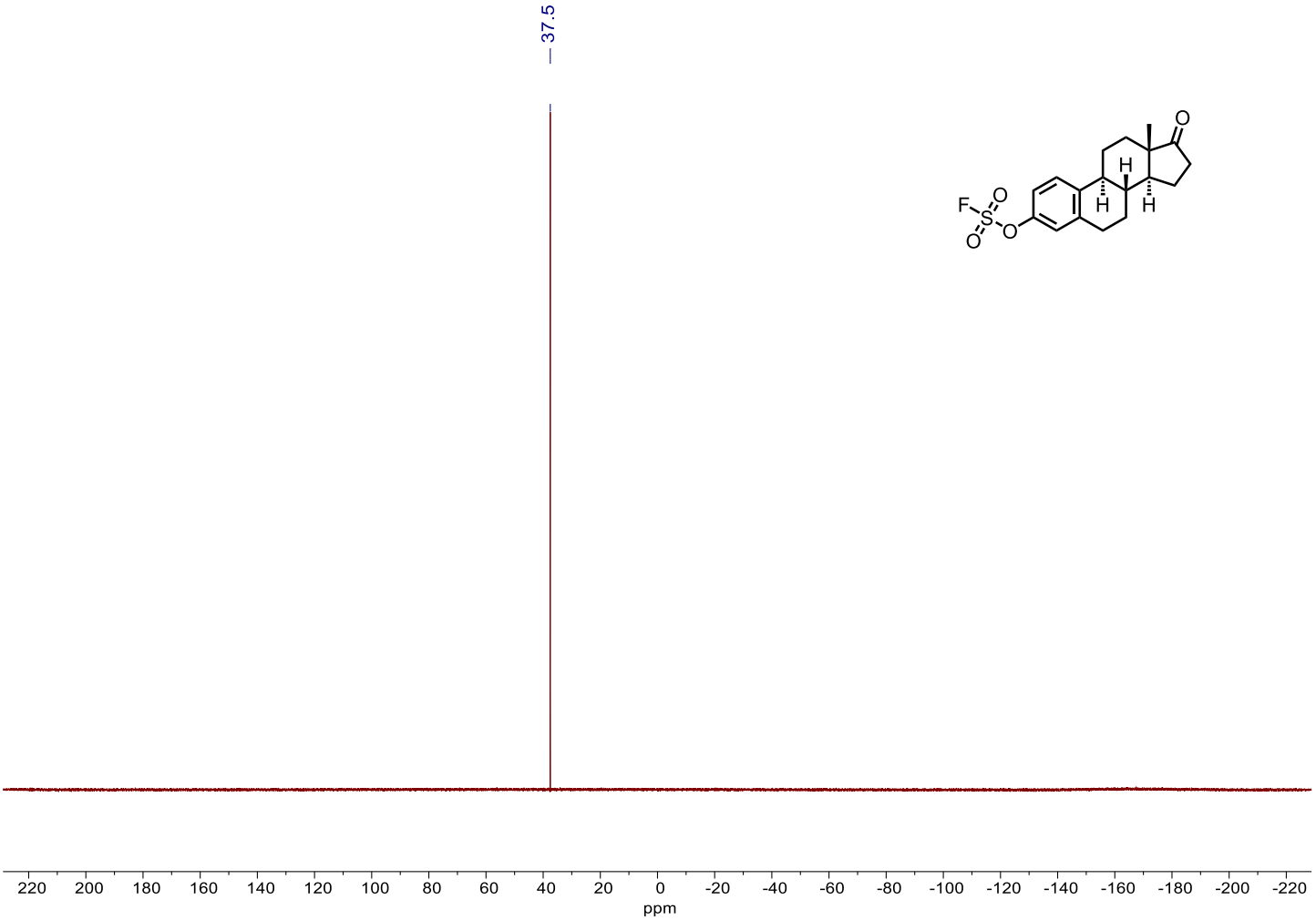

^{1}H NMR Spectrum for Compound **1-I02** (400 MHz, $CDCl_3$)

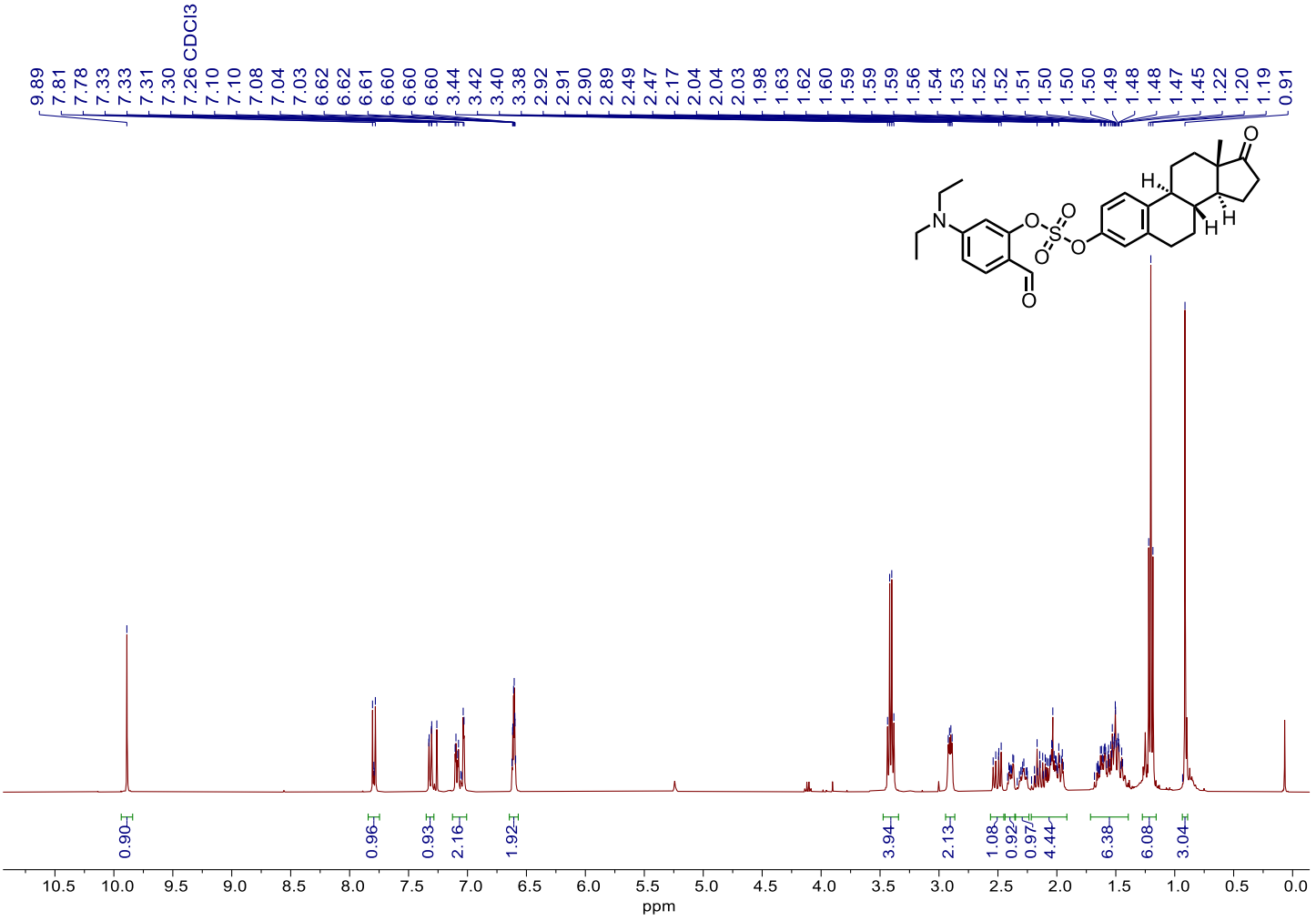

^{13}C NMR Spectrum for Compound **7-I02** (101 MHz, $CDCl_3$)

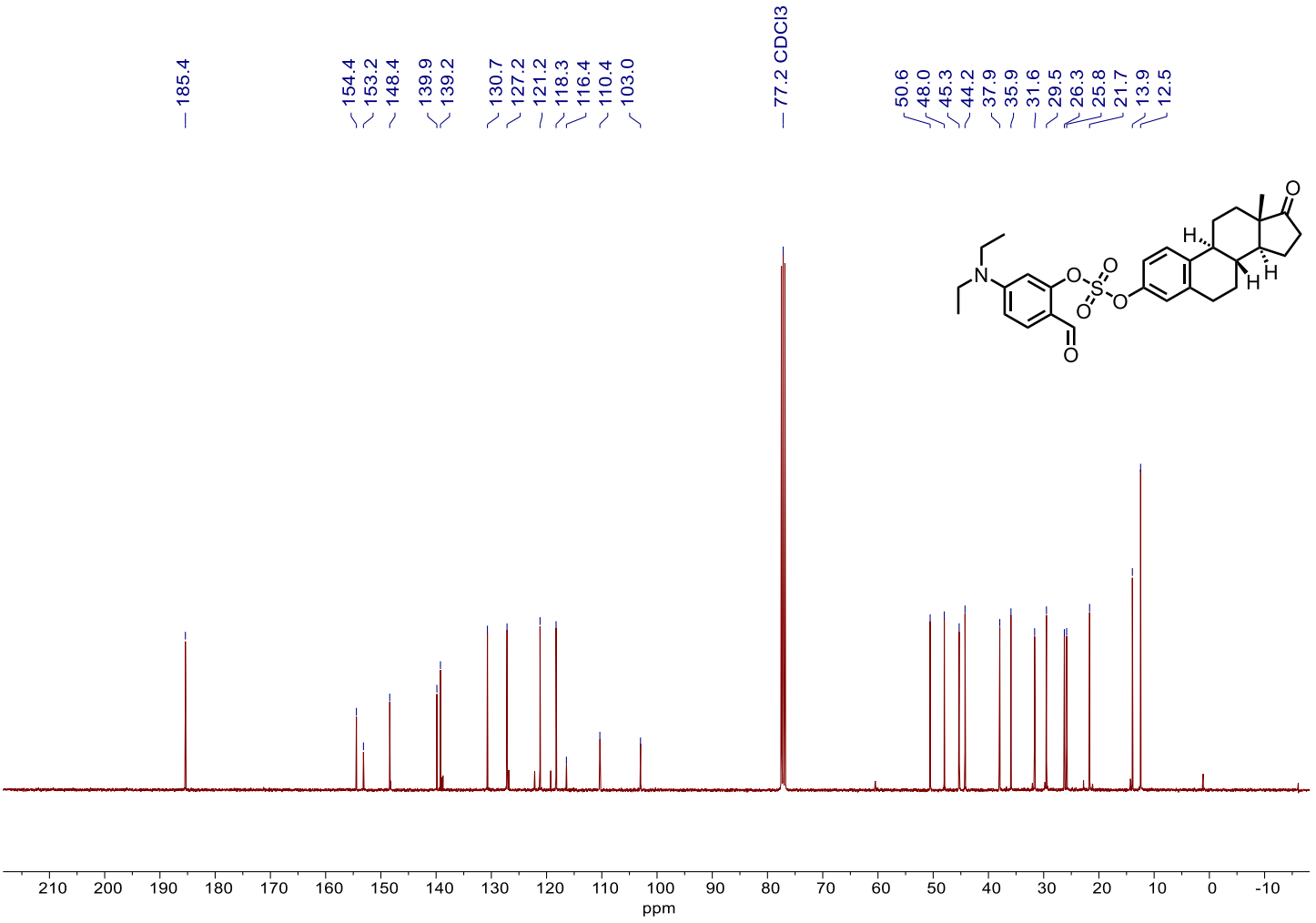

^{1}H NMR Spectrum for Compound **1-J08** (400 MHz, $CDCl_3$)

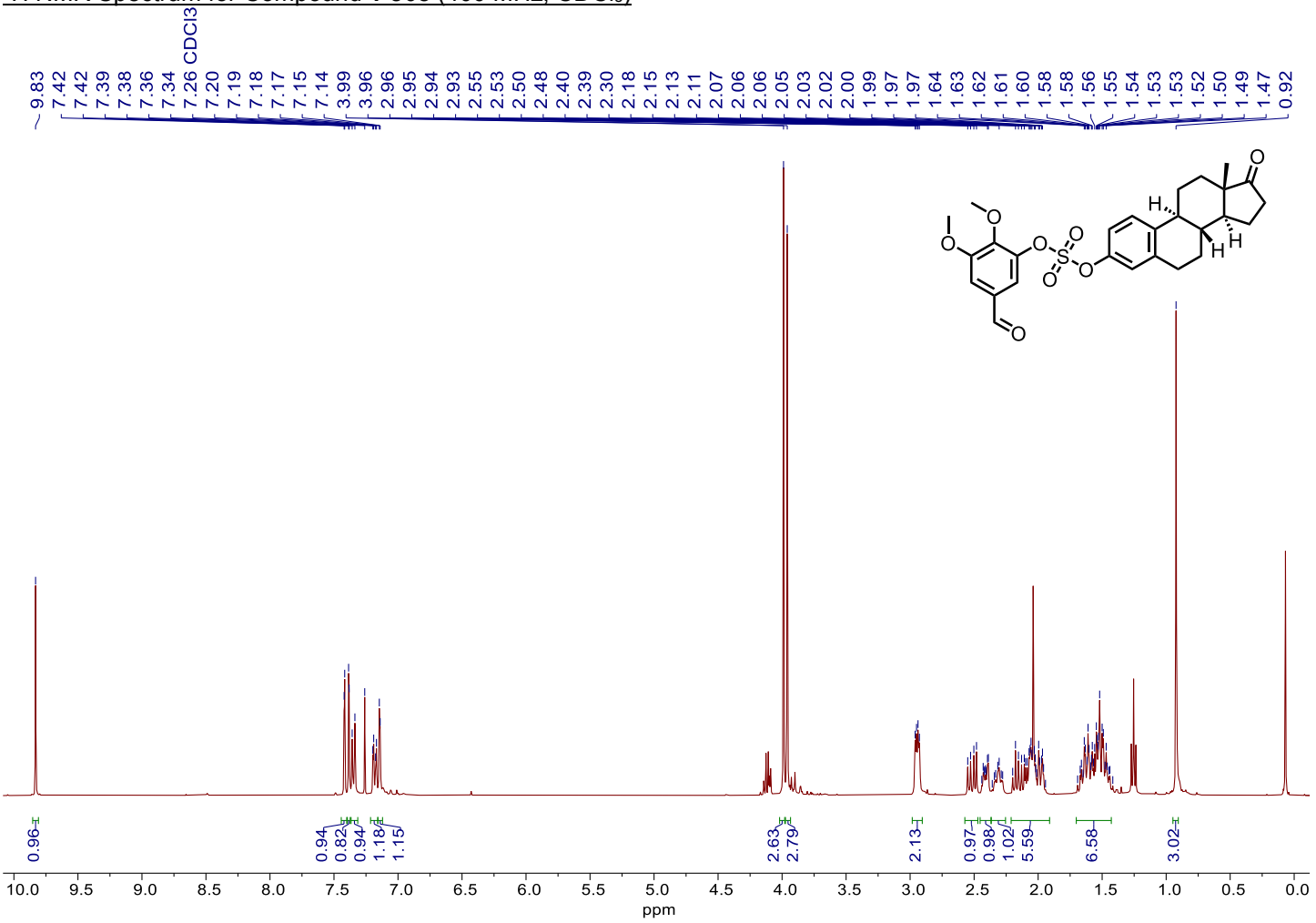

^{13}C NMR Spectrum for Compound **7-J08** (101 MHz, $CDCl_3$)

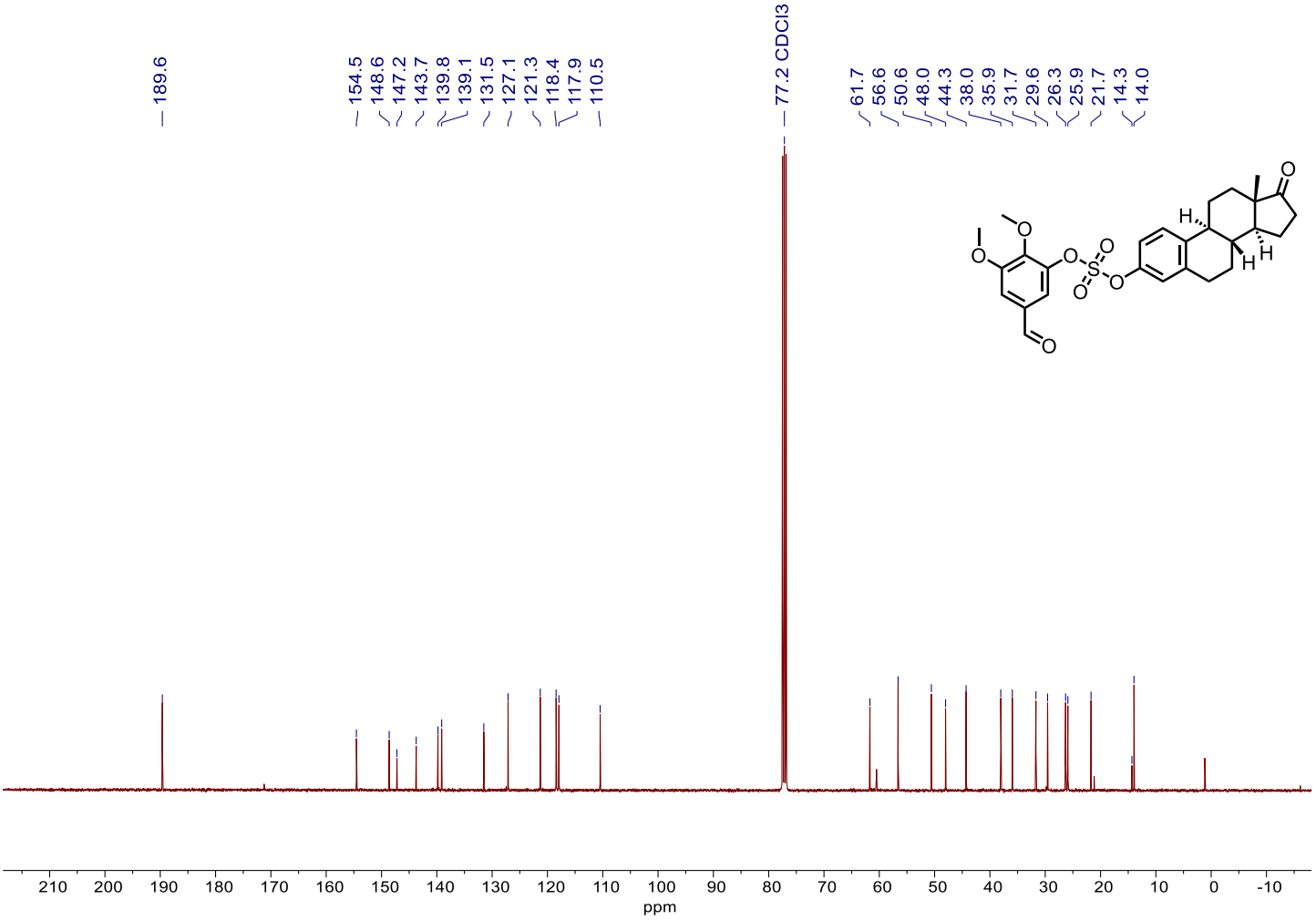

^{1}H NMR Spectrum for Compound **1-K07** (400 MHz, $CDCl_3$)

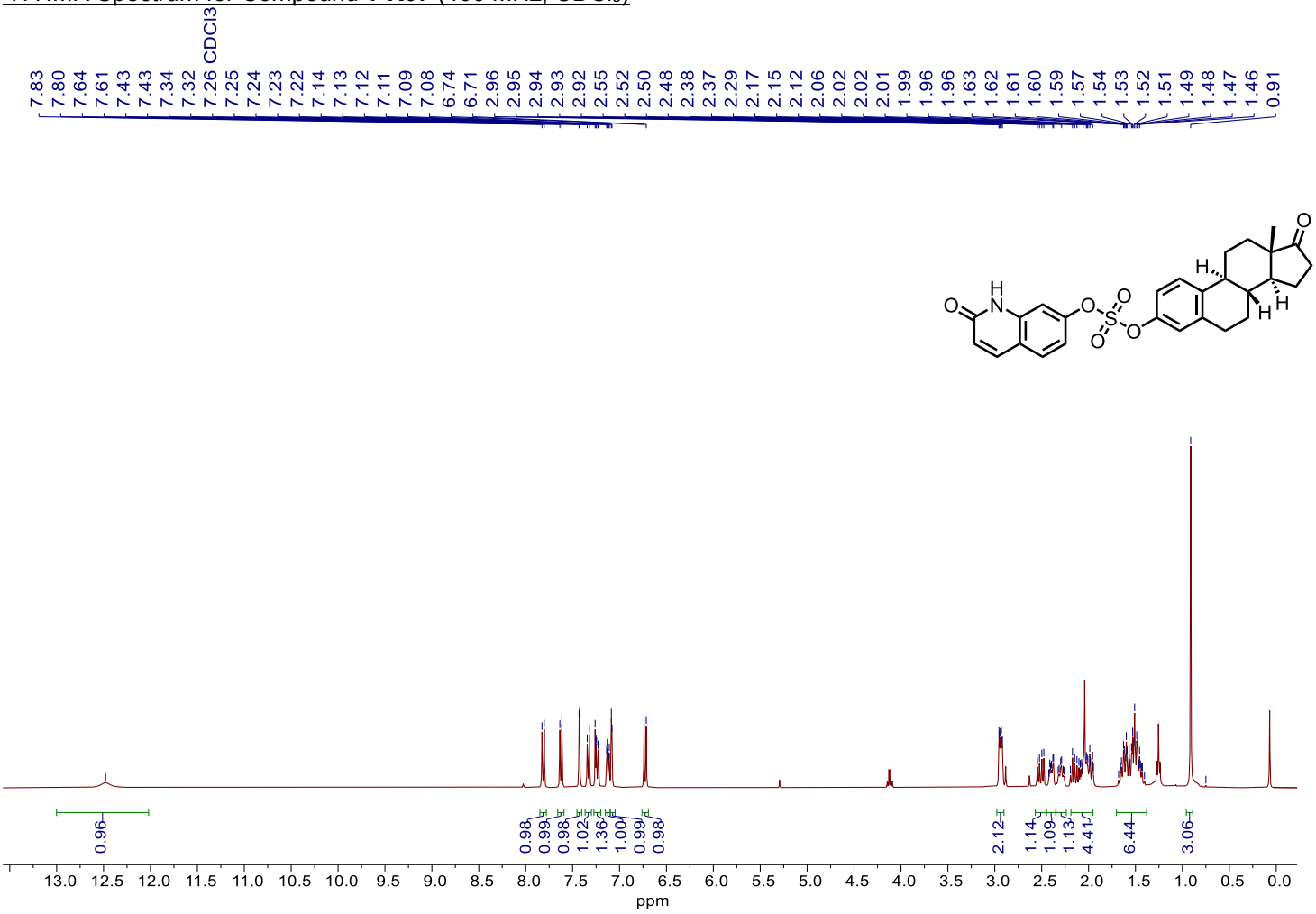

^{13}C NMR Spectrum for Compound **7-K07** (101 MHz, $CDCl_3$)

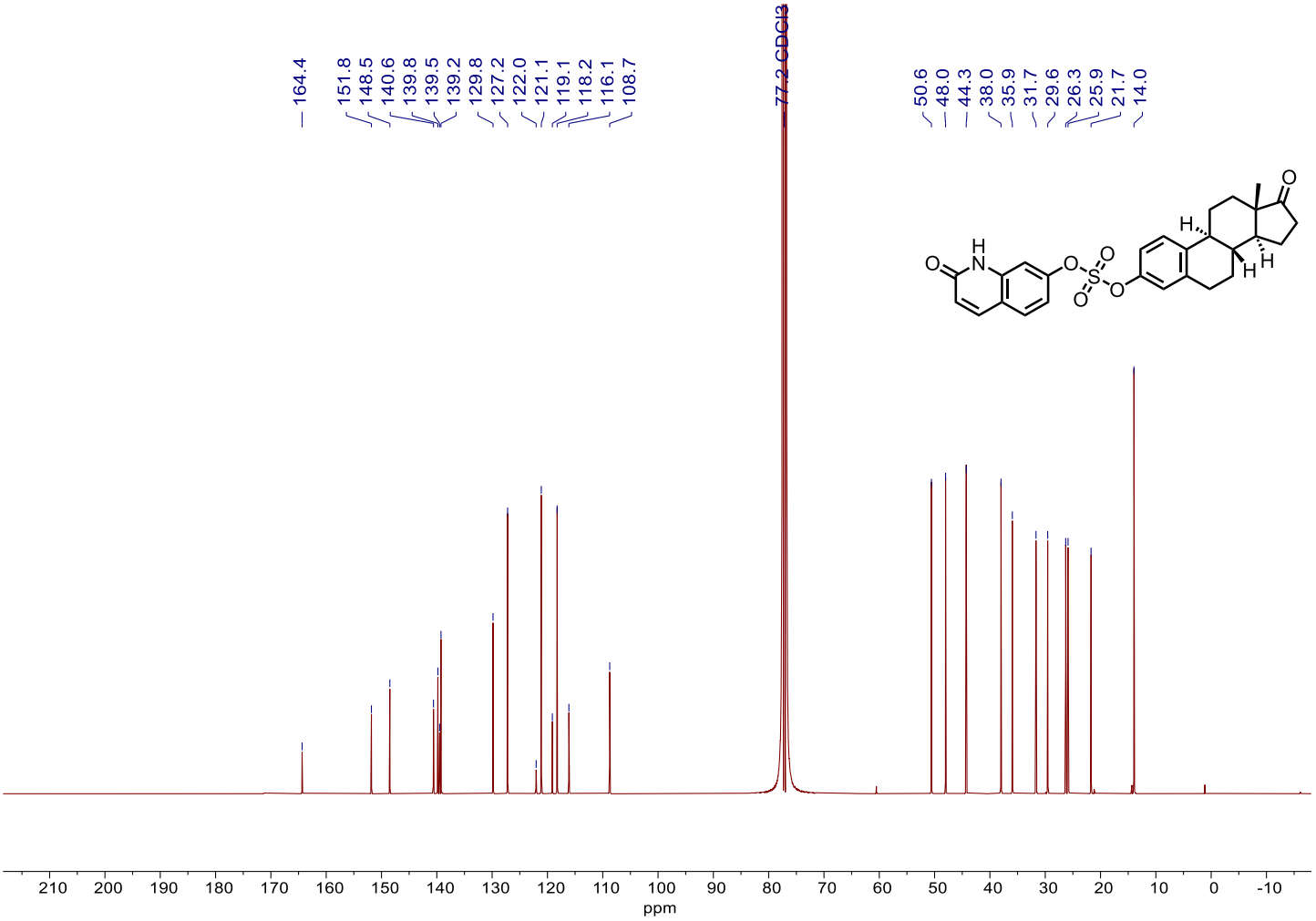

^{1}H NMR Spectrum for Compound **1-K08** (400 MHz, $CDCl_3$)

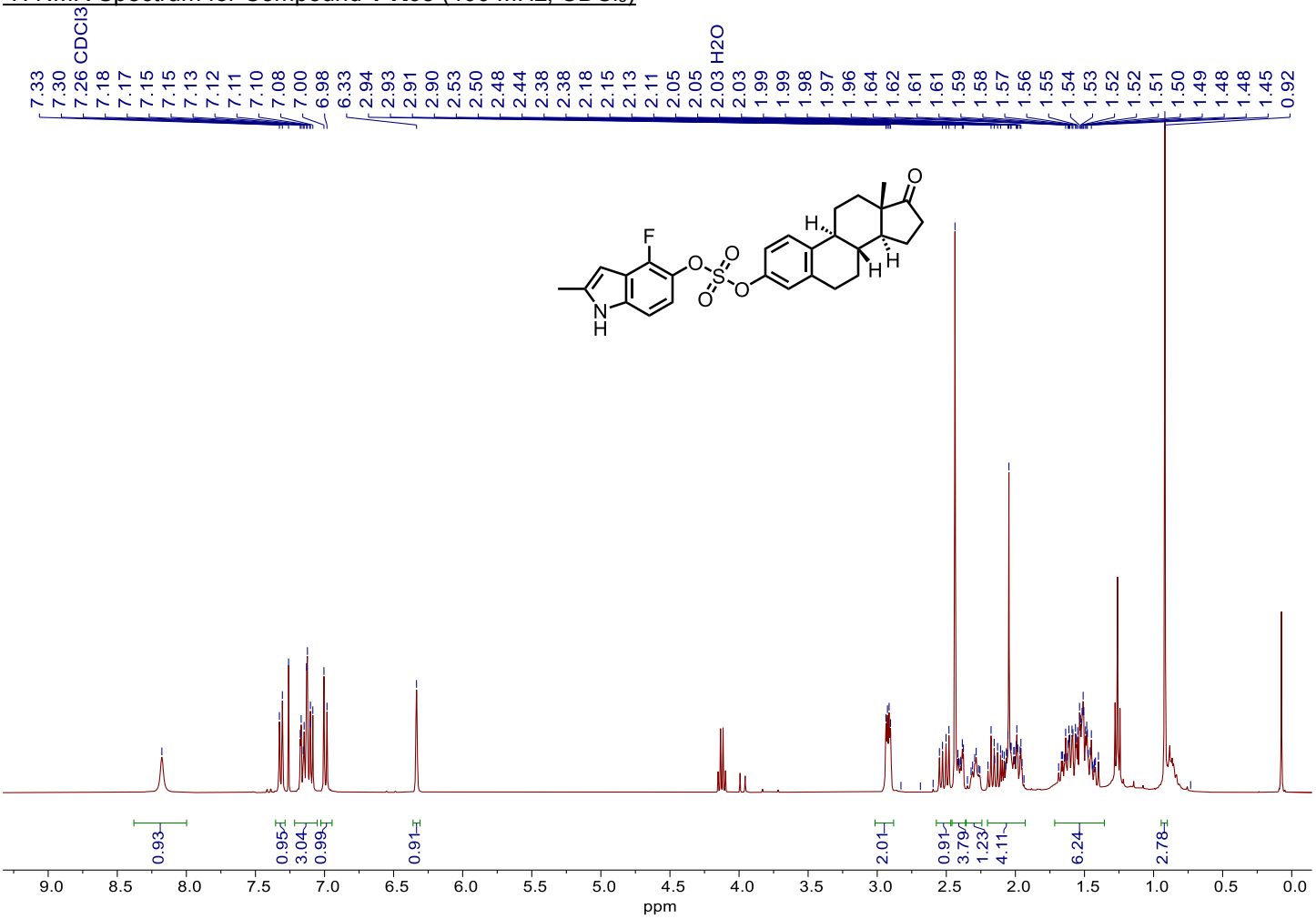

^{13}C NMR Spectrum for Compound **7-K08** (101 MHz, $CDCl_3$)

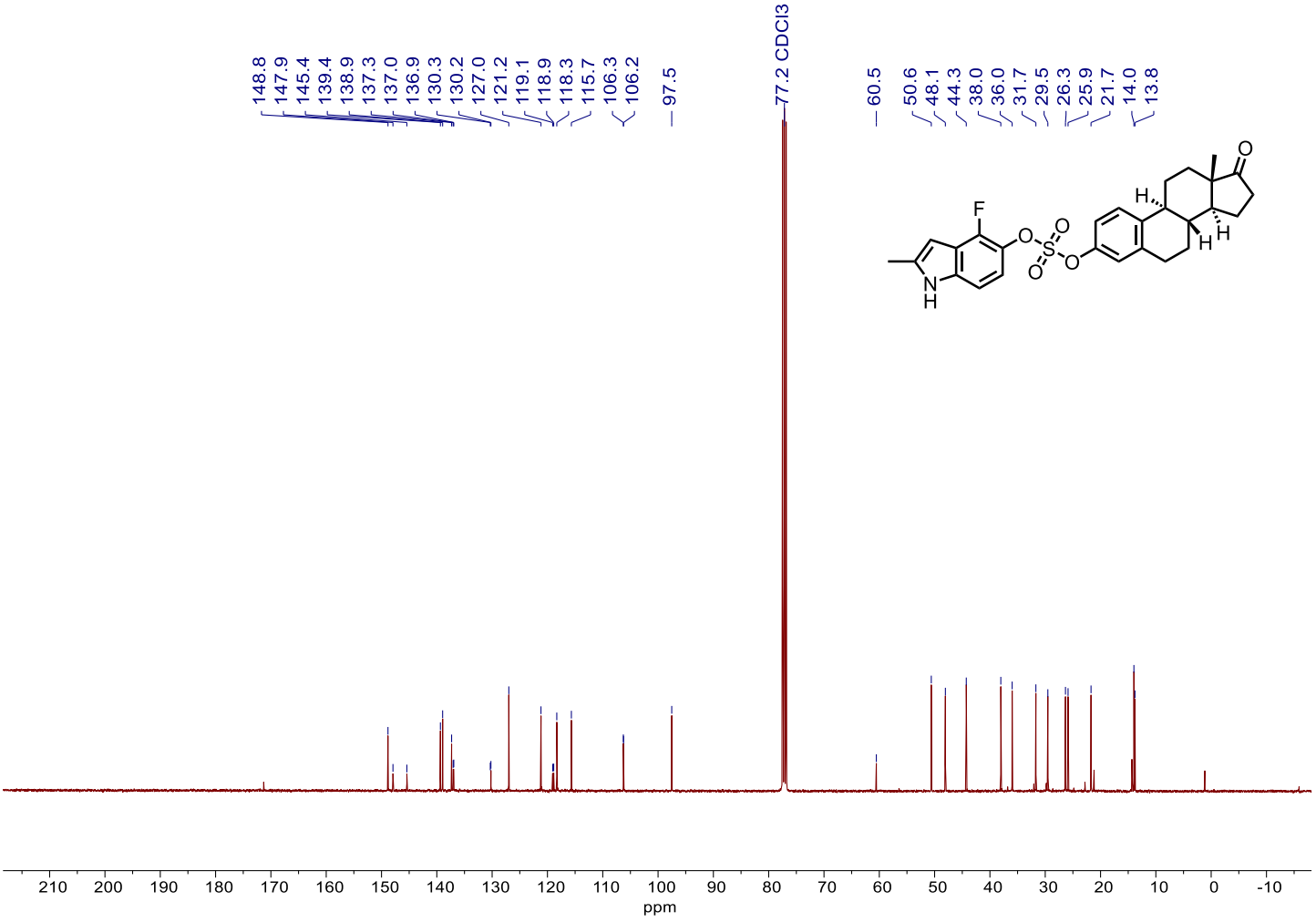

[1]H NMR Spectrum for Compound **9** (400 MHz, DMSO)

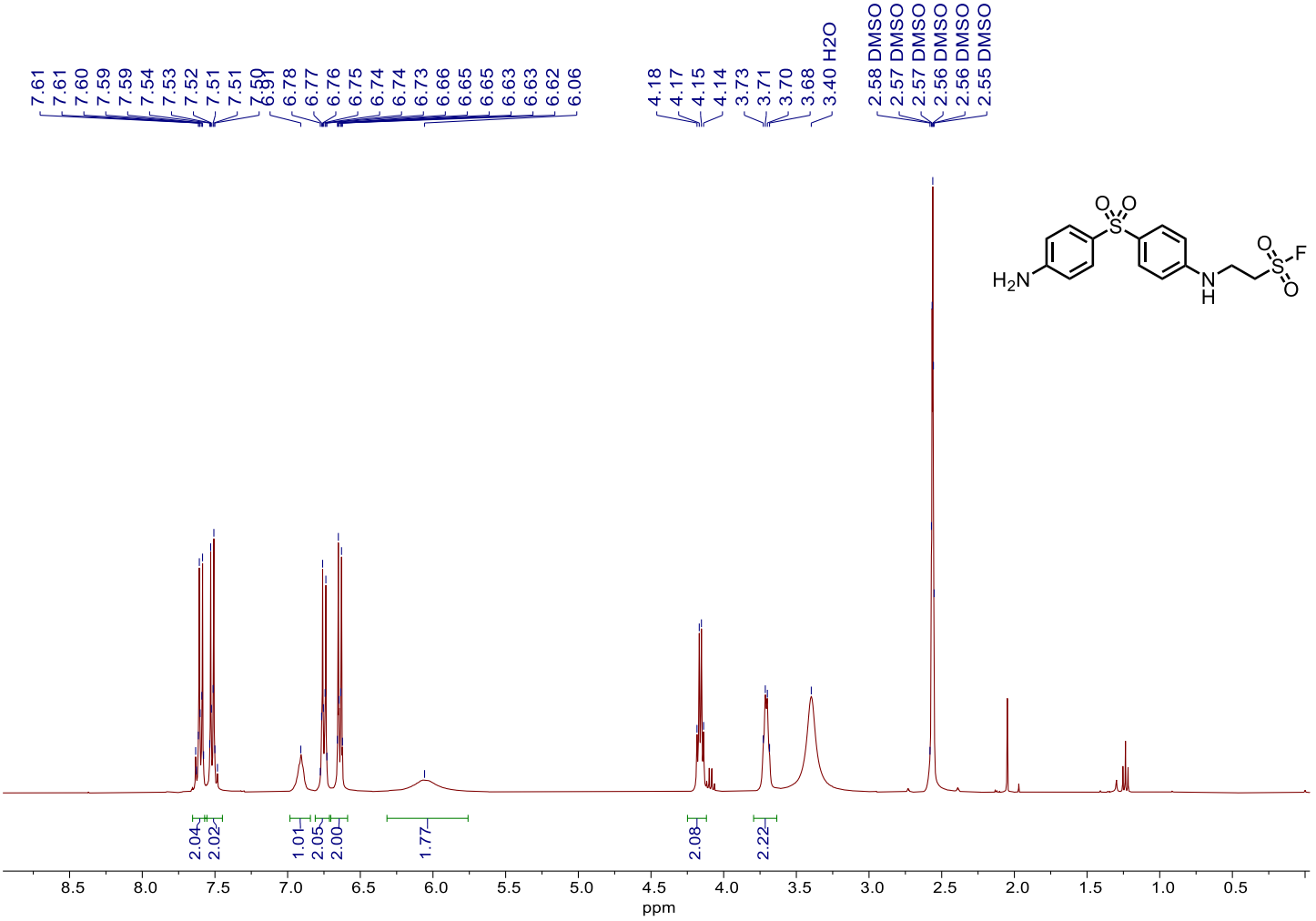

^{13}C NMR Spectrum for Compound **9** (101 MHz, DMSO)

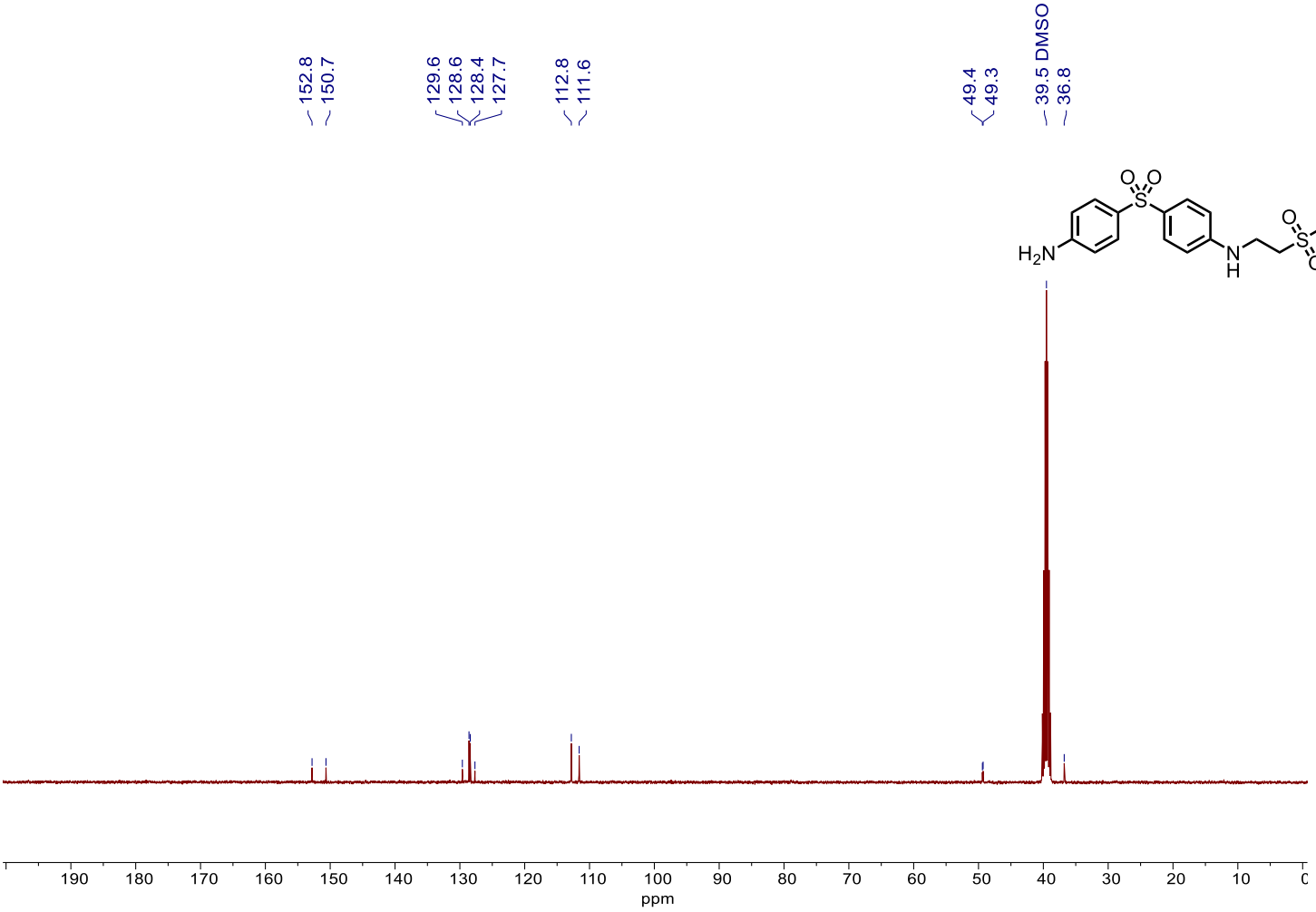

^{19}F NMR Spectrum for Compound **9** (376 MHz, DMSO)

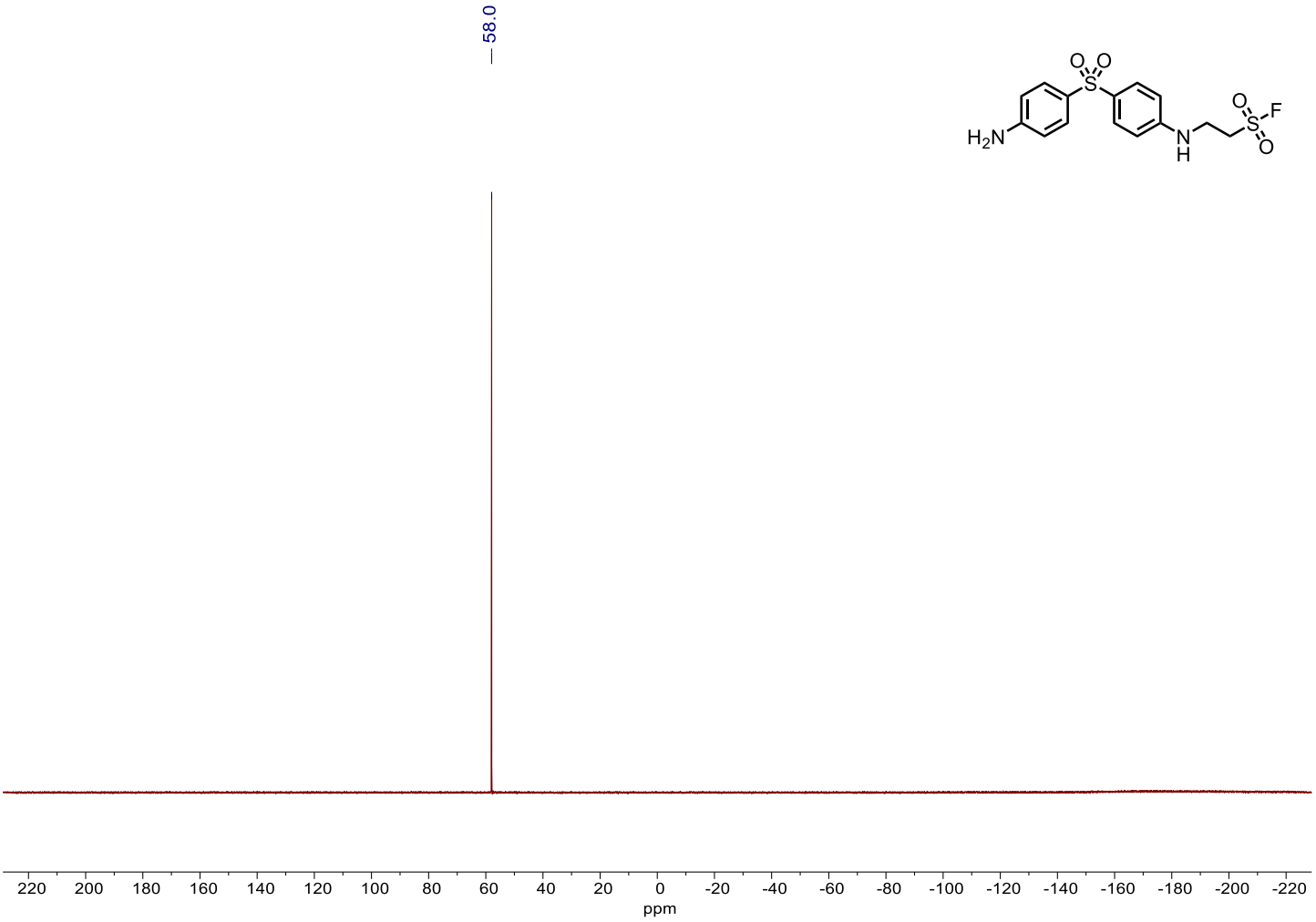

^{1}H NMR Spectrum for Compound **13** (400 MHz, $CDCl_3$)

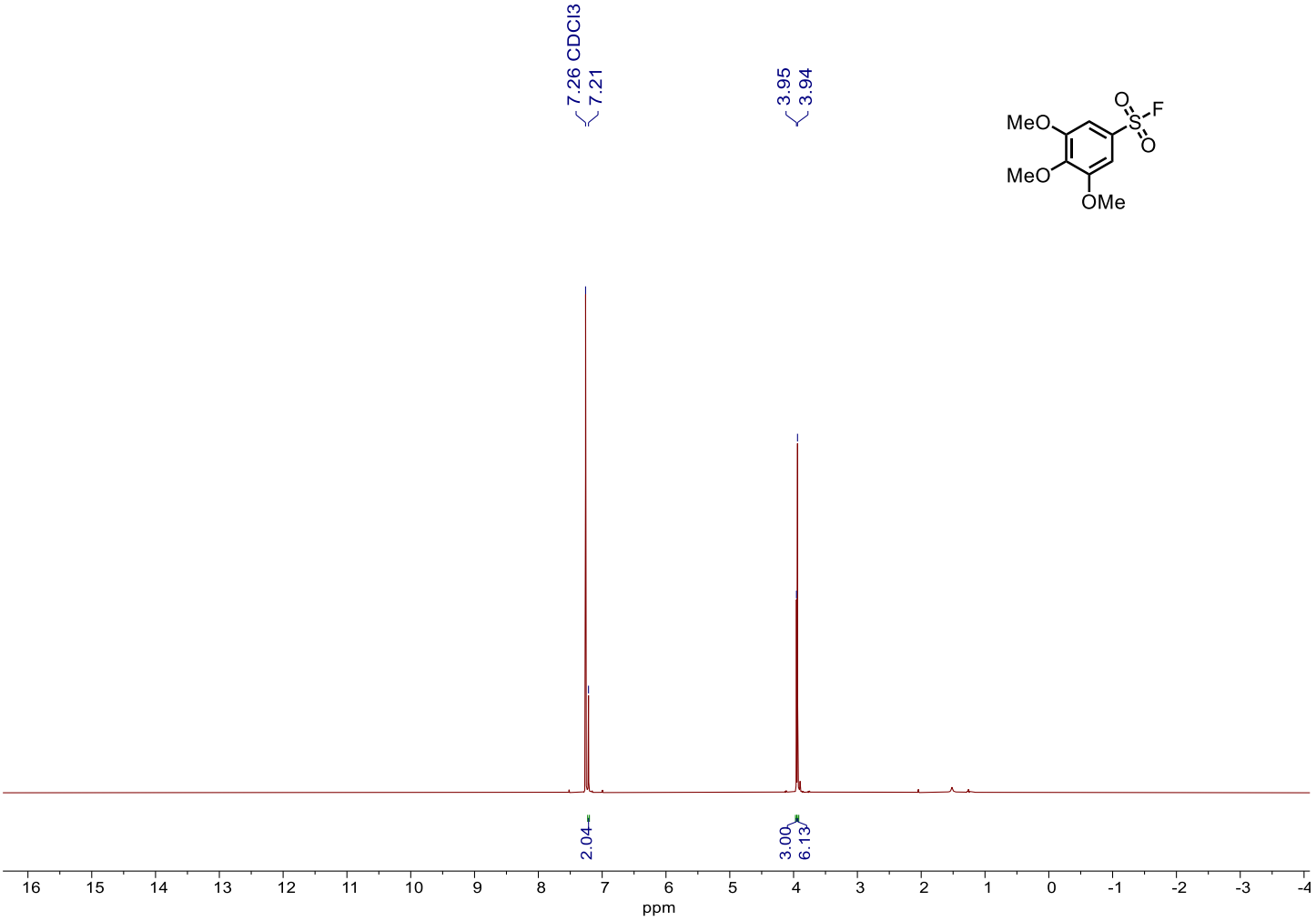

^{19}F NMR Spectrum for Compound **13** (376 MHz, $CDCl_3$)

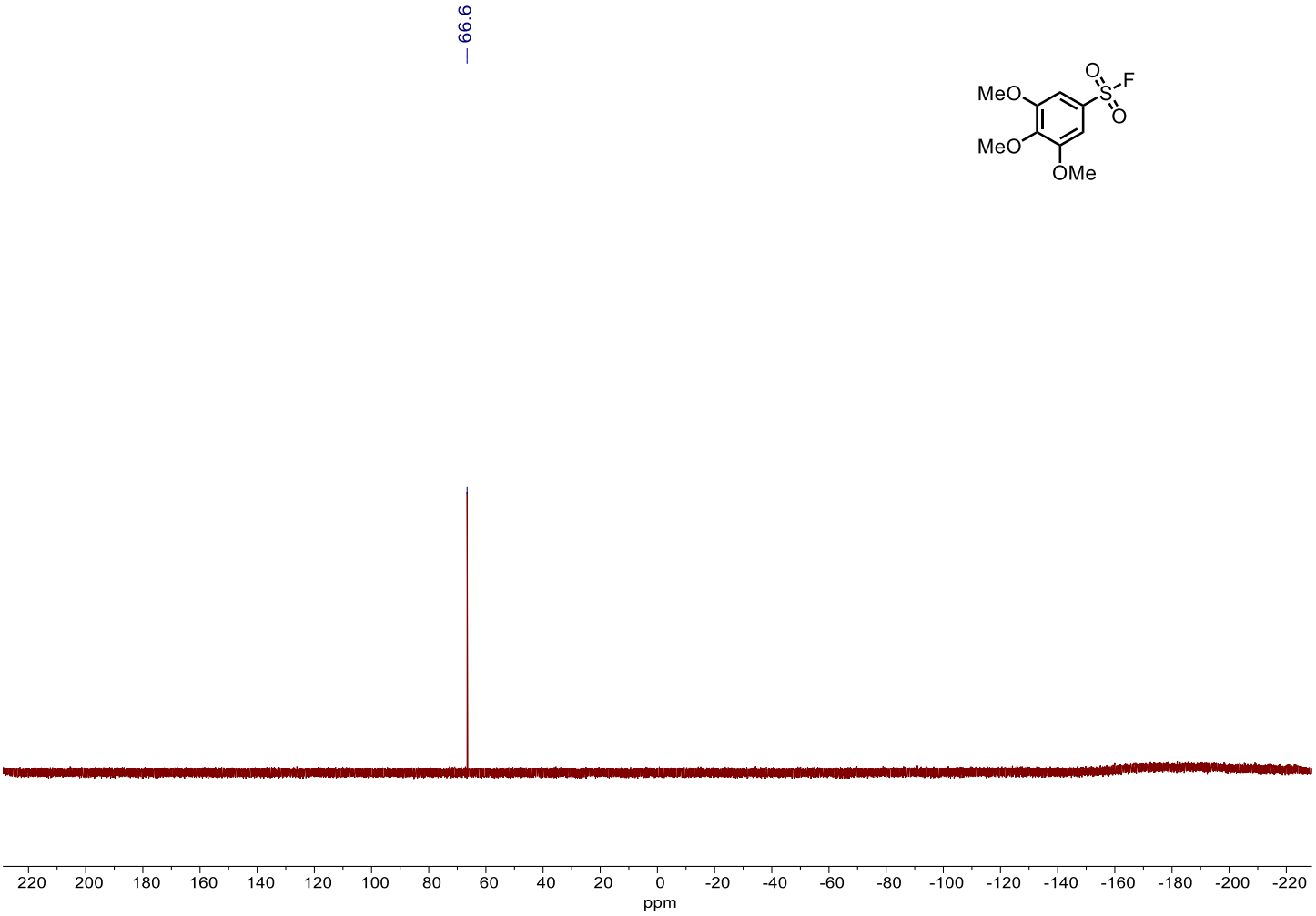

^{1}H NMR Spectrum for Compound **1-L01** (400 MHz, $CDCl_3$)

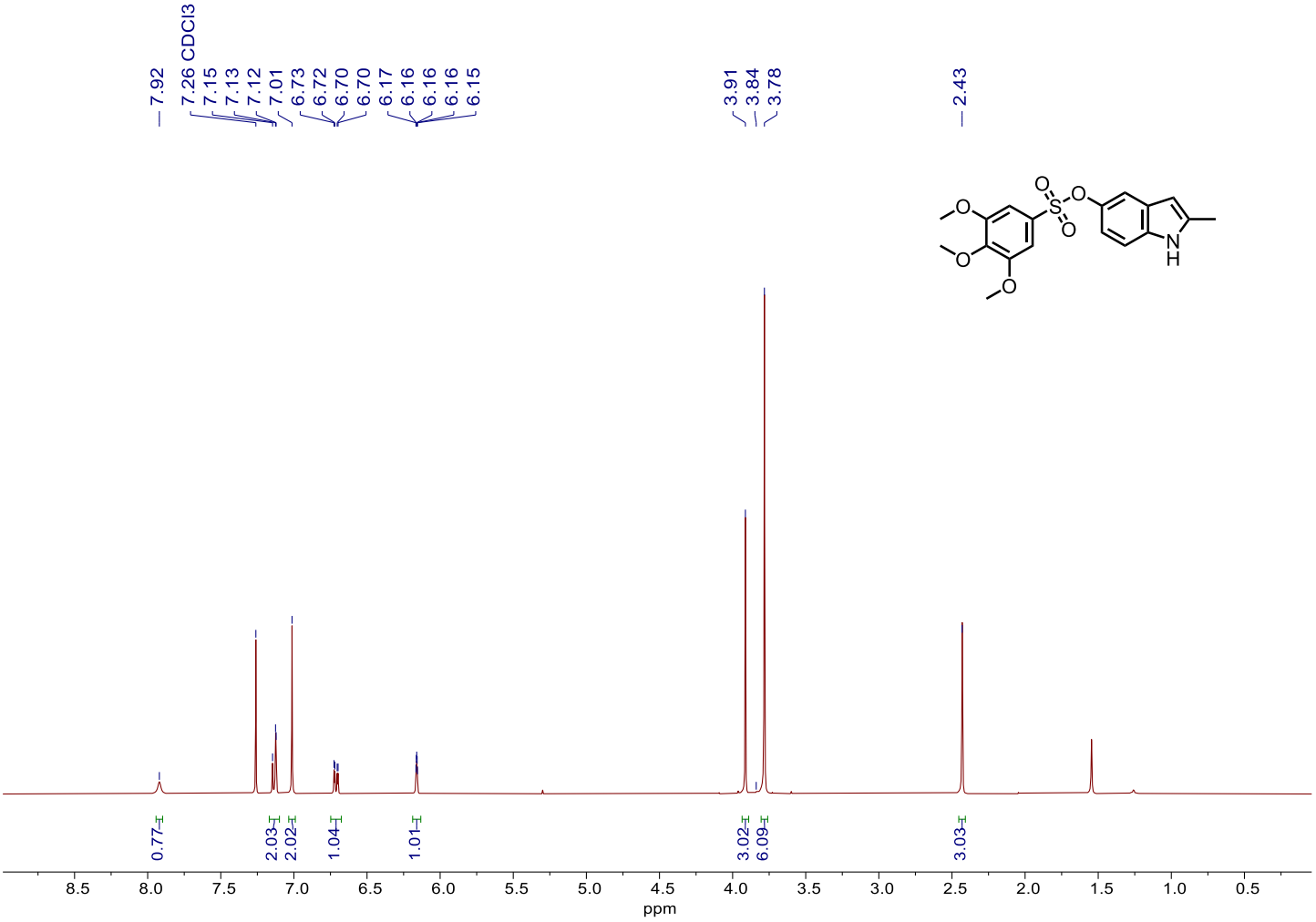

^{13}C NMR Spectrum for Compound **1-L01** (101 MHz, $CDCl_3$)

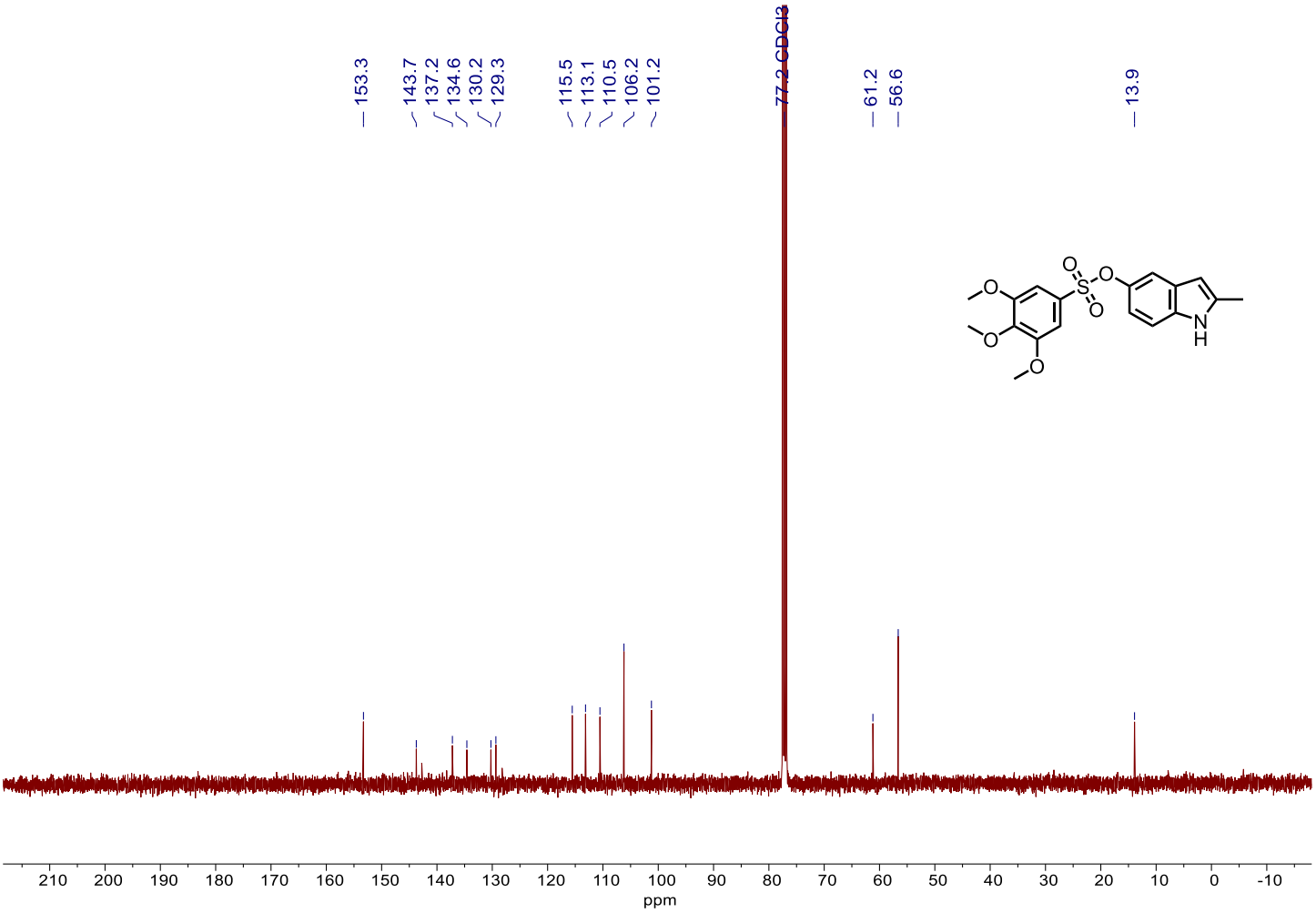

^{1}H NMR Spectrum for Compound **1-K08** (400 MHz, $CDCl_3$)

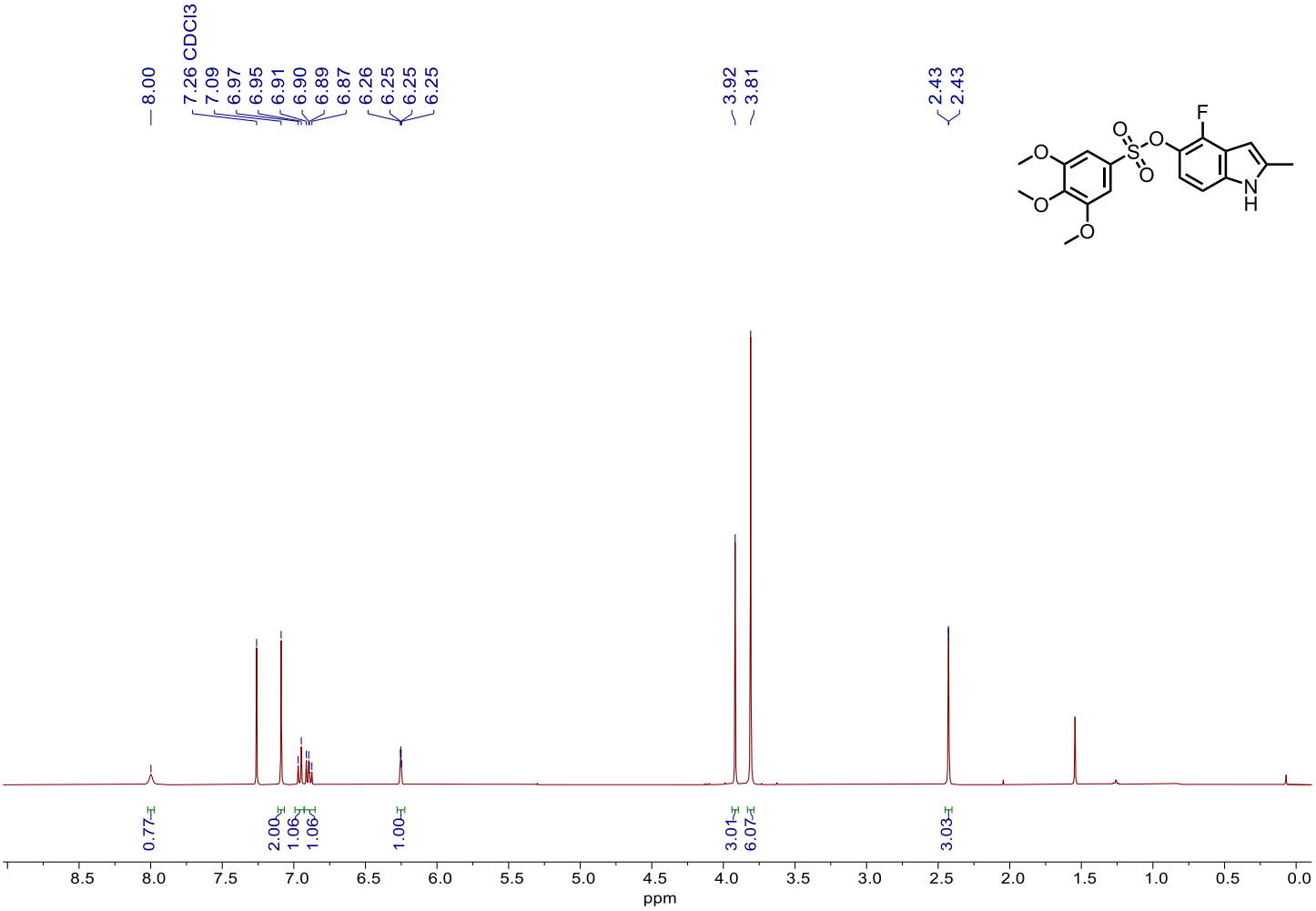

^{13}C NMR Spectrum for Compound **1-K08** (101 MHz, $CDCl_3$)

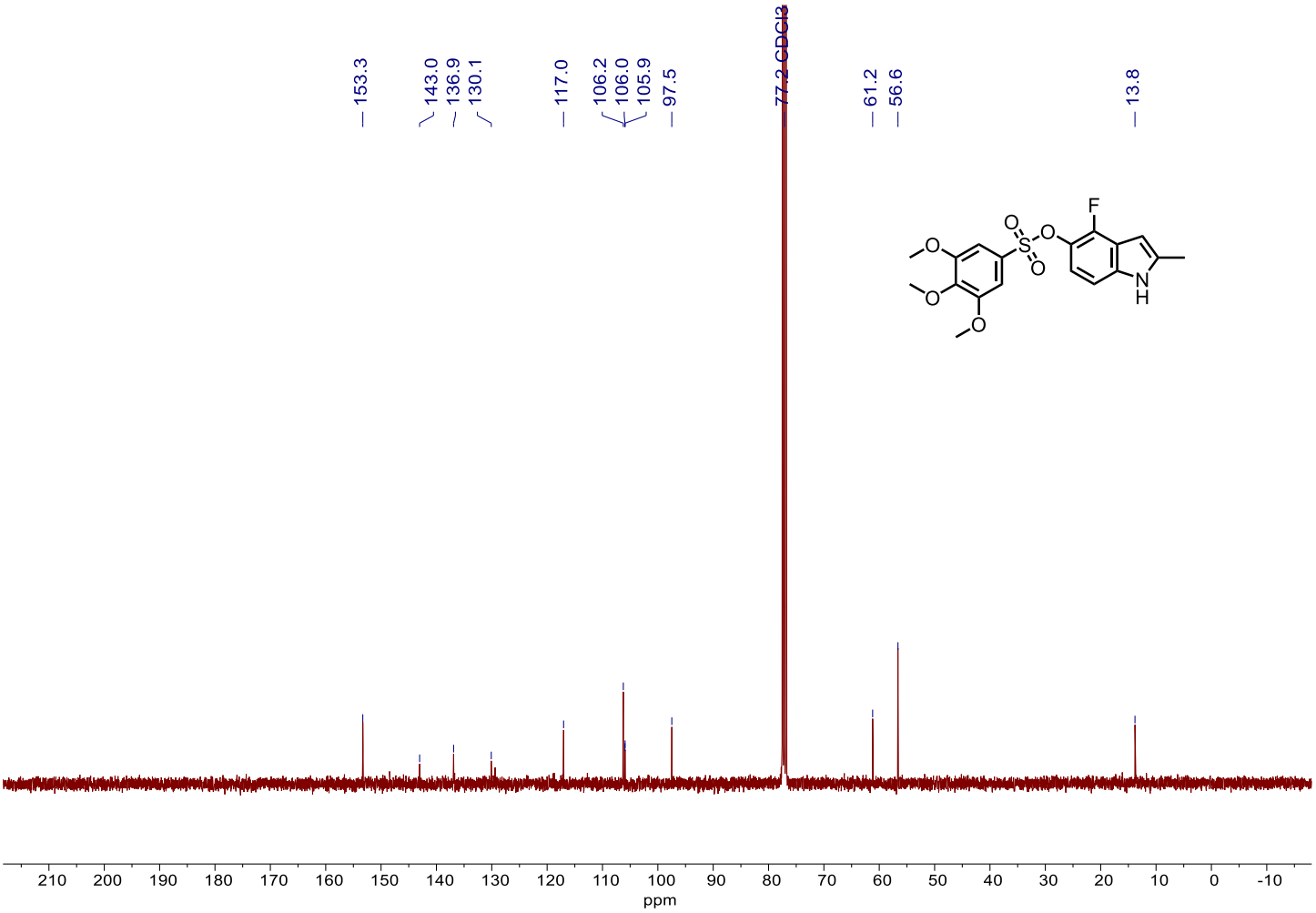

^{19}F NMR Spectrum for Compound **1-K08** (376 MHz, $CDCl_3$)

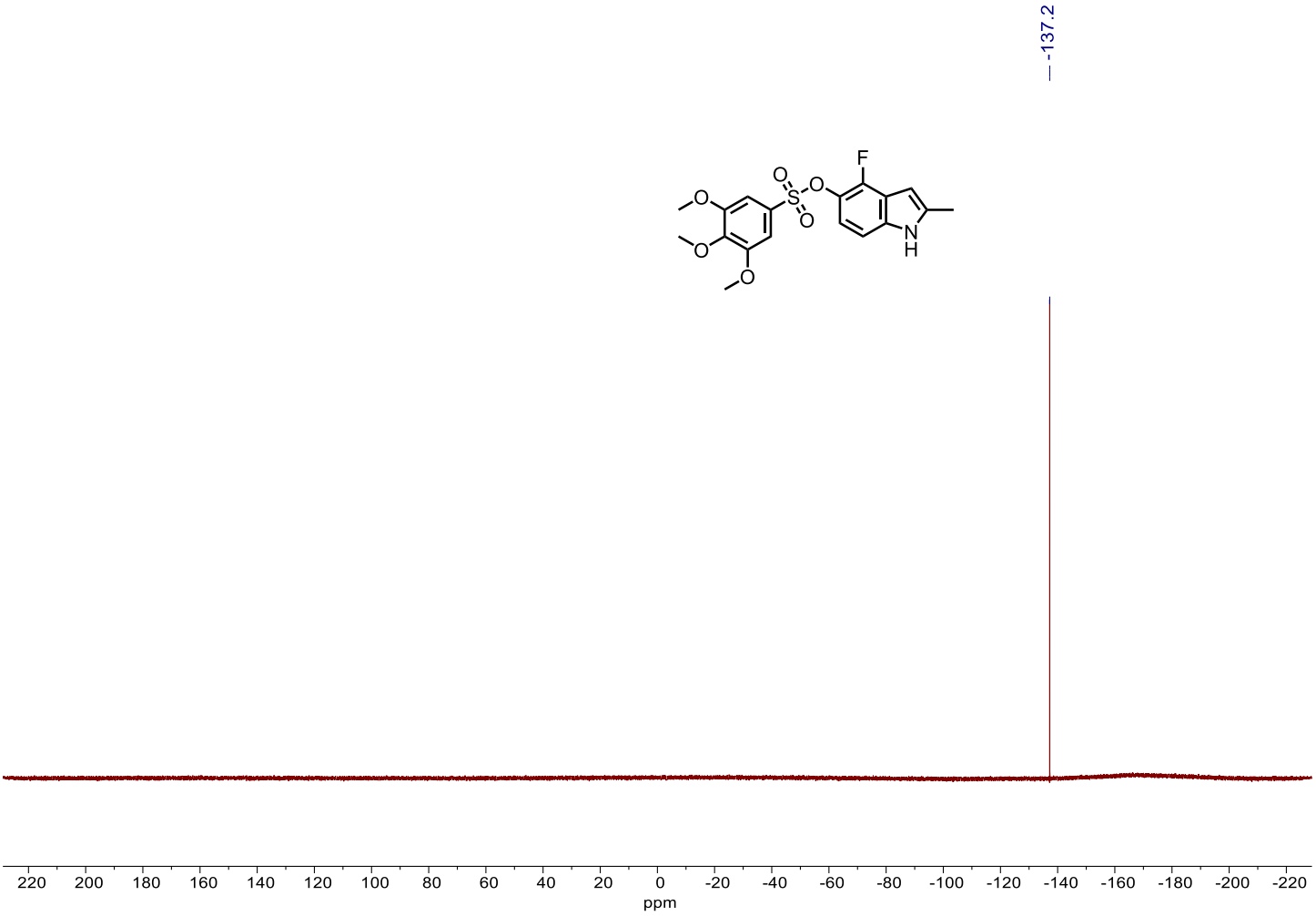

^{1}H NMR Spectrum for Compound **S1** (400 MHz, $CDCl_3$)

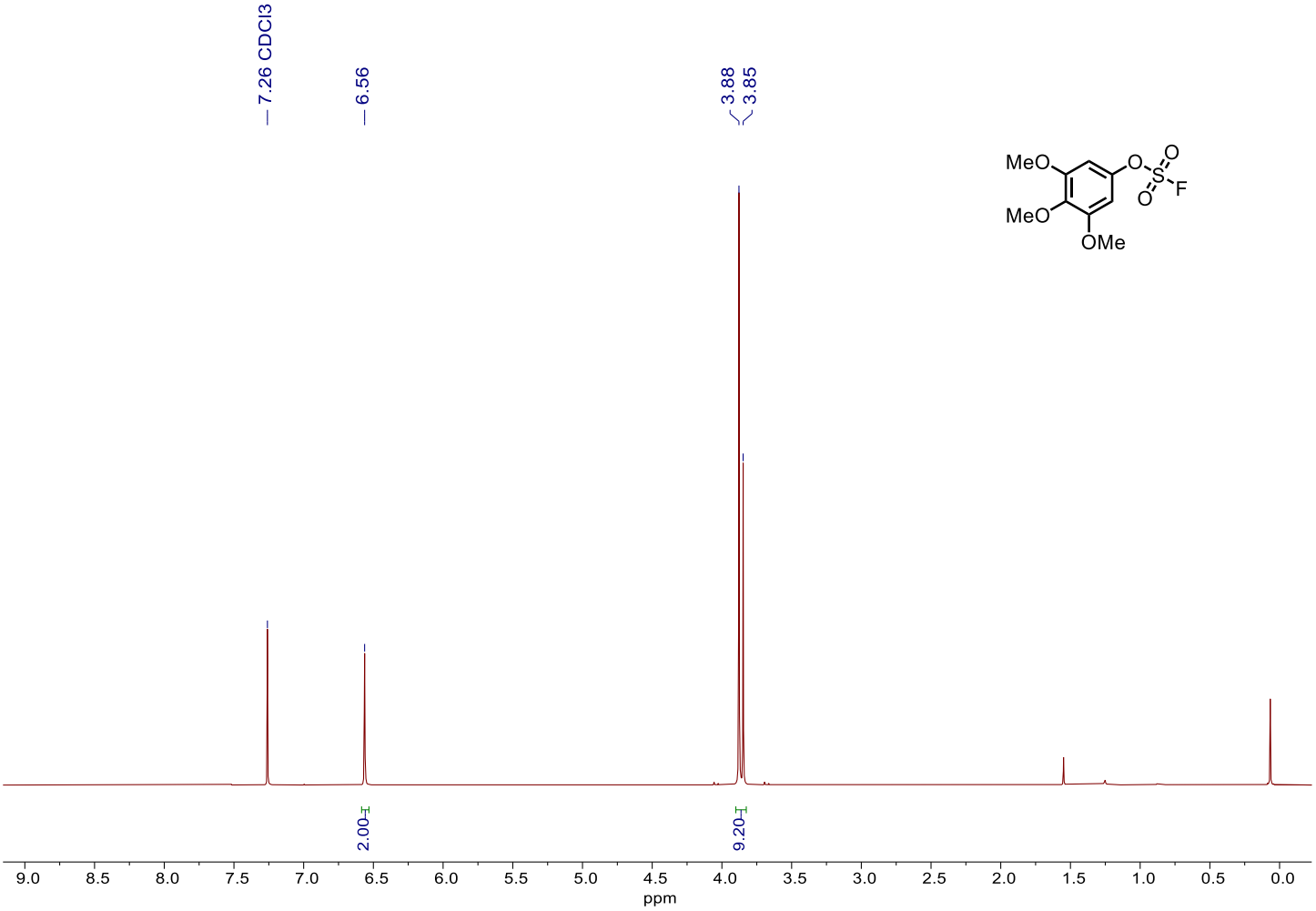

^{13}C NMR Spectrum for Compound **S1** (101 MHz, $CDCl_3$)

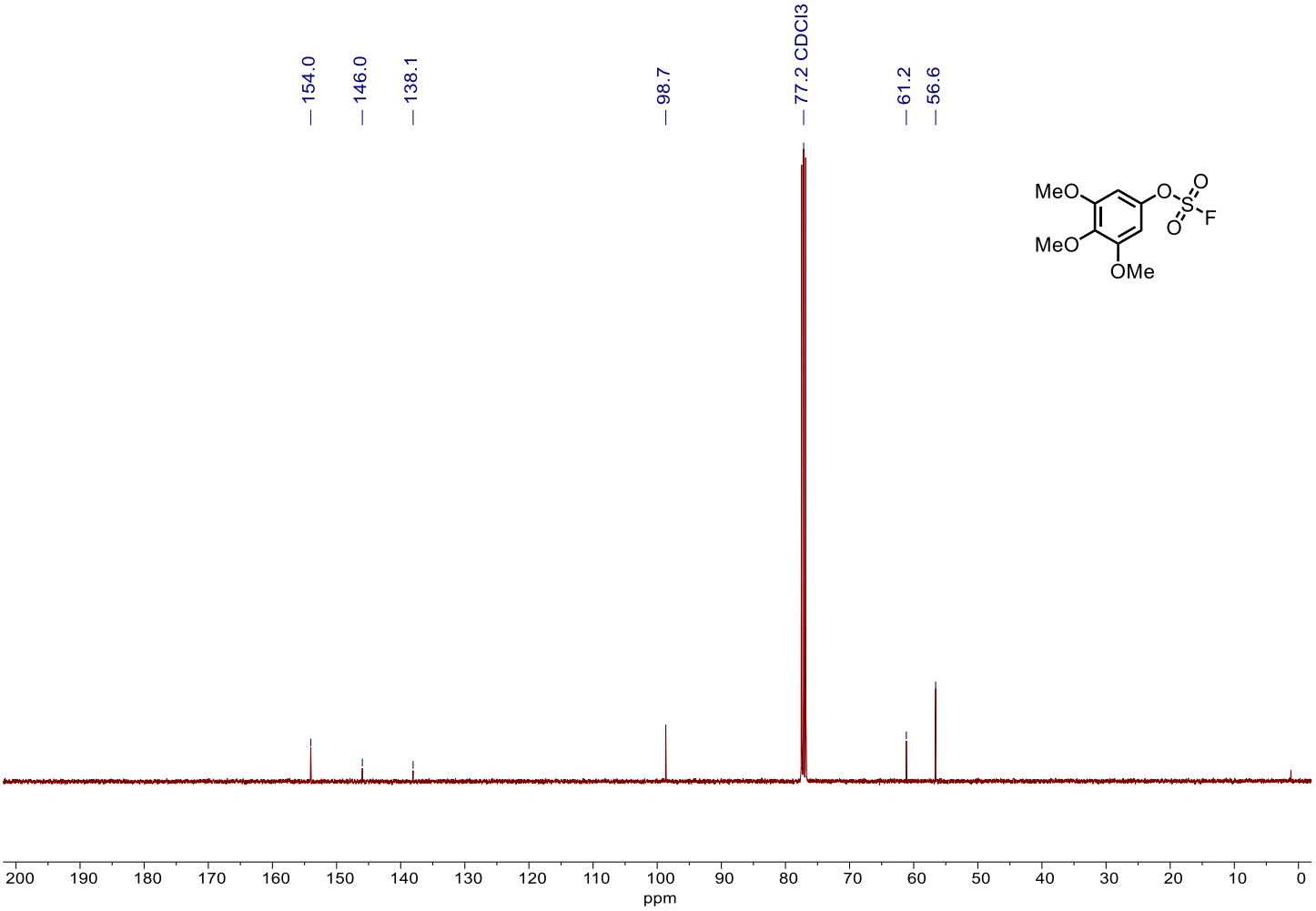

^{19}F NMR Spectrum for Compound **S1** (376 MHz, $CDCl_3$)

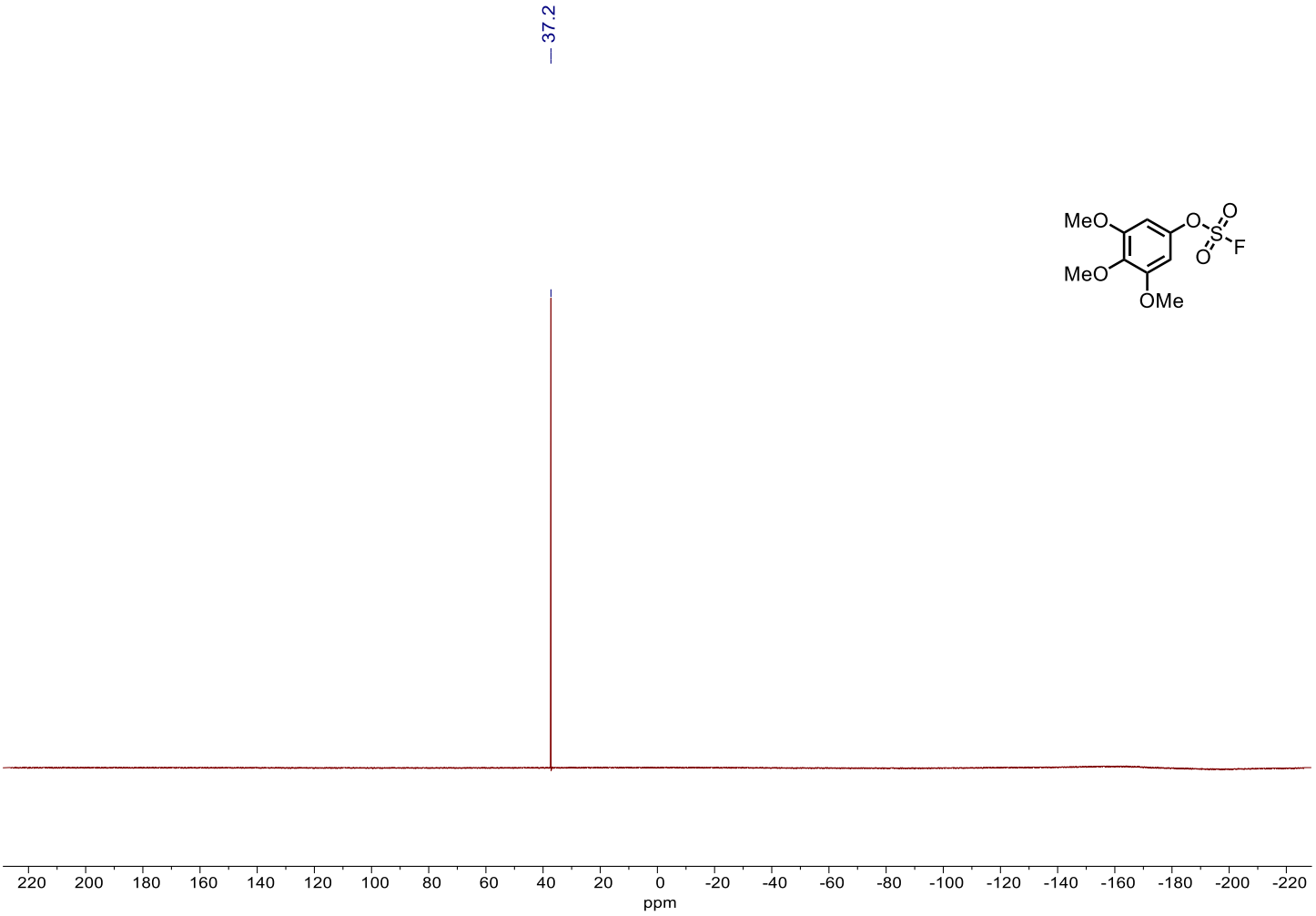

^{1}H NMR Spectrum for Compound **14-L01** (400 MHz, $CDCl_3$)

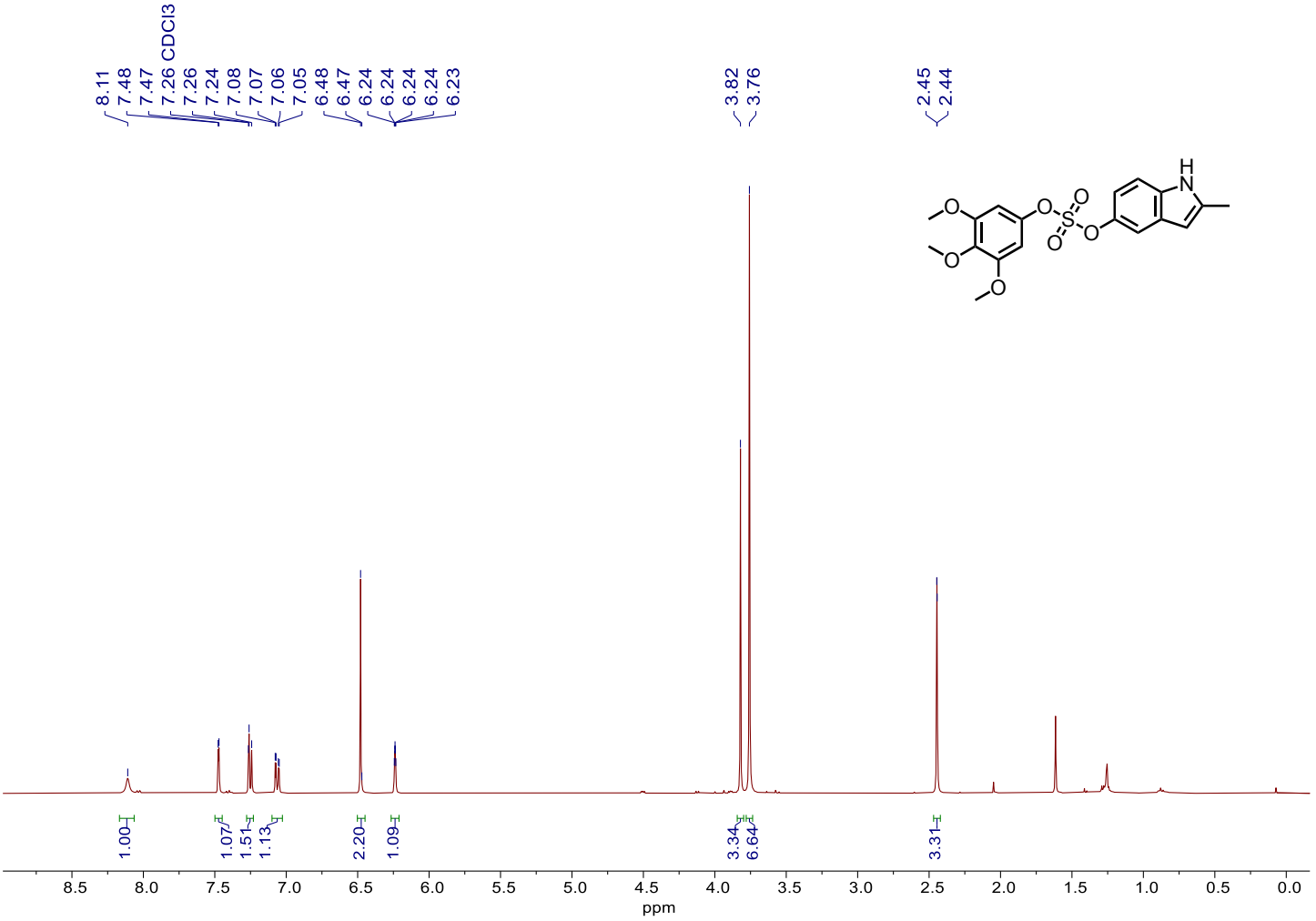

^{13}C NMR Spectrum for Compound **14-L01** (101 MHz, $CDCl_3$)

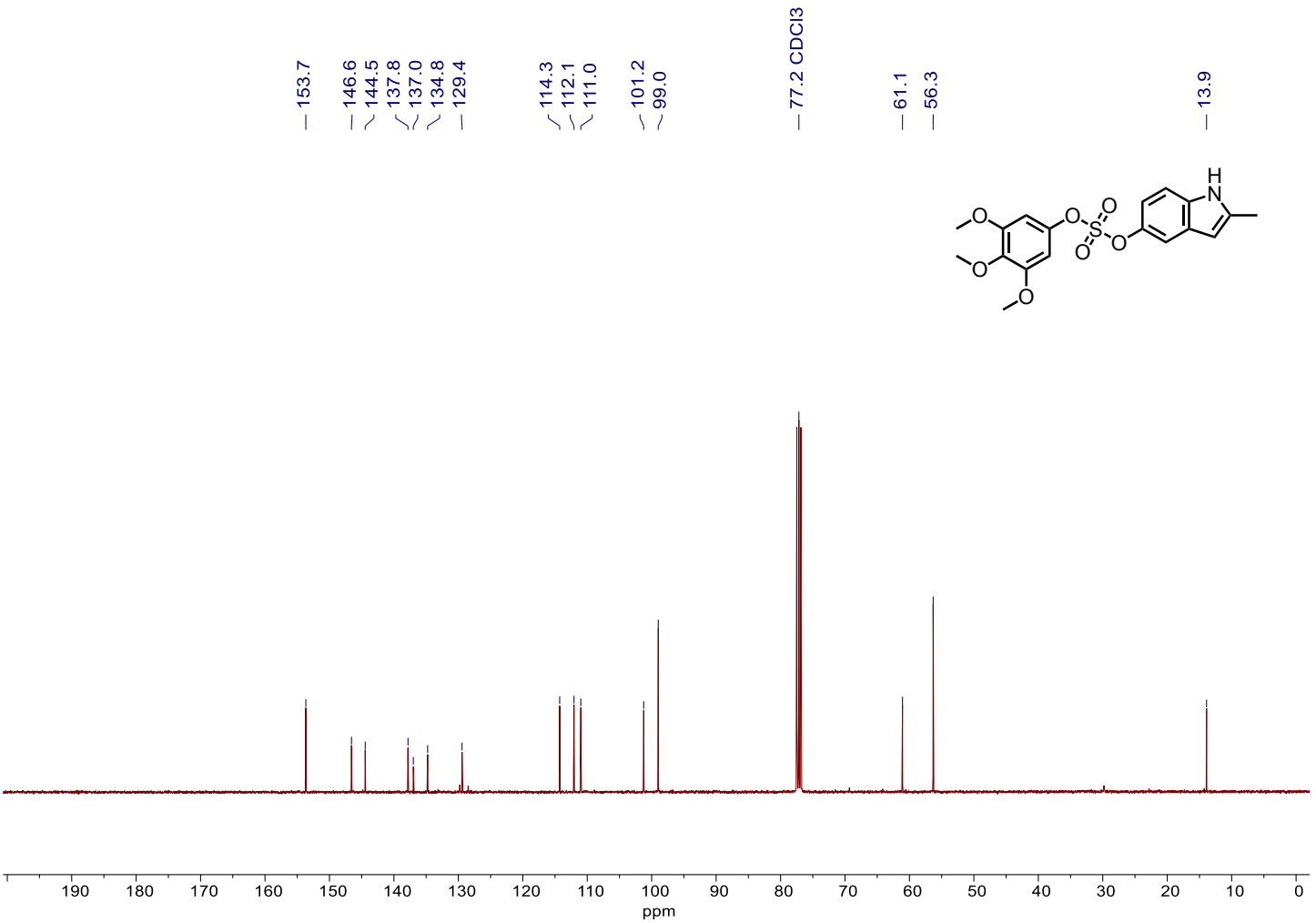

^{1}H NMR Spectrum for Compound **14-K08** (400 MHz, $CDCl_3$)

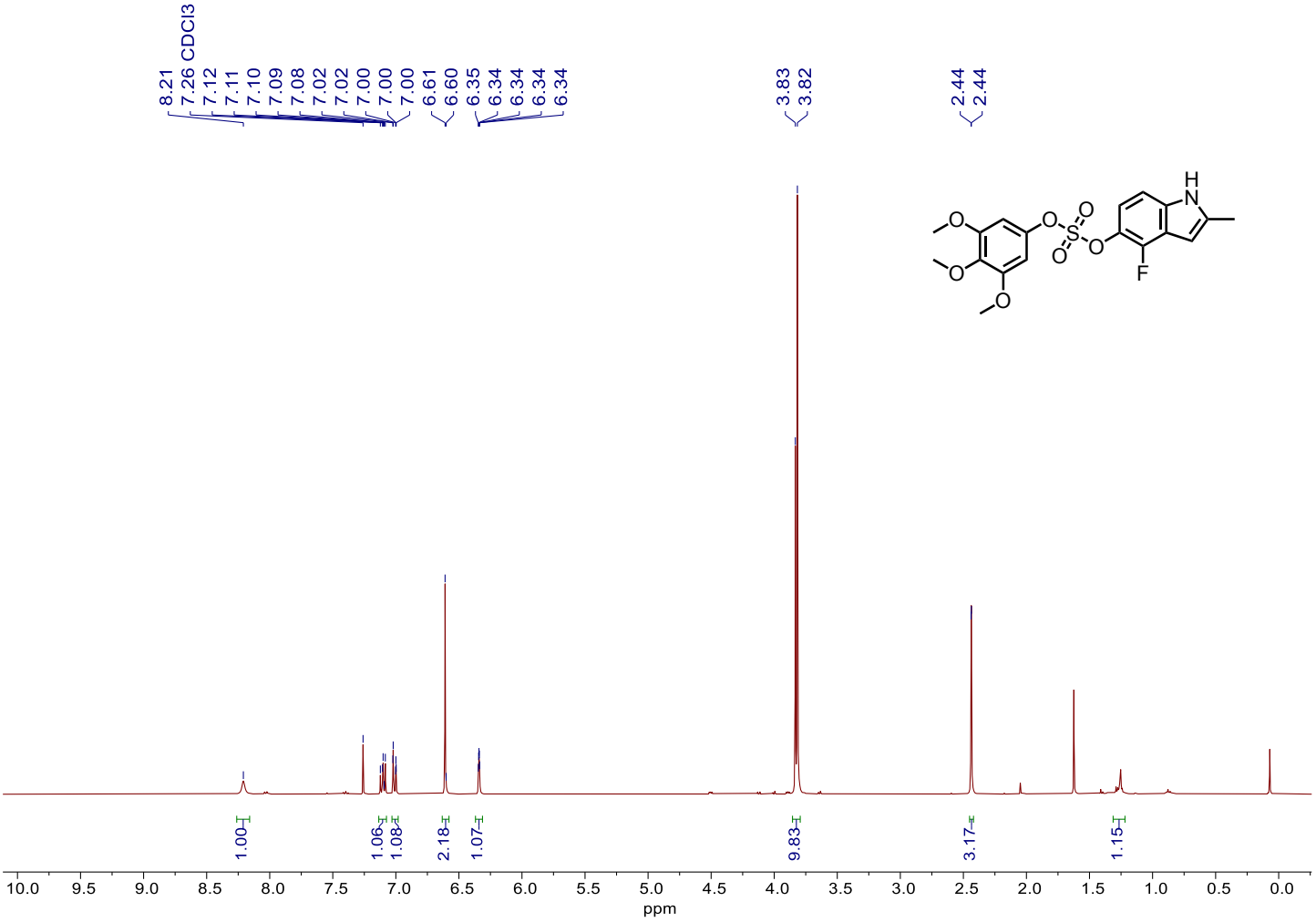

^{13}C NMR Spectrum for Compound **14-K08** (101 MHz, $CDCl_3$)

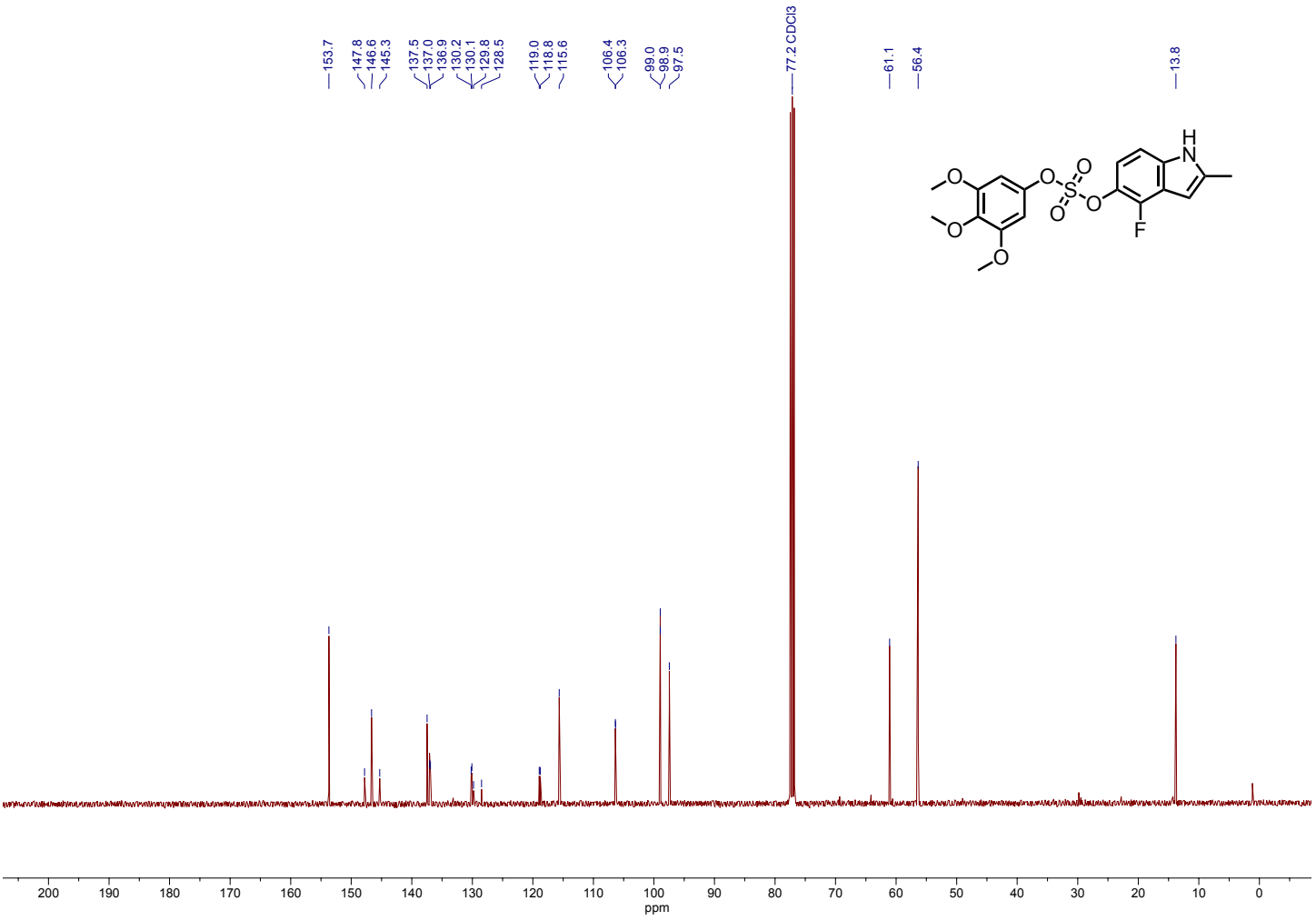

[1]H NMR Spectrum for Compound **S2** (400 MHz, DMSO)

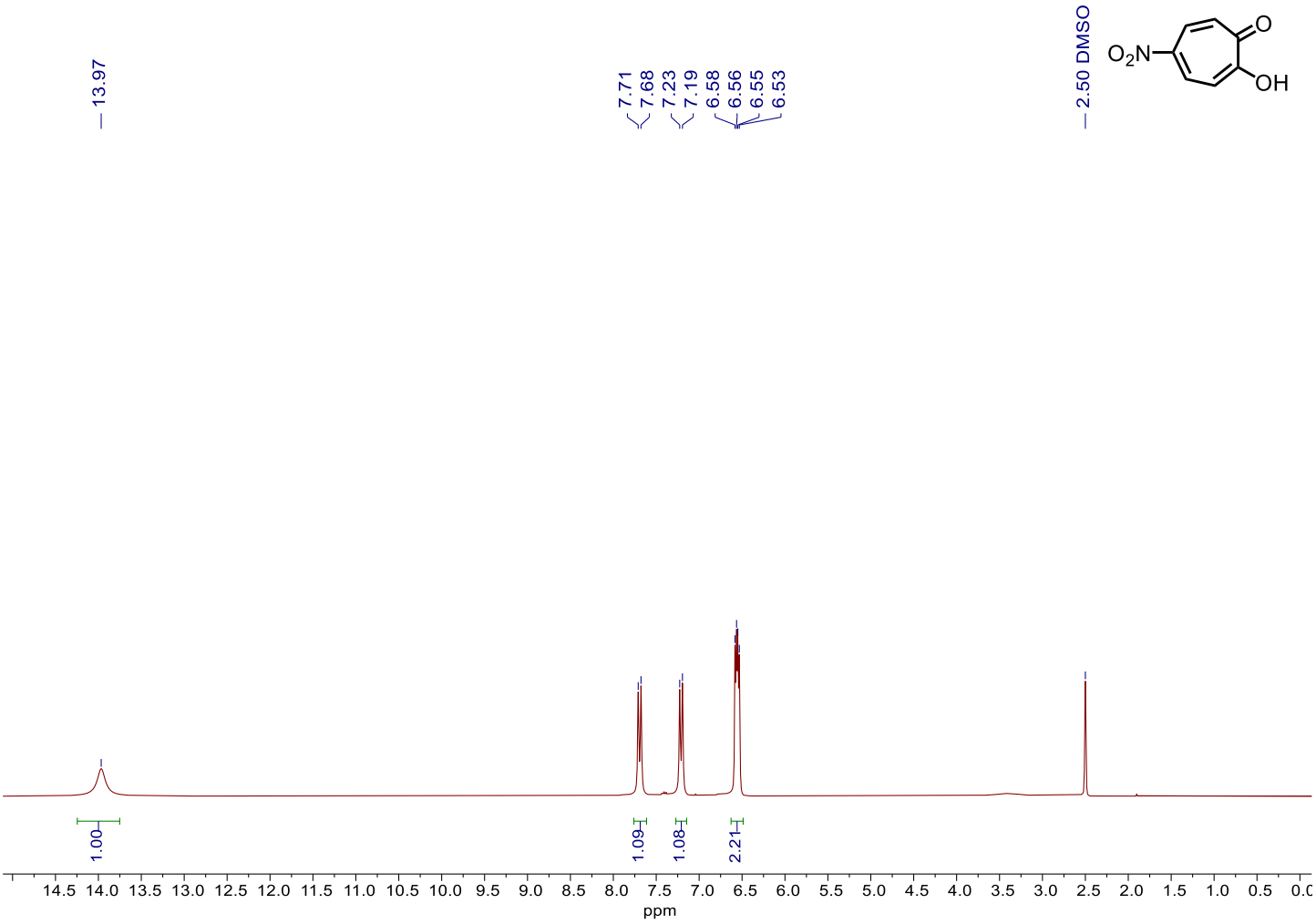

^{13}C NMR Spectrum for Compound **S2** (101 MHz, DMSO)

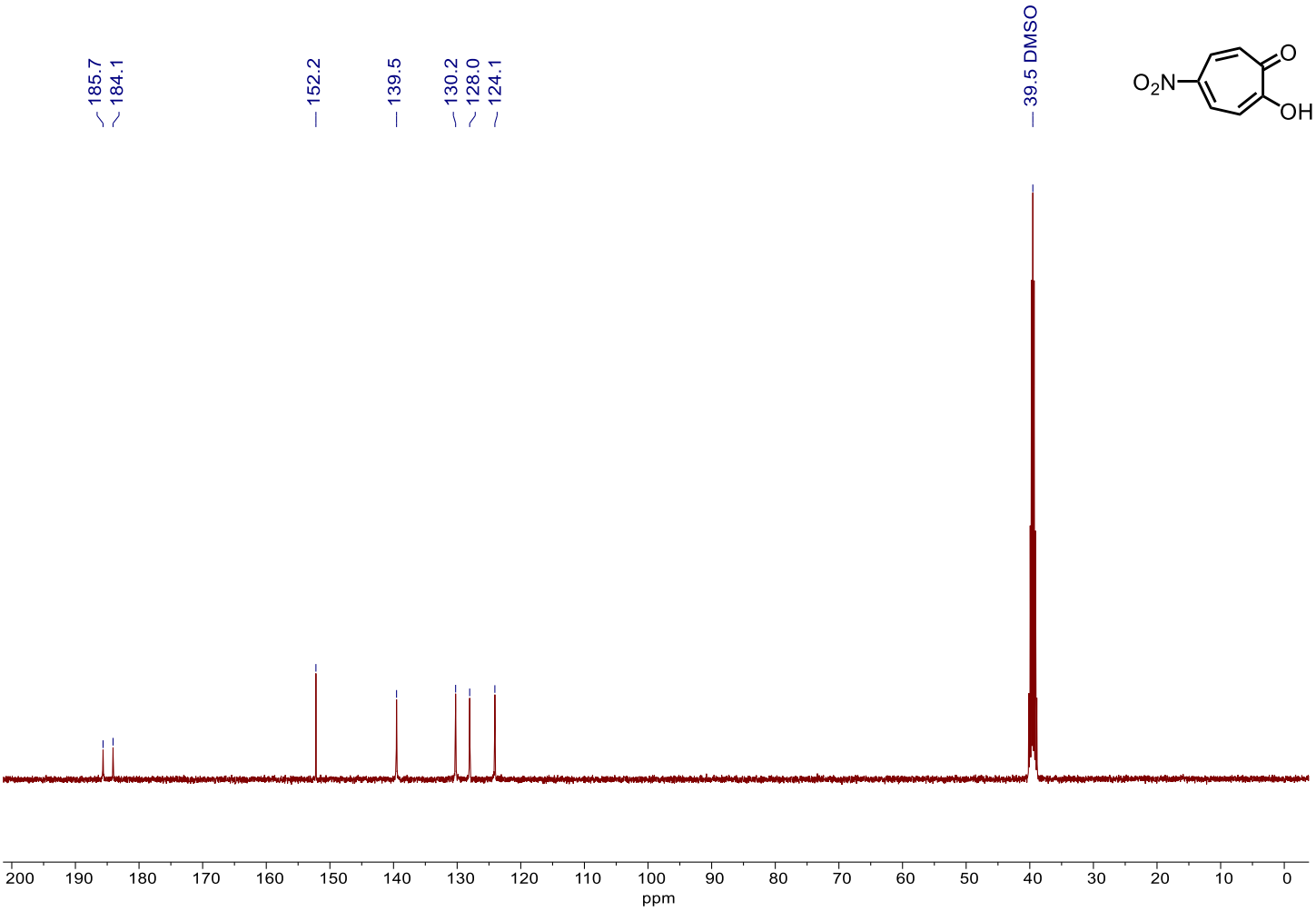

^{1}H NMR Spectrum for Compound **S3** (400 MHz, DMSO)

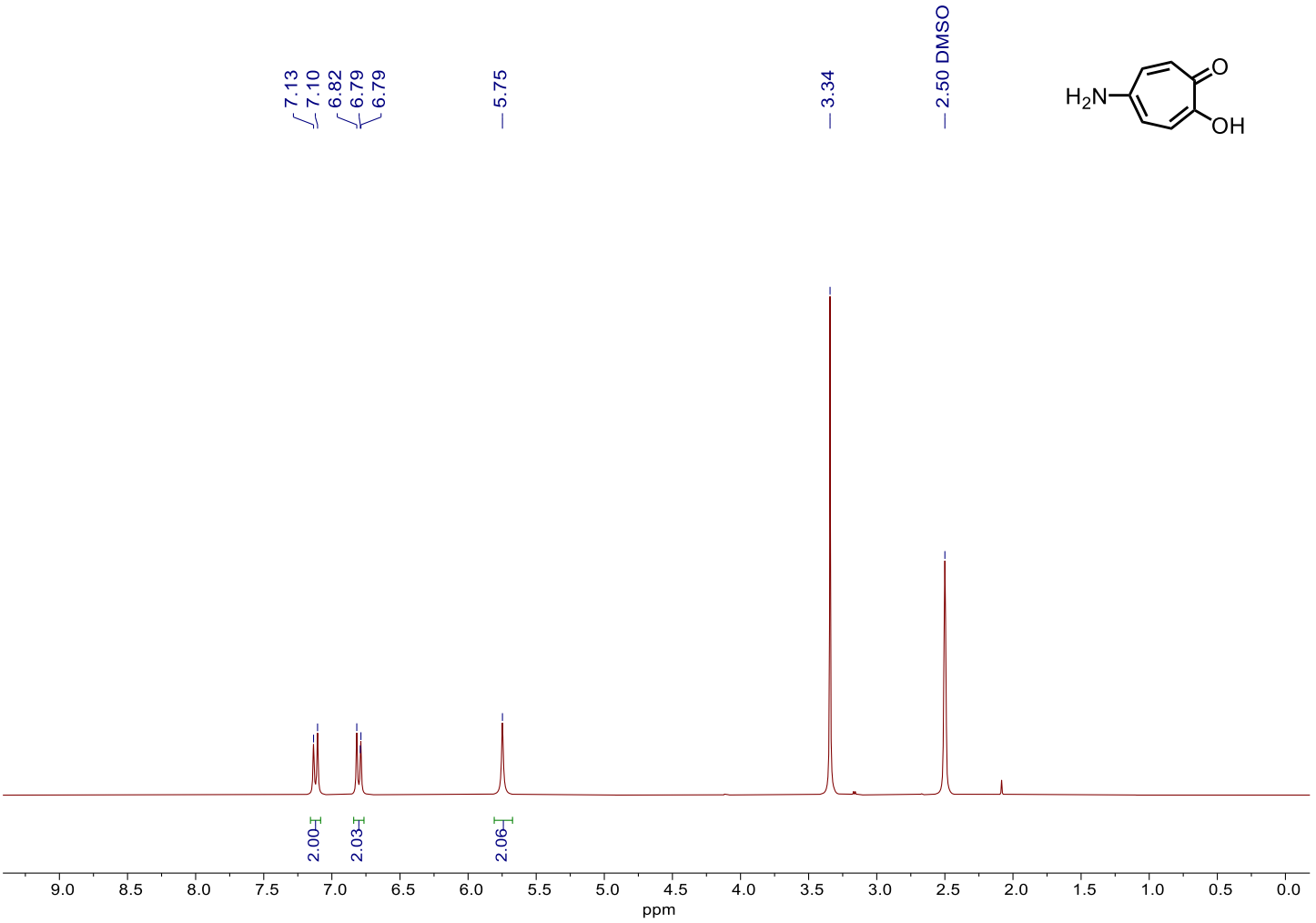

^{13}C NMR Spectrum for Compound **S3** (101 MHz, DMSO)

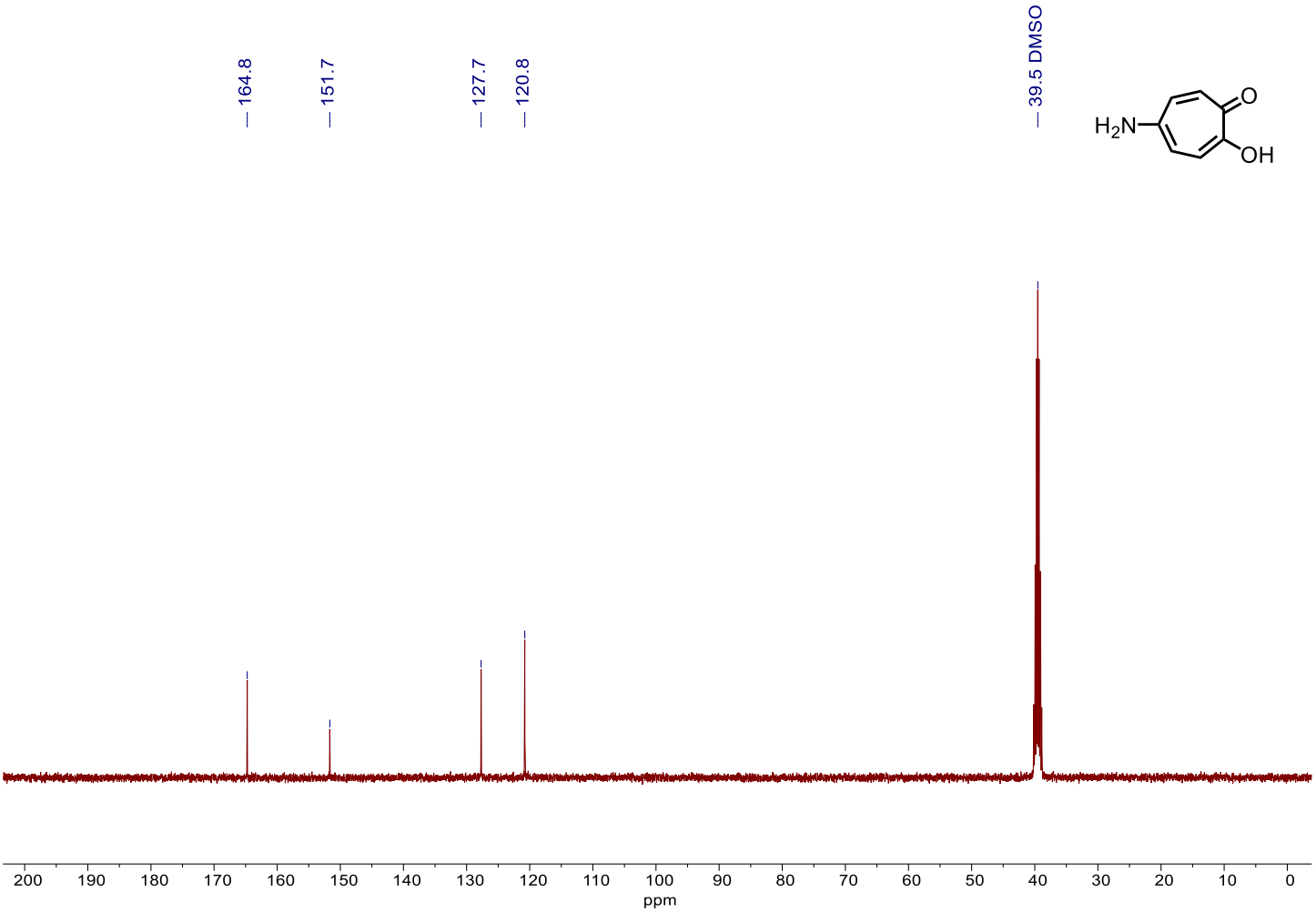

^{1}H NMR Spectrum for Compound **S4** (400 MHz, DMSO)

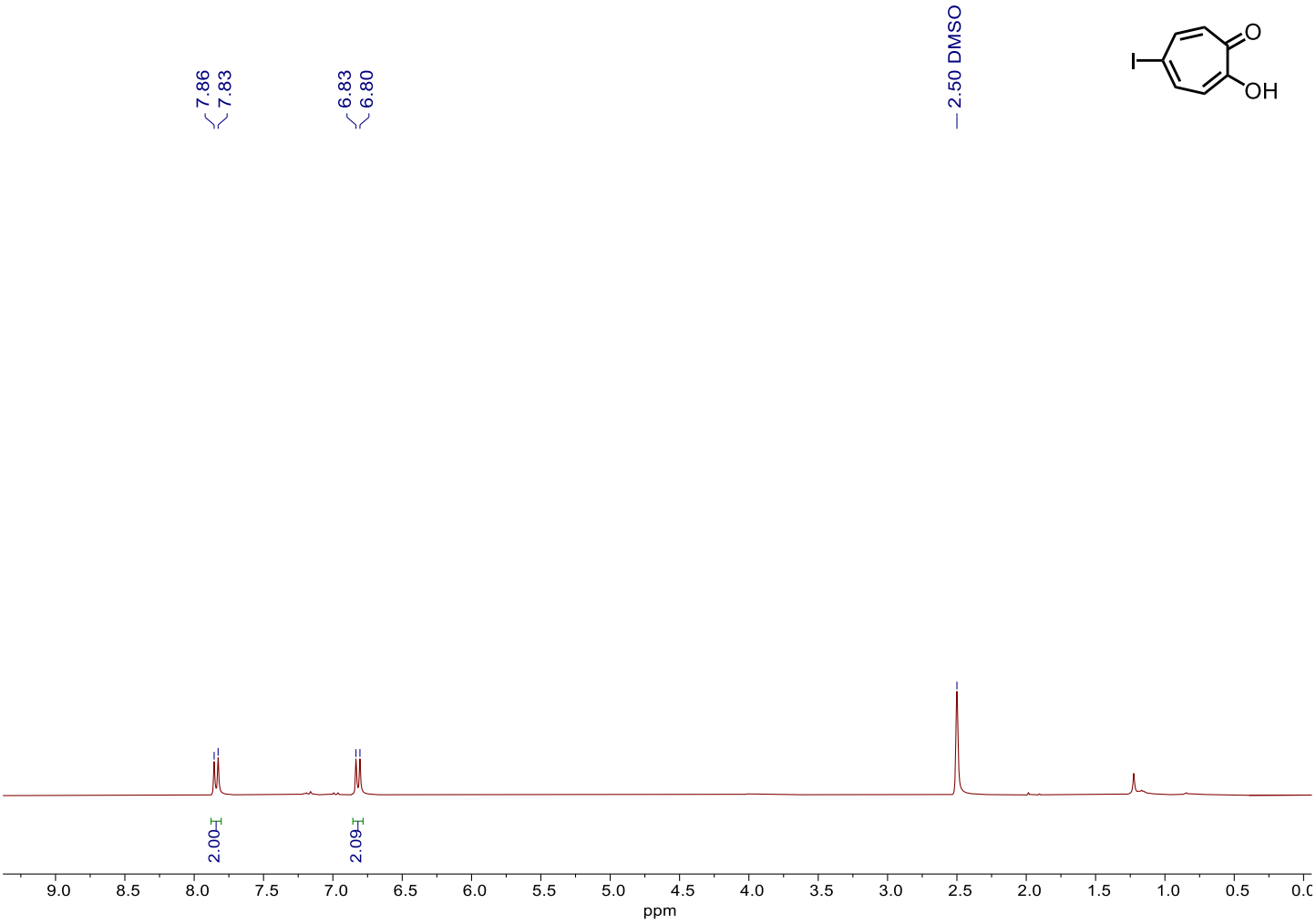

^{13}C NMR Spectrum for Compound **S4** (101 MHz, DMSO)

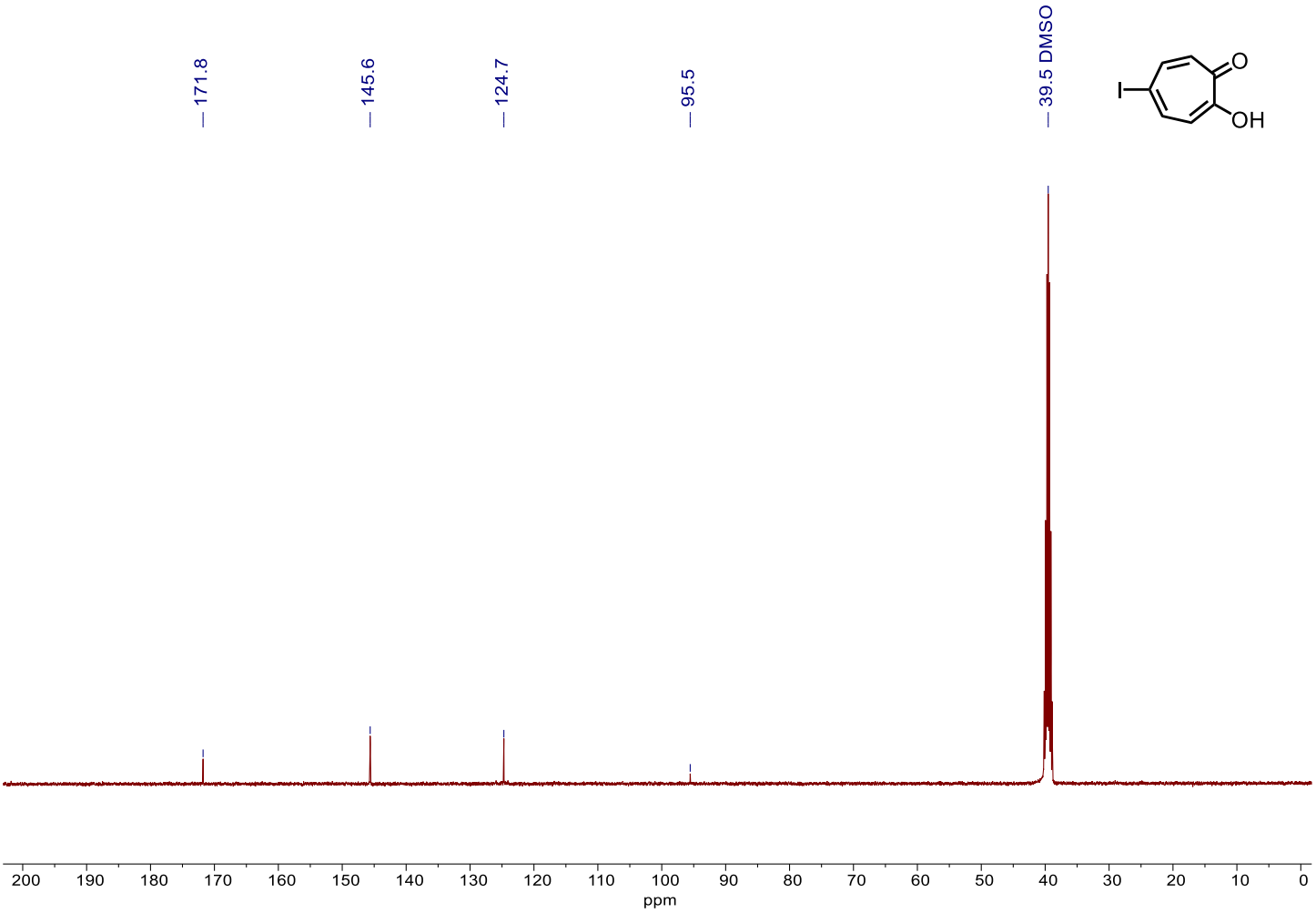

[1]H NMR Spectrum for Compound **S5** (400 MHz, DMSO)

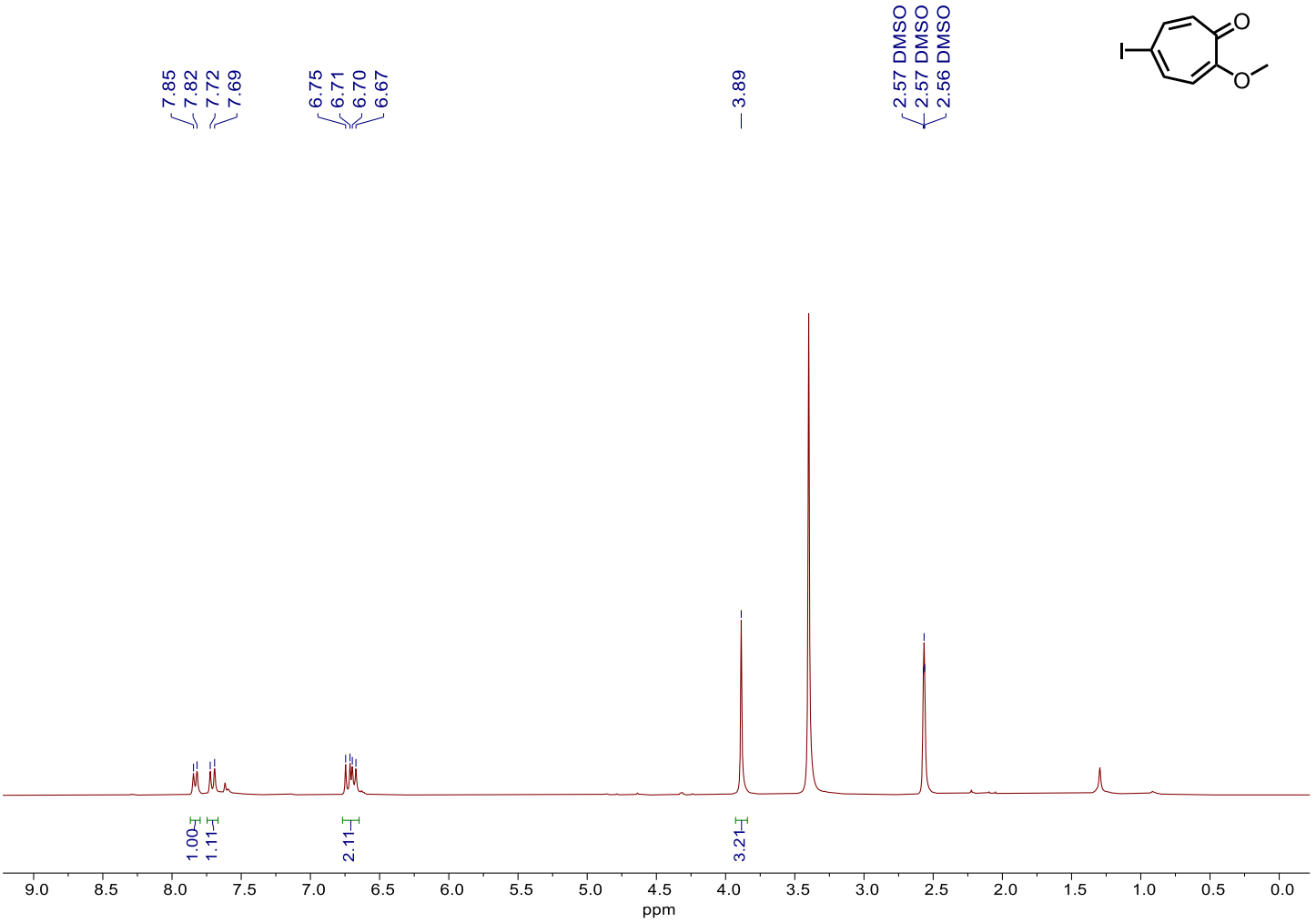

^{13}C NMR Spectrum for Compound **S5** (101 MHz, DMSO)

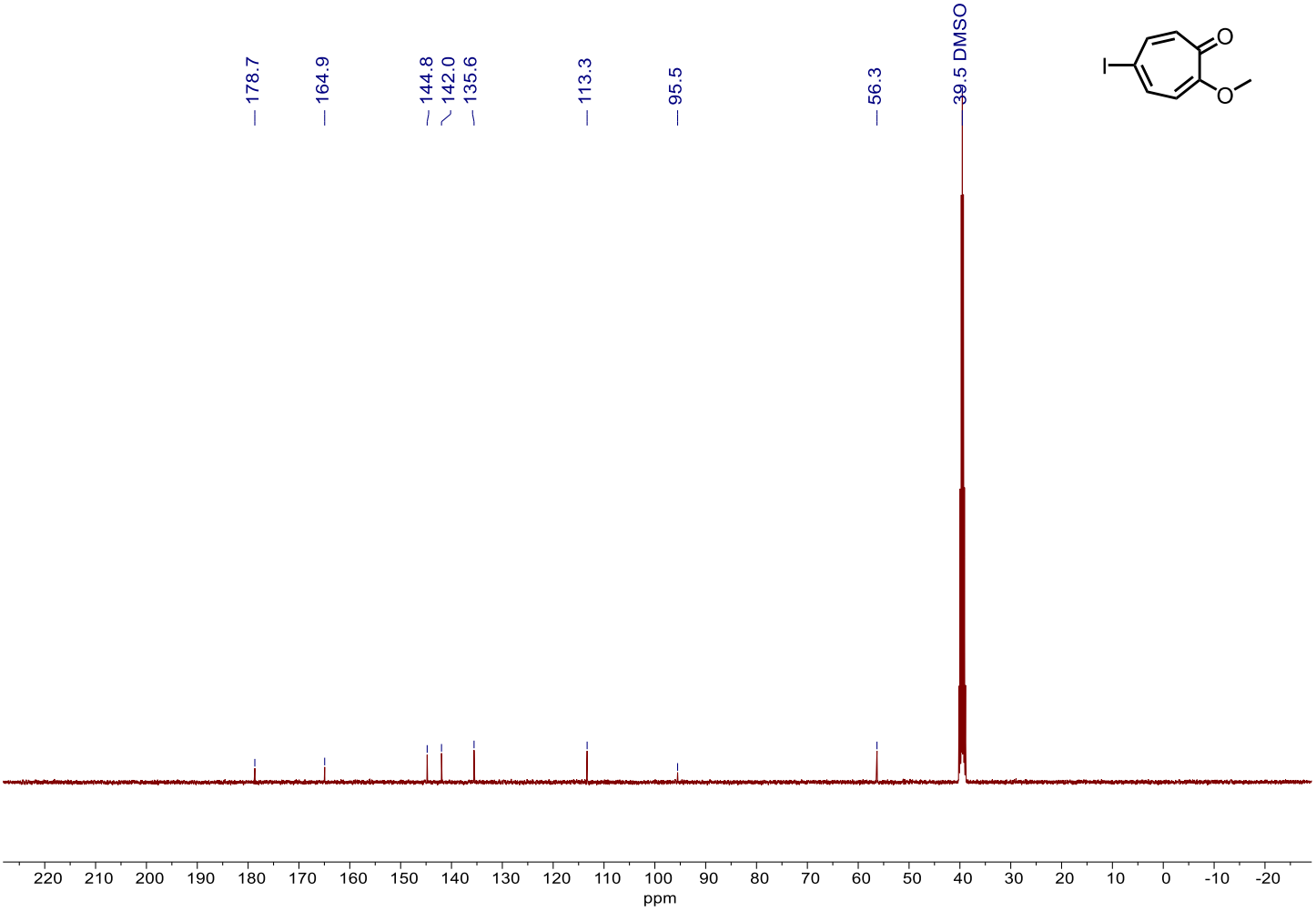

^{1}H NMR Spectrum for **MTC** (400 MHz, $CDCl_3$)

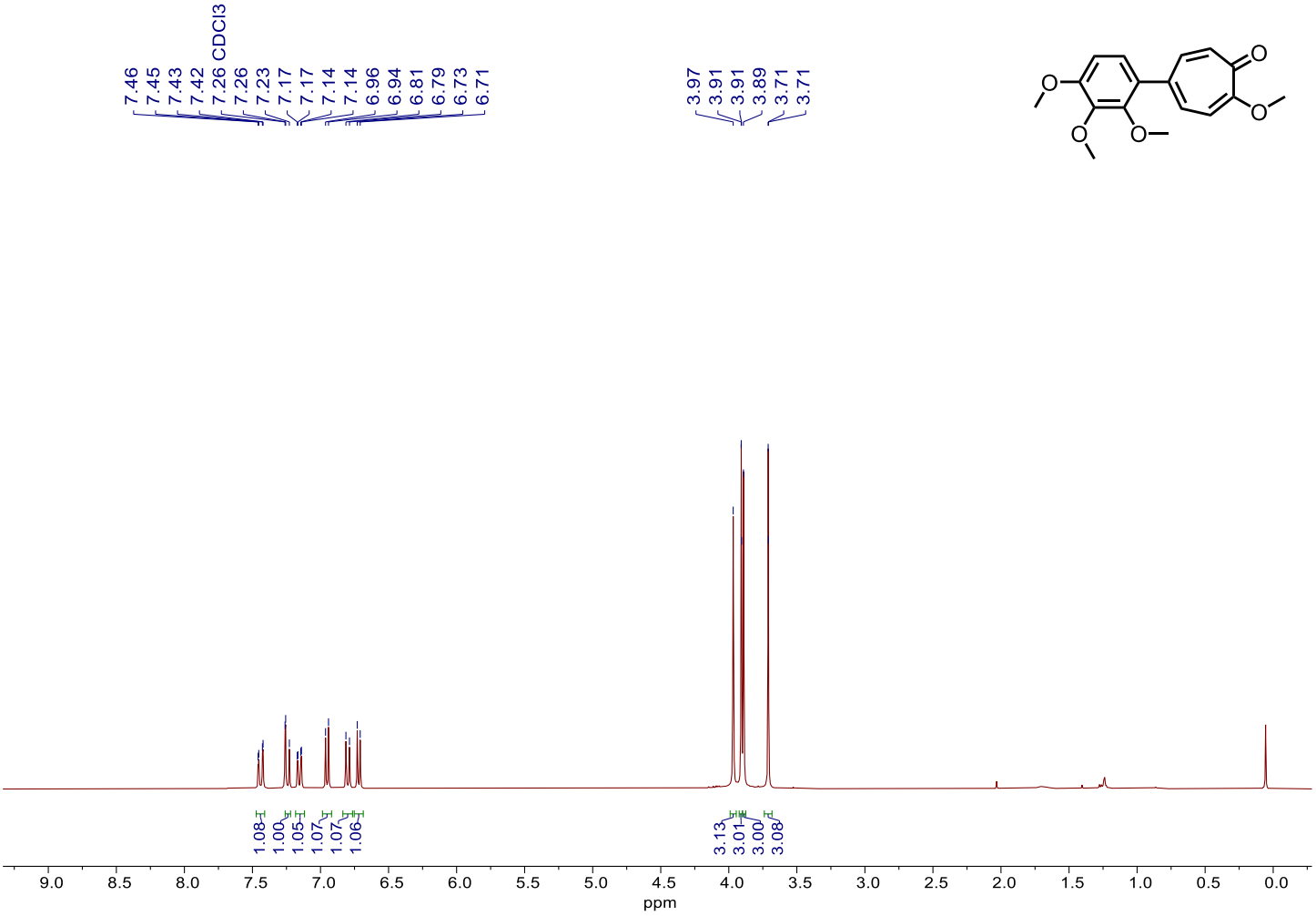

^{13}C NMR Spectrum for **MTC** (101 MHz, $CDCl_3$)